B U L L E T I N

DE LA SOCIÉTÉ DES SCIENCES ET DES LETTRES DE ŁÓDŹ

SÉRIE:
RECHERCHES SUR LES DÉFORMATIONS

Volume LXV, no. 2

B U L L E T I N

DE LA SOCIÉTÉ DES SCIENCES ET DES LETTRES DE ŁÓDŹ

SÉRIE:
RECHERCHES SUR LES DÉFORMATIONS

Volume LXV, no. 2

ŁÓDŹ 2015

ŁÓDZKIE TOWARZYSTWO NAUKOWE
PL-90-505 Łódź, ul. M. Curie-Skłodowskiej 11
tel. (42) 66-55-459, fax (42) 66 55 464
sprzedaż wydawnictw: tel. (42) 66 55 448, http://sklep.ltn.lodz.pl
e-mail: biuro@ltn.lodz.pl; http://www.ltn.lodz.pl/

**Wydano z pomocą finansową Ministerstwa Nauki
i Szkolnictwa Wyższego**

PL ISSN 0459–6854

Wydanie 1.
Nakład 200 egz.
Skład komputerowy: Zofia Fijarczyk
Druk i oprawa: 2K Łódź sp. z o.o.
Łódź, ul. Płocka 35/45
www.2k.com.pl, 2k@2k.com.pl

The journal appears in the bases *Copernicus* and *EBSCOhost*

INSTRUCTION AUX AUTEURS

1. La présente Série du Bulletin de la Société des Sciences et des Lettres de Łódź comprend des communications du domaine des mathématiques, de la physique ainsi que de leurs applications liées aux déformations au sense large.
2. Toute communications est présentée à la séance d'une Commission de la Société par un des members (avec deux opinions de spécialistes designés par la Rédaction). Elle doit lui être adressée directement par l'auteur.
3. L'article doit être écrit en anglais, français, allemand ou russe et débuté par un résumé en anglais ou en langue de la communication présentée. Dans tous les travaux écrits par des auteurs étrangers le titre et le résumé en polonais seront préparés par la rédaction. Il faut fournir le texte original qui ne peut contenir plus de 15 pages (plus 2 copies).
4. Comme des articles seront reproduits par un procédé photographique, les auteurs sont priés de les préparer avec soin. Le texte tapé sur un ordinateur de la classe IBM PC avec l'utilisation d'un imprimante de laser, est absolument indispensable. Il doit être tapé préférablement en *AMS-TEX* ou, exceptionnellement, en *Plain-TEX* ou *LATEX*. Après l'acceptation de texte les auteurs sont priés d'envoyer les disquettes (PC). Quelle que soient les dimensions des feuilles de papier utilisées, le texte ne doit pas dépasser un cadre de frappe de 12.3×18.7 cm (0.9 cm pour la page courante y compris). Les deux marges doivent être le la même largeur.
5. Le nom de l'auteur (avec de prénom complet), écrit en italique sera placé à la 1ère page, 5.6 cm au dessous du bord supérieur du cadre de frappe; le titre de l'acticle, en majuscules d'orateur 14 points, 7.1 cm au dessous de même bord.
6. Le texte doit être tapé avec les caractères Times 10 points typographiques et l'interligne de 14 points hors de formules longues. Les résumés, les rénvois, la bibliographie et l'adresse de l'auteurs doivent être tapés avec le petites caractères 8 points typographiques et l'interligne de 12 points. Ne laissez pas de "blancs" inutiles pour respecter la densité du texte. En commençant le texte ou une formule par l'alinéa il faut taper 6 mm ou 2 cm de la marge gauche, respectivement.
7. Les texte des thèorémes, propositions, lemmes et corollaries doivent être écrits en italique.
8. Les articles cités seront rangés dans l'ordre alphabétique et précédés de leurs numéros placés entre crochets. Après les références, l'auteur indiquera son adress complète.
9. Envoi par la poste: protégez le manuscript à l'aide de cartons.
10. Les auteurs recevront une copie de fascicule correspondant à titre gratuit.

Adresse de la Rédaction de la Série:
Département de la Physique d'etat solide
de l'Université de Łódź
Pomorska 149/153, PL-90-236 Łódź, Pologne

Name and surname of the authors

TITLE – INSTRUCTION FOR AUTHORS SUBMITTING THE PAPERS FOR BULLETIN

Summary

Abstract should be written in clear and concise way, and should present all the main points of the paper. In particular, new results obtained, new approaches or methods applied, scientific significance of the paper and conclusions should be emphasized.

Keywords and phrases:

1. General information

The paper for BULLETIN DE LA SOCIÉTÉ DES SCIENCES ET DES LETTRES DE ŁÓDŹ should be written in LaTeX, preferably in LaTeX 2e, using the style (the file **bull.cls**).

2. How to prepare a manuscript

To prepare the LaTeX 2e source file of your paper, copy the template file **instruction.tex** with **Fig1.eps**, give the title of the paper, the authors with their affiliations/addresses, and go on with the body of the paper using all other means and commands of the standard class/style 'bull.cls'.

2.1. Example of a figure

Figures (including graphs and images) should be carefully prepared and submitted in electronic form (as separate files) in Encapsulated PostScript (EPS) format.

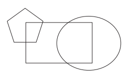

Fig. 1: The figure caption is located below the figure itself; it is automatically centered and should be typeset in small letters.

2.2. Example of a table

Tab. 1: The table caption is located above the table itself; it is automatically centered and should be typeset in small letters.

Description 1	Description 2	Description 3	Description 4
Row 1, Col 1	Row 1, Col 2	Row 1, Col 3	Row 1, Col 4
Row 2, Col 1	Row 2, Col 2	Row 2, Col 3	Row 2, Col 4

2.3. “Ghostwriting” and “guest authorship” are strictly forbiden

The printed version of an article is primary (comparing with the electronic version). Each contribution submitted is sent for evaluation to two independent referees before publishing.

3. How to submit a manuscript

Manuscripts have to be submitted in electronic form, preferably via e-mail as attachment files sent to the address **zofija@uni.lodz.pl**. If a whole manuscript exceeds 2 MB composed of more than one file, all parts of the manuscript, i.e. the text (including equations, tables, acknowledgements and references) and figures, should be ZIP-compressed to one file prior to transfer. If authors are unable to send their manuscript electronically, it should be provided on a disk (DOS format floppy or CD-ROM), containing the text and all electronic figures, and may be sent by regular mail to the address: **Department of Solid State Physics, University of Lodz, Bulletin de la Société des Sciences et des Lettres de Łódź, Pomorska 149/153, 90-236 Łódź, Poland**.

References

[1]

Affiliation/Address

TABLE DES MATIÈRES

Professor
Pierre Dolbeault
* 10.10.1924 † 12.06.2015

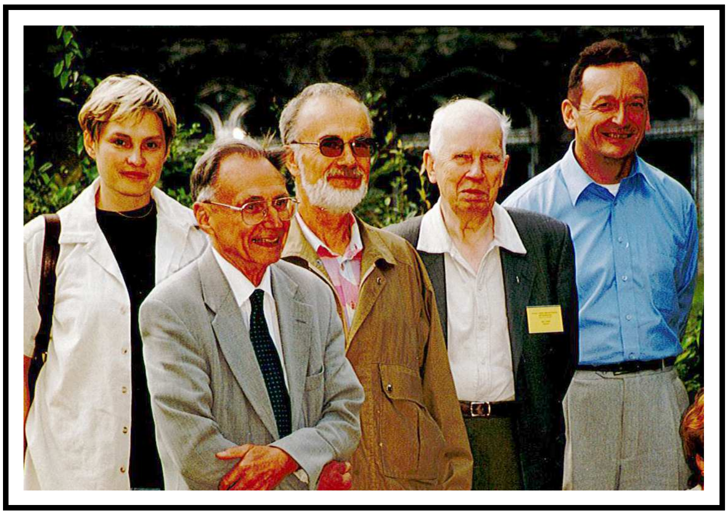

Professor Pierre Dolbeault among the participants
of the XIII International Conference on Analytic Functions at Będlewo, Poland, 2002

Cher ami Jean Dolbeault,

C'est avec une immense tristesse que nous venons d'apprendre le décès de notre cher collègue et ami, Professeur Pierre Dolbeault. Il était non seulement un chercheur impliqué et professionnel, mais essentiellement, nous nous souvenons de lui en tant qu'un vrai ami – gentil, cordial, avec la riche personnalité pleine d'empathie.

Nous allons manquer de ses conseils amicaux, et de son sens de l'humour qui a toujours enrichi nos discussions autour d'une tasse de café ou d'un verre du vin.

Nous prions pour Pierre et pour vous.

Nous espérons que vous recevrez la consolation chrétienne dans votre douleur et perte.

Dear Friend Jean Dolbeault,

It is with great pain and sorrow that we received your information about the death of our friend and colleague Professor Pierre Dolbeault.

He was not only an involved and highly professional researcher but, first of all, we remember Pierre as a true friend – kind, warm and of rich and empathic personality.

We will miss his friendly advice and his rich sense of humour, always enriching our informal talks over a cup of coffee or a glass of wine.

We pray for Pierre and for you.

We hope that you will receive Christian consolidation in your pain and loss.

PL ISSN 0459-6854

B U L L E T I N

DE LA SOCIÉTÉ DES SCIENCES ET DES LETTRES DE ŁÓDŹ

2015 Vol. LXV

Recherches sur les déformations no. 2

pp. 11–18

Katarzyna Lubnauer and Hanna Podsędkowska

CLONING AND ENTROPY IN VON NEUMANN ALGEBRAS

Summary

Under quantum measurement, the state of the system changes from the initial state into the final state. We investigate cloning property of final states of a quantum instrument associated with a minimal state entropy measurement.

Keywords and phrases: von Neumann algebra, entropy, cloning

Introduction

Cloning and broadcasting of quantum states have recently become important topics in Quantum Information Theory. Since its first appearance in [6,10] in the form of a no-cloning theorem it has been investigated in various settings, e.g. [1,3,7]. Another concept important from the point of quantum statistics is the state entropy. The definition we employ comes from Segal [9], and properties of entropy of measurement was presented in [8]. The entropy of the final state of the system after measurement is bounded and it attends its lower bound for the "minimal entropy measuremant". This paper presents results of reasearch on correlations between such measurement and possibility of broadcasting the final state.

1. Preliminaries and notation

Let $\mathcal{M}$ be an arbitrary von Neumann algebra with identity $\mathbb{1}$ acting on a Hilbert space $\mathcal{H}$. The predual $\mathcal{M}_*$ of $\mathcal{M}$ is a Banach space of all *normal*, i.e. continuous in the σ-weak topology linear functionals on $\mathcal{M}$.

A *state* on $\mathcal{M}$ is a bounded positive linear functional $\rho\colon \mathcal{M} \to \mathbb{C}$ of norm one. For a normal state ρ its *support*, denoted by $\mathrm{s}(\rho)$, is defined as the smallest projection in $\mathcal{M}$ such that $\rho(\mathrm{s}(\rho)) = \rho(\mathbb{1})$.

Let $\mathcal{A}$ and $\mathcal{B}$ be W^*-algebras. A linear map $T\colon \mathcal{A} \to \mathcal{B}$ is said to be *normal* if it is continuous in the σ-weak topologies on $\mathcal{A}$ and $\mathcal{B}$, respectively. It is called *unital* if it maps the identity of $\mathcal{A}$ to the identity of $\mathcal{B}$.

The map T is said to be *Schwarz* (or $1\frac{1}{2}$ *-positive* or *strongly positive*) if for each $a \in \mathcal{A}$ the following Schwarz inequality holds

$$T(a)^*T(a) \leqslant \|T\|T(a^*a),$$

which for a unital map amounts simply to

$$T(a)^*T(a) \leqslant T(a^*a).$$

2. Cloning and broadcasting

Let $\mathcal{M}$ be a von Neumann algebra. Consider now the tensor product $\mathcal{M}\overline{\otimes}\mathcal{M}$. We have obvious counterparts $\Pi_{1,2}\colon (\mathcal{M}\overline{\otimes}\mathcal{M})_* \to \mathcal{M}_*$ of the customary notion of partial trace, employed in the case $\mathcal{M} = \mathbb{B}(\mathcal{H})$, defined as

$$(\Pi_1\widetilde{\rho})(a) = \widetilde{\rho}(a \otimes \mathbb{1}),\ (\Pi_2\widetilde{\rho})(a) = \widetilde{\rho}(\mathbb{1} \otimes a),\ \widetilde{\rho} \in (\mathcal{M}\overline{\otimes}\mathcal{M})_*,\ a \in \mathcal{M}.$$

The main objects of our interest are the following two operations of *broadcasting* and *cloning* of states.

A linear map $K_*\colon \mathcal{M}_* \to (\mathcal{M}\overline{\otimes}\mathcal{M})_*$ sending states to states, and such that its dual $K\colon \mathcal{M}\overline{\otimes}\mathcal{M} \to \mathcal{M}$ is a unital Schwarz map will be called a *channel*. A state $\rho \in \mathcal{M}_*$ is *broadcast* by channel K_* if $(\Pi_i \circ K_*)(\rho) = \rho$, $i = 1, 2$; in other words, ρ is broadcast by K_* if for each $a \in \mathcal{M}$

$$\rho(K(a \otimes \mathbb{1})) = \rho(K(\mathbb{1} \otimes a)) = \rho(a).$$

A family of states is said to be *broadcastable* if there is a channel K_* that broadcasts each member of this family.

A state $\rho \in \mathcal{M}_*$ is *cloned* by channel K_* if $K_*\rho = \rho \otimes \rho$. A family of states is said to be *cloneable* if there is a channel K_* that clones each member of this family. An arbitrary family Γ of normal states on $\mathcal{M}$ is broadcastable if and only if there exists a family $\{\rho_i\}$ of normal states with pairwise orthogonal supports such that each $\rho \in \Gamma$ is a convex combination of ρ_i. Moreover the states ρ_i are clonable by some channel which also broadcasts the states in $\rho \in \Gamma$. This result was proved in [4].

3. Instruments in quantum measurement theory

An *instrument* on $(\Omega, \mathcal{F})$, a measurable space of values of an observable of the system, is a map

$$\mathcal{E}\colon \mathcal{F} \to \mathcal{L}^+(\mathcal{M}_*)$$

from the σ-field $\mathcal{F}$ into the set of all positive linear transformations on the predual $\mathcal{M}_*$ such that

(i) $(\mathcal{E}_\Omega \rho)(\mathbb{1}) = \rho(\mathbb{1})$ for all $\rho \in \mathcal{M}_*$,

(ii) $\mathcal{E}_{\bigcup_{n=1}^\infty \Delta_n} \rho = \sum_{n=1}^{\infty} \mathcal{E}_{\Delta_n} \rho$
for any $\rho \in \mathcal{M}_*$ and pairwise disjoint sets Δ_n from $\mathcal{F}$, where the series on the right hand side is convergent in the
$\sigma(\mathcal{M}_*, \mathcal{M})$-topology on $\mathcal{M}_*$.

Considering now for each $\mathcal{E}_\Delta$ its dual map $\mathcal{E}^*_\Delta \colon \mathcal{M} \to \mathcal{M}$ defined by

$$\rho(\mathcal{E}^*_\Delta(x)) = (\mathcal{E}_\Delta \rho)(x), \quad \rho \in \mathcal{M}_*,\ x \in \mathcal{M},$$

we come to the notion of *dual instrument* which is defined as a map $\mathcal{E}^* \colon \mathcal{F} \to \mathcal{L}^+_n(\mathcal{M})$ from $\mathcal{F}$ into the set of all positive normal linear transformations on $\mathcal{M}$ such that

(i*) $\mathcal{E}^*_\Omega(\mathbb{1}) = \mathbb{1}$,

(ii*) $\mathcal{E}^*_{\bigcup_{n=1}^\infty \Delta_n}(x) = \sum_{n=1}^{\infty} \mathcal{E}^*_{\Delta_n}(x)$
for any $x \in \mathcal{M}$ and pairwise disjoint sets Δ_n from $\mathcal{F}$, where the series on the right hand side is convergent in the $\sigma(\mathcal{M}, \mathcal{M}_*)$-topology on $\mathcal{M}$.

For a given instrument $\mathcal{E}$ its *associated observable* is defined as a map $e \colon \mathcal{F} \to \mathcal{M}$ by the formula

$$e(\Delta) = \mathcal{E}^*_\Delta(\mathbb{1}),$$

thus e is a positive operator-valued measure (POVM, semispectral measure). If $e(\Delta)$ is a projection for any Δ, then e is a projection-valued measure (PVM, spectral measure).

Among many important classes of instruments there are repeatable instruments which satisfy the celebrated von Neumann repeatability hypothesis: if the physical quantity is measured twice in succession in a system, then we get the same value each time. The definition of a *repeatable* instrument is a follows:

An instrument $\mathcal{E}$ is called *repeatable* if for any $\Delta_1, \Delta_2 \in \mathcal{F}$

$$\mathcal{E}_{\Delta_1} \mathcal{E}_{\Delta_2} = \mathcal{E}_{\Delta_1 \cap \Delta_2},$$

or equivalently

$$\mathcal{E}^*_{\Delta_1} \mathcal{E}^*_{\Delta_2} = \mathcal{E}^*_{\Delta_1 \cap \Delta_2}.$$

4. Entropy of measurements

Let $\mathcal{M}$ be a von Neumann algebra with normal finite faithful trace τ, $\tau(\mathbb{1}) = 1$. For any normal state ρ there exists a unique nonnegative selfadjoint operator D_ρ affiliated with $\mathcal{M}$, called *density* of ρ, such that for each $a \in \mathcal{M}$, we have

$$\rho(a) = \tau(aD_\rho).$$

In particular, if D_ρ is bounded, then $D_\rho \in \mathcal{M}$. The entropy of ρ, denoted by $H(\rho)$, is defined for bounded D_ρ as

$$H(\rho) = \tau(D_\rho log D_\rho)$$

that is, by spectral decomposition of the D_ρ, ($D_\rho = \int_0^\infty \lambda e(d\lambda)$),

$$H(\rho) = \int_0^\infty \lambda log\lambda \tau(e(d\lambda)),$$

in which $\tau(e(\cdot))$ is a measure defined as

$$\mathcal{B}(\mathbb{R}) \ni \Delta \mapsto \tau(e(\Delta)).$$

Theorem 1. *The entropy, as a function of a state, has the following properties*

(i) *Entropy is bounded from below and in particular it is nonnegative for a state:*

$$H(\rho) \geqslant \rho(\mathbb{1}) - 1.$$

(ii) *Since D_ρ is bounded thus the function $\lambda \mapsto \lambda log\lambda$ is bounded on its spectrum which yields that entropy is bounded from above.*

(iii) *For $\rho, \varphi \in \mathcal{M}_*$, with bounded densities D_ρ and D_φ respectively:*

$$H(\rho) + H(\varphi) \leqslant H(\rho + \varphi)$$

with equality if and only if $D_\rho D_\varphi = 0$

(iv) *Entropy is a convex function of ρ.*

The above theorem was discussed and proved in [8].

Let us consider now the measurement represented by an instrument $\mathcal{E}$. Let the system be in the initial state $\rho \in \mathcal{M}_*$. The final state of the system is $\mathcal{E}_\Omega \rho$. For any reading scale i.e.

$$\mathcal{R} = \{\Delta_i : i = 1, 2, \ldots, n;\ \ \Delta_i \cap \Delta_j = \emptyset,\ \bigcup_i \Delta_i = \Omega\}$$

we have

$$\mathcal{E}_\Omega \rho = \sum_{i=1}^n \mathcal{E}_{\Delta_i} \rho.$$

Considering only the non-zero summands, denote

$$\frac{\mathcal{E}_{\Delta_i}\rho}{(\mathcal{E}_{\Delta_i}\rho)(\mathbb{1})} = \rho_i, \qquad (\mathcal{E}_{\Delta_i}\rho)(\mathbb{1}) = \alpha_i;$$

ρ_i are normal states, moreover , $\alpha_i > 0$ and $\sum_{i=1}^n \alpha_i = 1$. We have the following theorem (proved in [8])

Theorem 2. *For every normal state ρ of the system such that $\mathcal{E}_\Omega\rho$ has bounded density the following equation holds:*

$$\sum_i H(\rho_i) + H((\alpha_i)) \leqslant H(\mathcal{E}_\Omega\rho) \leqslant \sum_i H(\rho_i) \tag{1}$$

where $H((\alpha_i))$ is the (minus) classical entropy of the sequence α_i:

$$H((\alpha_i)) = \sum_i \alpha_i \log \alpha_i.$$

The lower bound of (1) can be rewritten in the form

$$\sum_i H(\rho_i) + H((\alpha_i)) = \sum_i H(\alpha_i\rho_i) = \sum_i H(\mathcal{E}_{\Delta_i}\rho).$$

By the property (iii) of Theorem 1

$$\sum_i H(\mathcal{E}_{\Delta_i}\rho) = H(\sum_i \mathcal{E}_{\Delta_i}\rho) = H(\mathcal{E}_\Omega\rho)$$

if and only if $\mathcal{E}_{\Delta_i}\rho$, and consequently ρ_i, have orthogonal supports, and we have the following:

Corollary 1. *The lower bound of* (1) *is attained if and only if the family $(\rho_i)_i$ have orthogonal supports.*

We say that the measurement associated with instrument $\mathcal{E}$ is minimal state entropy one if for any initial state ρ and any reading scale $\mathcal{R}$ it attains the lower bound of (1).

The characterization of instruments given in [8] shows the equivalent conditions for minimal state entropy measurements. That is for instrument $\mathcal{E}$ having as its observable a spectral measure the following conditions are equivalent

(i) $\mathcal{E}^*_\Omega = (\mathcal{E}^*_\Omega)^2$ and $\mathcal{E}$ is a minimal state entropy

(ii) $\mathcal{E}$ is repeatable.

Theorem 3. *Let ρ be an arbitrary initial state of the system and $\mathcal{E}$ an instrument associated with a minimal state entropy measurement. For family of states $\Gamma = \{\rho_i : i \in \mathbb{N}\}$ with*

$$\rho_i = \frac{\mathcal{E}_{\Delta_i}\rho}{\mathcal{E}_{\Delta_i}\rho(\mathbb{1})}$$

where Δ_i is an arbitrary reading scale $\mathcal{R}$, there exist the channel K_* which clones the family Γ. Moreover, the final state of the system $\mathcal{E}_\Omega\rho$ is broadcast by the same channel K_*.

Proof. State $\mathcal{E}_\Omega\rho$ is a convex combination of states

$$\rho_i = \frac{\mathcal{E}_{\Delta_i}\rho}{\mathcal{E}_{\Delta_i}\rho(\mathbb{1})}$$

with coefficients $\alpha_i = \mathcal{E}_{\Delta_i}\rho(\mathbb{1})$. As the instruments $\mathcal{E}$ is associated with a minimal state entropy measurement, the states $\rho_i \in \Gamma$ have orthogonal supports. For such a family exists a channel K_* cloning each state ρ_i, $i = 1, 2, \dots$ and broadcasting the state

$$\mathcal{E}_\Omega \rho = \sum_i \alpha_i \rho_i.$$

□

It is worth noticing that the following theorem holds:

Theorem 4. *Each repeatable or even weakly repeatable instrument $\mathcal{E}$ (i.e. such that for all $\Delta_1, \Delta_2 \in \mathcal{F}$ $\mathcal{E}^*_{\Delta_1}(\mathcal{E}^*_{\Delta_2}(\mathbb{1})) = \mathcal{E}^*_{\Delta_1 \cap \Delta_1}(\mathbb{1})$ holds) transforms the initial state ρ to $\mathcal{E}_\Omega\rho$ broadcastable by the same channel K_* which clones the family*

$$\Gamma = \{\rho_i, i = 1, 2, \dots\}$$

Proof. Indeed, for a weakly repeatable instrument and any $\Delta, \Theta \in \mathcal{F}$ such that $\Delta \cap \Theta = \emptyset$ we have

$$\mathcal{E}^*_\Delta(s(\mathcal{E}^*_\Delta)e(\Theta)s(\mathcal{E}^*_\Delta)) = \mathcal{E}^*_\Delta(e(\Theta)) = \mathcal{E}^*_\Delta(\mathcal{E}^*_\Theta(\mathbb{1})) = 0$$

which yields

$$s(\mathcal{E}^*_\Delta)e(\Theta)s(\mathcal{E}^*_\Delta) = 0$$

and thus

$$s(\mathcal{E}^*_\Delta)e(\Theta) = 0.$$

From the weak repeatability of $\mathcal{E}$, it follows that

$$\mathcal{E}^*_\Theta(e(\Theta)) = e(\Theta) = \mathcal{E}^*_\Theta(\mathbb{1})$$

so

$$\mathcal{E}^*_\Theta(\mathbb{1} - e(\Theta)) = 0$$

and

$$s(\mathcal{E}^*_\Theta)(\mathbb{1} - e(\Theta))s(\mathcal{E}^*_\Theta) = 0$$

then we have

$$s(\mathcal{E}^*_\Theta) = e(\Theta)s(\mathcal{E}^*_\Theta)$$

and finally

$$s(\mathcal{E}^*_\Delta)s(\mathcal{E}^*_\Theta) = s(\mathcal{E}^*_\Delta)e(\Theta)s(\mathcal{E}^*_\Theta) = 0.$$

Let us also notice that for $\rho_i = \frac{\mathcal{E}_{\Delta_i}\rho}{\mathcal{E}_{\Delta_i}\rho(\mathbb{1})}$

$$\mathcal{E}_{\Delta_i}\rho_i = \frac{\mathcal{E}_{\Delta_i}(\mathcal{E}_{\Delta_i}\rho)}{\mathcal{E}_{\Delta_i}\rho(\mathbb{1})} = \frac{\mathcal{E}_{\Delta_i}\rho}{\mathcal{E}_{\Delta_i}\rho(\mathbb{1})} = \rho_i$$

and

$$\rho_i(s(\mathcal{E}^*_{\Delta_i})) = \mathcal{E}_{\Delta_i}\rho_i(s(\mathcal{E}^*_{\Delta_i})) = \rho_i(\mathcal{E}^*_{\Delta_i}(s(\mathcal{E}^*_{\Delta_i}))) =$$
$$= \rho_i(\mathcal{E}^*_{\Delta_i}(\mathbb{1})) = \mathcal{E}_{\Delta_i}\rho_i(\mathbb{1}) = \mathbb{1} = \rho_i(\mathbb{1})$$

and we have

$$s(\rho_i) \subset s(\mathcal{E}^*_{\Delta_i}).$$

The orthogonality of the supports of $\mathcal{E}^*_{\Delta_i}$'s implies orthogonality of $s(\rho_i)$'s. According to [4, Theorem 4.3] there exists a channel K_* which clones the family $\Gamma = \{\rho_i\}\ \ i \in I$ and broadcas the final state $\mathcal{E}_\Omega = \sum_i \alpha_i \rho_i$ where $\alpha_i = \mathcal{E}_{\Delta_i}\rho_i(\mathbb{1})$. □

Corollary 2. *For a minimal state entropy measurement (associated with an instrument $\mathcal{E}$) the channel which clones family of states $\Gamma = \{\rho_i, i = 1, 2, \dots\}$ and broadcasts final state $\mathcal{E}_\Omega\rho$ is given by the formula*

$$K_*(\varphi) = \sum_i \varphi(s(\mathcal{E}^*_{\Delta_i}))\frac{\mathcal{E}_{\Delta_i}\rho}{\mathcal{E}_{\Delta_i}\rho(\mathbb{1})} \otimes \frac{\mathcal{E}_{\Delta_i}\rho}{\mathcal{E}_{\Delta_i}\rho(\mathbb{1})}.$$

Proof.

Let denote $\rho_i = \frac{\mathcal{E}_{\Delta_i}\rho}{\mathcal{E}_{\Delta_i}\rho(\mathbb{1})}$.

$$K_*(\rho_j) = \sum_i \rho_j(s(\mathcal{E}^*_{\Delta_i}))\frac{\mathcal{E}_{\Delta_i}\rho}{\mathcal{E}_{\Delta_i}\rho(\mathbb{1})} \otimes \frac{\mathcal{E}_{\Delta_i}\rho}{\mathcal{E}_{\Delta_i}\rho(\mathbb{1})}.$$

Observe that

$$\rho_j(s(\mathcal{E}^*_{\Delta_i})) = \begin{cases} 0 & \text{for } i \neq j \\ 1 & \text{for } i = j \end{cases}$$

thus $K(\rho_j) = \rho_j \otimes \rho_j$. Moreover,

$$\begin{aligned} K_*(\mathcal{E}_\Omega\rho) &= \textstyle\sum_i \mathcal{E}_\Omega\rho(s(\mathcal{E}^*_{\Delta_i}))\rho_i \otimes \rho_i = \sum_i \sum_j \mathcal{E}_{\Delta_i}\rho(s(\mathcal{E}^*_{\Delta_i}))\rho_i \otimes \rho_i \\ &= \textstyle\sum_i \sum_j \rho(\mathcal{E}^*_{\Delta_j} s(\mathcal{E}^*_{\Delta_i}))\rho_i \otimes \rho_i = \sum_i \rho(\mathcal{E}^*_{\Delta_i} s(\mathcal{E}^*_{\Delta_i}))\rho_i \otimes \rho_i \\ &= \textstyle\sum_i \rho(\mathcal{E}^*_{\Delta_i}(\mathbb{1}))\rho_i \otimes \rho_i = \sum_i \mathcal{E}_{\Delta_i}\rho(\mathbb{1})\rho_i \otimes \rho_i \end{aligned}$$

and

$$\Pi_i(K_*(\mathcal{E}_\Omega\rho)) = \sum_i \mathcal{E}_{\Delta_i}\rho(\mathbb{1})\rho_i = \sum_i \mathcal{E}_{\Delta_i}\rho = \mathcal{E}_\Omega\rho.$$

□

References

[1] H. Barnum, J. Barrett, M. Leifer, and A. Wilce, *Generalized no-broadcasting theorem*, Phys. Rev. Lett. **99** (2007), 240501.

[2] H. Barnum, C. M. Caves, C. A. Fuchs, R. Jozsa, and B. Schumacher, *Noncommuting mixed states cannot be broadcast* Phys. Rev. Lett. **76**(15) (1996), 2818–2821.

[3] D. Dieks, *Communication by EPR devices*, Phys. Lett. A **92**(6) (1982), 271–272.

[4] K. Kaniowski, K. Lubnauer, and A. Łuczak, *Cloning and broadcasting in von Neumann algebras*, doi: 10.1093/qmath/hau028, Quart. J. Math.

[5] K. Kaniowski, K. Lubnauer, and A. Łuczak, *Cloning in C^*-algebras*, preprint.

[6] G. Lindblad, *A general no-cloning theorem*, Lett. Math. Phys. **47** (1999), 189–196.

[7] A. Łuczak, *Cloning by positive maps in von Neumann algebras*, Positivity. **19** (2015), 317–332.

[8] H. Podsędkowska, *Entropy of Quantum Measurement*, Entropy (2015), DOI:10.33.90/e17031181.

[9] I. E. Segal, *A note on the concept of entropy*, J. Math. Mech. **9(4)** (1960), 623–629.

[10] W. K. Wooters, and W. H. Zurek, *A single quantum state cannot be cloned*, Nature **299** (1982), 802.

Faculty of Mathematics and Computer Science
University of Łódź
Banacha 22, PL-90-238 Łódź
Poland
e-mail: lubnauer@math.uni.lodz.pl
hpodsedk@math.uni.lodz.pl

Presented by Andrzej Łuczak at the Session of the Mathematical-Physical Commission of the Łódź Society of Sciences and Arts on November 30, 2015

KLONOWANIE I ENTROPIA W ALGEBRACH VON NEUMANNA

S t r e s z c z e n i e

Klonowanie stanów kwantowych oraz badanie ich entropii to dwa ważne aspekty teorii informacji kwantowej.

W pracy wykorzystana została definicja entropii stanu kwantowego, reprezentowanego przez element preduala algebry von Neumanna, zaczerpnięta od Segala. Przedstawione zostały również własności entropii jako funkcji stanu.

Podczas pomiaru, stan początkowy systemu kwantowego ulega przekształceniu. Jeżeli pomiar jest reprezentowany przez instrument powtarzalny będący jednocześnie odwzorowaniem idempotentnym, wówczas entropia stanu końcowego osiąga najmniejszą wartość, a pomiar nazywamy "pomiarem o minimalnej entropii stanu".

Z każdym stanem końcowym związana jest rodzina stanów zdeterminowana przez tzw. skalę odczytu pomiaru. Jeżeli pomiar jest pomiarem o minimalnej entropii stanu, wówczas dla dowolnej skali odczytu istnieje kanał "brodcastujący" stan końcowy i jednocześnie klonujący rodzinę stanów zdeterminowaną przez tę skalę odczytu.

Słowa kluczowe: algebra von Neumanna, entropia, klonowanie

PL ISSN 0459-6854

B U L L E T I N

DE LA SOCIÉTÉ DES SCIENCES ET DES LETTRES DE ŁÓDŹ

2015 Vol. LXV

Recherches sur les déformations no. 2

pp. 19–25

Marek Bienias and Filip Strobin

SPACEABILITY OF THE SET OF CONTINUOUS LINEAR INJECTIONS FROM ℓ_p TO ℓ_p WITH NOWHERE CONTINUOUS INVERSES

Summary

Let $1 \leq p < \infty$. We show that, in the Banach space of all bounded linear operators from ℓ_p to ℓ_p, the subset consisting of all injections with nowhere continuous inverses, is isometrically ℓ_p-spaceable, i.e., it contains an isometric copy of ℓ_p. The proof uses the ideas from a recent paper of M. Balcerzak and F. Strobin, in which a similar result (in particular, without linearity) was proved, and from a recent paper of S. Creswell where one example of such a mapping was given.

We also show how to modify the proof of mentioned result of M. Balcerzak and F. Strobin to get a relatively more natural version of it.

Keywords and phrases: spaceability, special continuous mappings, ℓ_p-spaces, bounded linear operators

1. Introduction

In the last decade a new notion of largeness has become very popular. Namely, one can call a set **big** whenever it contains an algebraic structure inside - like a vector space, a closed vector space, an algebra etc. (For a comprehensive description of these concepts we refer the reader for example to the survey papers [8, 9].)

For our purposes we need to recall the notion of spaceability, that firstly appeared in the works of R. Aron, A. Bartoszewicz, S. Głąb, V. Gurariy, D. Pérez-García and J. B. Seoane-Sepúlveda (see [4–7])

Definition 1. Let X be a Banach space and a set $A \subseteq X$. We say that A is **spaceable** if $A \cup \{0\}$ contains an infinite dimensional closed vector subspace. Moreover, if $A \cup$

$\{0\}$ contains an isometric copy of some Banach space V then we say that A is **isometrically V-spaceable**.

Having $1 \leq p < \infty$ and a field $\mathbb{K} \in \{\mathbb{R}, \mathbb{C}\}$, by $\ell_p^{\mathbb{K}}$ we denote the space of sequences of elements from $\mathbb{K}$, summable with the p^{th} power (with respect to the absolute value of coefficients). An element $x \in \ell_p^{\mathbb{K}}$ will denote a sequence $x = (x_n)_{n\in\mathbb{N}}$. The standard norm in $\ell_p^{\mathbb{K}}$ will be denoted by the symbol $\|\cdot\|_p$ and for $n \in \mathbb{N}$, e_n will denote the sequence $(0, ..., 0, 1, 0, ...)$ where 1 occurs on the n^{th} coordinate only. Moreover, $B(\ell_p^{\mathbb{K}}, \ell_p^{\mathbb{K}})$ stands for the Banach space of all continuous linear operators from $\ell_p^{\mathbb{K}}$ to $\ell_p^{\mathbb{K}}$ equipped with the standard operator norm, and $Cb(B_{\ell_p^{\mathbb{K}}}, \ell_p^{\mathbb{K}})$ stands for the Banach space of all continuous **bounded** mappings (not necessarily linear) on the open unit ball $B_{\ell_p^{\mathbb{K}}} \subseteq \ell_p^{\mathbb{K}}$ to $\ell_p^{\mathbb{K}}$, equipped with the supremum norm.

S. Creswell [2] described a continuous bijection T from $\ell_2^{\mathbb{R}}$ onto a subset of $\ell_2^{\mathbb{R}}$ such that its inverse T^{-1} is discontinuous everywhere. In the paper [1] this example (modified a bit) was exploit to prove the following:

Theorem 1. *Let $1 < p < \infty$ and $W \subseteq Cb(B_{\ell_p^{\mathbb{R}}}, \ell_p^{\mathbb{R}})$ be a set of all injections with nowhere continuous inverses. The set W is isometrically $\ell_p^{\mathbb{R}}$-spaceable.*

In the Section 2 we show how to modify the original proof from [1] to get analogous (to the one from [1]) result, but for mappings defined on a **closed** unit ball $\overline{B}_{\ell_p^{\mathbb{R}}}$ (as was pointed out by Z. Lipecki during seminar in Wrocław Univeristy of Technology, such a result for the closed unit ball seems to be more natural). Namely, our goal is to modify the proof (from [1]) of Theorem 1 to get the following result (we equip the space $Cb(\overline{B}_{\ell_p^{\mathbb{R}}}, \ell_p^{\mathbb{R}})$ of bounded continuous mappings from $\overline{B}_{\ell_p^{\mathbb{R}}}$ to ℓ_p also with the supremum norm):

Theorem 2. *Let $1 < p < \infty$ and $W \subseteq Cb(\overline{B}_{\ell_p^{\mathbb{R}}}, \ell_p^{\mathbb{R}})$ be a set of all injections with nowhere continuous inverses. The set W is isometrically $\ell_p^{\mathbb{R}}$-spaceable.*

Moreover, in the Section 3, we use another S. Creswell's example ([3]) to obtain related, but essentially different result. Namely, we prove that for $1 \leq p < \infty$ (so we allow $p = 1$) and $\mathbb{K} \in \{\mathbb{R}, \mathbb{C}\}$, the set of all continuous **linear** injections from $\ell_p^{\mathbb{K}}$ to $\ell_p^{\mathbb{K}}$ is isometrically $\ell_p^{\mathbb{K}}$-spaceable in the space $B(\ell_p^{\mathbb{K}}, \ell_p^{\mathbb{K}})$.

2. Proof of Theorem 2

In this section we show how to modify original proof of Theorem 1 to get a proof Theorem 2. For simplicity, in this section we write ℓ_p instead of $\ell_p^{\mathbb{R}}$.

Proof. (of Theorem 2) We start in a similar way as in the proof of Theorem 1 in [1]. Let $(A_k)_{k\in\mathbb{N}}$ be a decomposition of $\mathbb{N}$ (i.e. sequence of pairwise disjoint sets that covers $\mathbb{N}$) into infinite sets. For $k \in \mathbb{N}$ let $\sigma_k : A_k \to \mathbb{N}$ be a bijection. For $t \in \ell_p$ and $x \in \ell_p$ let us define a sequence $\big((F_t(x))_j\big)_{j\in\mathbb{N}}$ by the formula:

$$(F_t(x))_j := t_k s^+(x_{\sigma_k(j)})|x_{\sigma_k(j)}|^p$$

for all $j \in \mathbb{N}$, where k is such that $j \in A_k$, and $s^+ : \mathbb{R} \to \{-1, 1\}$ is the sign function.

In the same way as in the proof of Theorem 1 in [1], we can see that the mapping $\overline{B}_p \ni t \to F_t \in Cb(\overline{B}_p, \ell_p)$ is an isometry. It remains to show that for any $t \in \ell_p \setminus \{0\}$, $h := F_t \in W''$. We only focus on showing that h^{-1} is discontinuous everywhere in $h[\overline{B}_{\ell_p}]$.

So we fix $y \in h[\overline{B}_{\ell_p}]$, and take $x \in \overline{B}_{\ell_p}$ such $h(x) = y$. If $x \in B_{\ell_p}$ (i.e., $\|x\|_p < 1$), then we proceed exactly as in [1].

Hence assume that $\|x\|_p = 1$, and take $i_0 \in \mathbb{N}$ such that $x_{i_0} \neq 0$.

Now take $r \in \mathbb{N}$ so that $t_r \neq 0$ (recall that $t = (t_i) \neq 0$) and choose any $\delta > 0$. We can find $c, \eta > 0$ such that

$$|t_r|^{-1} \left(\sum_{j \in A_r} |y_j| + c - \eta \right) \leq 1 \tag{1}$$

$$\frac{\eta \|t\|_p}{|t_r|} < \delta \tag{2}$$

$$\eta < |y_{\sigma_r^{-1}(i_0)}| \tag{3}$$

Note that (1) is a counterpart of [1, condition (4)]. Such a c, η can be taken because $\|x\|_p \leq 1$ and $y_{\sigma_r^{-1}(i_0)} \neq 0$ (since $x_{i_0} \neq 0$ - see [1, condition (3)]).
By (2) we can take $n \in \mathbb{N}$ such that

$$|t_r|^{-p} \|t\|_p^p \left(\frac{c^p}{n^{p-1}} + \eta^p \right) < \delta^p \tag{4}$$

(note that it is a counterpart of [1, condition (5)]).
Then we proceed as in original proof of Theorem 1, with the change that we have to assure that, additionally, $j_1, ..., j_n \neq \sigma_r^{-1}(i_0)$. Then we define $v = (v_i)$ as in [1], but with additional condition:

$$v_{i_0} = s^+(t_r) s^+(y_{\sigma_r^{-1}(i_0)}) |t_r|^{-\frac{1}{p}} \left| y_{\sigma_r^{-1}(i_0)} - s^+(y_{\sigma_r^{-1}(i_0)}) \cdot \eta \right|^{\frac{1}{p}} \tag{5}$$

Then by (1) we have

$$\begin{aligned} \|v\|_p^p &= |t_r|^{-1} \left(\sum_{j \in A_r \setminus \{j_1, \dots, j_n, \sigma_r^{-1}(i_0)\}} |y_j| + \sum_{j \in \{j_1, \dots, j_n\}} \left| |y_j| + \frac{c}{n} \right| + \left(|y_{\sigma_r^{-1}(i_0)}| - \eta \right) \right) \\ &\leq |t_r|^{-1} \left(\sum_{j \in A_r} |y_j| + c - \eta \right) \leq 1, \end{aligned}$$

so $v \in \overline{B}_p$. Now setting $z := h(v)$, we have (proceeding similarly as in [1] and omitting one coefficient)

$$\|h^{-1}(z) - h^{-1}(y)\|_p > |t_r|^{-1} \frac{c}{2}$$

and for every $k \in \mathbb{N}$, following similar lines as in [1] and by (3), we have:

$$\sum_{j\in A_k} |y_j - z_j|^p = ... = |t_k|^p |t_r|^{-p} \sum_{j\in A_r} |y_j - z_j|^p = |t_k|^p |t_r|^{-p} \left(\frac{c^p}{n^{p-1}} + \eta^p \right)$$

(note that $z_{\sigma_r^{-1}(i_0)} = y_{\sigma_r^{-1}(i_0)} - s^+(y_{\sigma_r^{-1}(i_0)}) \cdot \eta)$. The above, together with (4), give us

$$\|z-y\|_p^p = \sum_{k\in\mathbb{N}} \left(\sum_{j\in A_k} |z_j - y_j|^p \right) = |t_r|^{-p} \left(\frac{c^p}{n^{p-1}} + \eta^p \right) ||t||_p^p < \delta^p$$

All in all, we proved the discontinuity of h^{-1} (for $\varepsilon := |t_r|^{-1}\frac{c}{2}$). □

Remark 3. It is worth to note that in the above proof it was more important that $\|x\|_p > 0$ rather than $\|x\|_p = 1$, since the fact that we were able to take $x_{i_0} \neq 0$ played some role.

3. Linear S. Creswell's example and ℓ_p-spaceability

Let us start with recalling the mentioned in the Introduction example of S. Creswell (see [3]; note that S. Creswell considered only the space $\ell_2^{\mathbb{R}}$, but his argument work withs a general case). Let $1 \leq p < \infty$, $\mathbb{K} \in \{\mathbb{R}, \mathbb{C}\}$, and let the mapping $T : \ell_p^{\mathbb{K}} \to \ell_p^{\mathbb{K}}$ be given by

$$T(x) := \left(x_1, \frac{x_2}{2}, \frac{x_3}{3}, ...\right) = \left(\frac{x_i}{i}\right)_{i\in\mathbb{N}}$$

for $x \in \ell_p^{\mathbb{K}}$. It is easy to see that T is linear, injective and that its inverse $T^{-1} : T[\ell_p^{\mathbb{K}}] \to \ell_p^{\mathbb{K}}$ is given by

$$T^{-1}(y) = (iy_i)_{i\in\mathbb{N}} \qquad \text{for} \qquad y \in T[\ell_p^{\mathbb{K}}].$$

Observe that:

$$\|T\| = \sup\{\|T(x)\|_p : \|x\|_p \leq 1\} = 1 \tag{6}$$

and T^{-1} is discontinuous everywhere, that means (since T^{-1} is linear):

$$\sup\{\|T^{-1}(y)\|_p : y \in T[\ell_p^{\mathbb{K}}],\ \|y\|_p \leq 1\} = \infty \tag{7}$$

To see (6), take $x \in \ell_p^{\mathbb{K}}$ with $\|x\|_p \leq 1$. Then

$$\|T(x)\|_p = \left(\sum_{i\in\mathbb{N}} \left(\frac{|x_i|}{i} \right)^p \right)^{\frac{1}{p}} \leq \left(\sum_{i\in\mathbb{N}} |x_i|^p \right)^{\frac{1}{p}} \leq 1$$

Moreover, $\|T(e_1)\|_p = 1$, so we have (6). Now fix $n \in \mathbb{N}$ and consider $e_n \in T[\ell_p^{\mathbb{K}}]$. Since $\|e_n\|_p = 1$ and $\|T^{-1}(e_n)\|_p = n$, we get (7).

The main result of this section is the following:

Theorem 4. *Let $1 \leq p < \infty$, and $W \subseteq B(\ell_p^{\mathbb{K}}, \ell_p^{\mathbb{K}})$ be a set of all injections with nowhere continuous inverses. The set W is isometrically $\ell_p^{\mathbb{K}}$-spaceable.*

Proof. We will write ℓ_p instead of $\ell_p^{\mathbb{K}}$. Let $(A_k)_{k\in\mathbb{N}}$ be, again, a decomposition of $\mathbb{N}$ into infinite sets and, for $k \in \mathbb{N}$, let $\sigma_k : A_k \to \mathbb{N}$ be a bijection. For $t \in \ell_p$ and $x \in \ell_p$ let us define a sequence $\big((F_t(x))_j\big)_{j\in\mathbb{N}}$ by the formula:

$$(F_t(x))_j = t_k \frac{1}{\sigma_k(j)} x_{\sigma_k(j)}$$

for $j \in \mathbb{N}$, where $k \in \mathbb{N}$ is such that $j \in A_k$. It is easy to see that for fixed $t \in \ell_p$, the mapping $\ell_p \ni x \mapsto F_t(x) \in \mathbb{K}^{\mathbb{N}}$ is linear. Moreover, for any $x \in \ell_p$ we have that

$$\begin{aligned}\left(\sum_{k\in\mathbb{N}}\sum_{j\in\mathbb{N}} |t_k \frac{1}{\sigma_k(j)} x_{\sigma_k(j)}|^p\right)^{\frac{1}{p}} &= \left(\sum_{k\in\mathbb{N}} |t_k|^p \sum_{j\in\mathbb{N}} |\frac{1}{j} x_j|^p\right)^{\frac{1}{p}} \\ &= \|t\|_p \cdot \|T(x)\|_p \le \|t\|_p \cdot \|T\| \cdot \|x\|_p \end{aligned} \tag{8}$$

where T is the Creswell's operator recalled at the beginning of this section. Hence, by (6) we have that $F_t(x) \in \ell_p$. Moreover, also by (8) and (6), $F_t : \ell_p \to \ell_p$ is continuous and

$$\begin{aligned}\|F_t\| &= \sup\{\|F_t(x)\|_p : \|x\|_p \le 1\} = \sup\{\|t\|_p \cdot \|T(x)\|_p : \|x\|_p \le 1\} \\ &= \|t\|_p \cdot \|T\| = \|t\|_p.\end{aligned}$$

The above calculations show that $\ell_p \ni t \overset{F}{\mapsto} F_t \in B(\ell_p, \ell_p)$ is an isometry.

Now, to finish the proof, it is enough to show that every element of $F[\ell_p] \setminus \{0\}$ has an everywhere discontinuous inverse. Let $t \in \ell_p$ be such that $F_t \in F[\ell_p] \setminus \{0\}$. Then clearly $t \neq 0$. By linearity of F_t^{-1} it is sufficient to prove that

$$\sup\{\|F_t^{-1}(y)\|_p : y \in F_t[\ell_p], \|y\|_p \le 1\} = \infty$$

or, equivalently, that for every $n \in \mathbb{N}$ there is $y^n \in F_t[\ell_p]$ with $\|y^n\|_p \le 1$ and

$$\|F_t^{-1}(y^n)\|_p \ge \frac{n}{\|t\|_p}.$$

Let $n \in \mathbb{N}$ and define $y^n \in \ell_p$ by the formula:

$$y_i^n = \begin{cases} \frac{t_k}{\|t\|_p}, \text{ when } \sigma_k(i) = n \text{ for } k \in \mathbb{N} \\ 0, \text{ elsewhere.} \end{cases}$$

Observe that

$$\|y^n\|_p = 1 \qquad \text{and} \qquad F_t\left(\frac{ne_n}{\|t\|_p}\right) = y^n,$$

hence

$$\|F_t^{-1}(y^n)\|_p = \frac{n}{\|t\|_p}.$$

To sum up, $F : \ell_p \to W \cup \{0\}$ is isometric embedding, hence W is ℓ_p-spaceable. $\square$

Remark 5. Observe that the family of all restrictions $F_{|\overline{B}_p}$, $F \in B(\ell_p, \ell_p)$, is a subspace of $Cb(\overline{B}_p, \ell_p)$ (the norms coincide), so there might be an attempt to deduce Theorem 2 directly from Theorem 4. However, it is not true that if $F : X \to Y$ is an injection such that F^{-1} is everywhere discontinuous, then also every restriction $F_{|A}$ has this property. Also, the proof of discontinuity of F_t^{-1} in Theorem 4 used strongly the fact that a family of elements $\frac{ne_n}{\|t\|}$ is unbounded.

Let us also mention that the above proof of Theorem 4 is shorter and less technically complicated than the proofs of Theorems 1 and 2, despite the fact that its range is wider (the complex case and $p = 1$). The reason is that the Creswell's operator T used here is nicer than the one used in the proofs of the latter theorems.

References

[1] M. Balcerzak and F. Strobin, *Spaceability of the set of continuous injections from B_{ℓ_p} into ℓ_p with nowhere continuous inverses*, Linear Algebra Appl. **450**, no. 1 (2014), 76–82.

[2] S. H. Creswell, *A continuous bijection from ℓ_2 onto a subset of ℓ_2 whose inverse is everywhere discontinuous*, Amer. Math. Monthly **117** (2010), 823–828.

[3] S. H. Creswell, *A continuous linear bijection from ℓ_2 onto a dense subset of ℓ_2 whose inverse is everywhere unboundedly discontinuous*, Missouri J. Math. Sci. **25**, no. 2 (2013), 213-214.

[4] R. M. Aron, V. I. Gurariy, and J. B. Seoane-Sepúlveda, Lineability and spaceability of sets of functions on $\mathbb{R}$, Proc. Amer. Math. Soc. **133**, no. 3 (2005), 795–803.

[5] R. M. Aron, D. Pérez-García, and J. B. Seoane-Sepúlveda, Algebrability of the set of non-convergent Fourier series, Studia Math. **175**, no. 1 (2006), 83–90.

[6] R. M. Aron and J. B. Seoane-Sepúlveda, Algebrability of the set of everywhere surjective functions on $\mathbb{C}$, Bull. Belg. Math. Soc. Simon Stevin **14**, no. 1 (2007), 25–31.

[7] A. Bartoszewicz and S. Głąb, Strong algebrability of sets of sequences and functions, Proc. Amer. Math. Soc. **141** (2013), 827–835.

[8] A. Bartoszewicz, M. Bienias, and S. Głąb, Lineability, algebrability and strong algebrability of some sets in $\mathbb{R}^{\mathbb{R}}$ and $\mathbb{C}^{\mathbb{C}}$, Traditional and present-day topics in real analysis, Faculty of Mathematics and Computer Science, University of Łódź, Łódź 2013, 213–232.

[9] L. Bernal-González, D. Pellegrino, and J. B. Seoane-Sepúlveda, Linear subsets of nonlinear sets in topological vector spaces. Bull. Amer. Math. Soc. (N. S.) **51**, no. 1 (2014), 71–130.

Institute of Mathematics
Łódź University of Technology
Wólczańska 215, PL-93-005 Łódź
Poland
e-mail: marek.bienias@p.lodz.pl
filip.strobin@p.lodz.pl

Presented by Władysław Wilczyński at the Session of the Mathematical-Physical Commission of the Łódź Society of Sciences and Arts on November 30, 2015

DOMKNIĘTA LINIOWALNOŚĆ ZBIORU CIĄGŁYCH LINIOWYCH INJEKCJI Z ℓ_p W ℓ_p O NIGDZIE-CIĄGŁYCH ODWROTNOŚCIACH

S t r e s z c z e n i e

Niech $p \in [1, \infty)$. W pracy pokazujemy, że w przestrzeni Banacha wszystkich operatorów liniowych ograniczonych z ℓ_p w ℓ_p, podzbiór operatorów różnowartościowych o nigdzie-ciągłych odwrotnościach, jest izometrycznie ℓ_p-domknięto liniowalny, czyli zawiera (wraz z zerem) izometryczną kopię przestrzeni ℓ_p. Dowód wykorzystuje pewne idee z wcześniejszej pracy M. Balcerzaka i F. Strobina, w której podobny wynik (w szczególności jednak bez założenia liniowości) został udowodniony, oraz niedawnej pracy S. Creswella, gdzie jeden konkretny przykład takiej funkcji został podany.

W pracy pokazujemy też w jaki sposób zmodyfikować dowód twierdzenia ze wspomnianej pracy M. Balcerzaka i F. Strobina aby uzyskać w pewnym sensie bardziej naturalną jego wersję.

Słowa kluczowe: domknięta liniowalność, szczególne funkcje ciągłe, przestrzenie ℓ_p, operatory liniowe ograniczone

PL ISSN 0459-6854

B U L L E T I N

DE LA SOCIÉTÉ DES SCIENCES ET DES LETTRES DE ŁÓDŹ

2015 Vol. LXV

Recherches sur les déformations no. 2

pp. 27–46

Julian Ławrynowicz, Małgorzata Nowak-Kępczyk, Anna Valianti, and Mariusz Zubert

PHYSICS OF COMPLEX ALLOYS – ONE DIMENSIONAL RELAXATION PROBLEM AND THE ROLE OF TOTAL ENERGY CALCULATION

Summary

We start with a brief description of an approach to physics of complex materials, in particular alloys, coming back to R. Kikuchi (1951). Then some algebras important when studying the stochastical relaxation problems are recalled as well as the background algebras involved in linearization of the initial second order differential equations, with help of the Cayley-Dickson process. Then (Sections 4 and 5) the four and two-sheeted Riemann-surface approach to the algebras in question is reported (the original content of this section is entirely due to the second-named author). In Section 4 we consider algebras with four and eight generators; in Section 5 with 9 and 18 generators – in addition this includes bridging of the related scales. Next an analysis of linearization of the one-dimensional stochastical relaxation problem is given together with a numerical procedure for calculating the six fundamental solutions. Three examples are attached for solving effectively the related boundary value problem. Finally two kinds of conclusions are given: concerning lines of forces and equipotential lines, and concerning physical and non-physical fundamental solutions. In addition, an example of calculation of total energy of an alloy is given.

Keywords and phrases: complex material, relaxation problem, nonlinear parabolic equation, para-quaternions

1. Introduction: an approach to physics of complex materials

Physics of complex materials is now of basic interest in physics and technology including, in particular, crystalline solidification [25–12]. In his theory of cooperative phenomena, Kikuchi [3] approximated a complex crystallographic structure with help

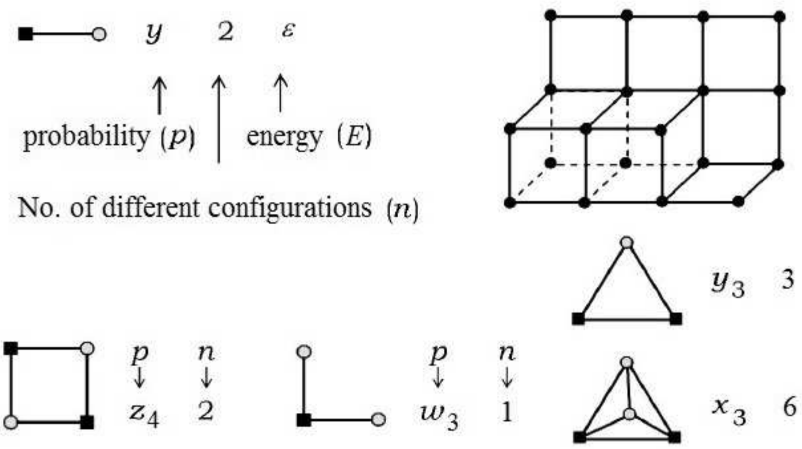

Fig. 1: Some basic configurations of pairs, triples and quadruples of neighbouring atoms in a binary alloy according to R. Kikuchi.

of different configurations like lattice edges, pairs of edges, triangles, squares, and regular pyramids (Fig. 1) which, in particular, gives rise for total energy calculations. Following this idea, Castillo Alvarado and two of us [1] constructed fractal modelling of alloys. In the case of an AB_3 binary alloy of fcc lattice and (111) surface orientation the first embranchment is shown in Fig. 2, where α- and β-vacancies are replaced by α- and β-sites respectively. Actually our Fig. 2 is an example of introducing some complexity: α- and β-vacancies because the AB_3 binary alloy of [1] has to be treated as a quaternary alloy.

Besides, owing to thermal dependence of vacancies, they are more dense close to the surfaces, so the fractal structure fails. In addition we may treat the AB_3-binary alloy with α- and β-vacancies as a quaternary alloy. Two of us were already treating the topic with help of decomposition of the staff to triangles or rectangles [14, 12]. Moreover, they inverted a method of replacing the description of quaternary alloy by description of ternary alloys and the description of ternary alloy by description of binary alloys [15] (cf. Figs 3, 4). On the level of linearization and Cayley-Dickson process this involves Clifford-Grassmann algebras with quaternions and para-quaternions for the background [27, 24, 6–8]. In connection with a four-and two-sheeted Riemann-surface approach, in analogy to Tamm's lectures on electromagnetism [32, 33, 9, 5] our description comes back to Sylvester [30, 31] and Peirce [26], and includes bridging of the related scales. Conclusions, following examples, for solving effectively the related boundary value problem, concern lines of force and equipotential lines, and discussion which fundamental solutions are physical. Also, an example of total energy calculation in an alloy is given.

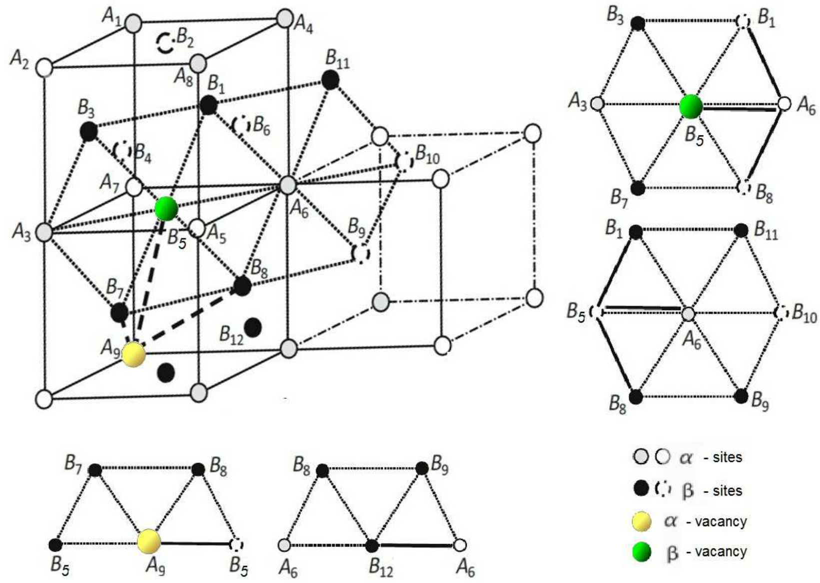

Fig. 2: AB_3 binary alloy with two types α β of vacancies of fcc lattice and (111) surface orientation.

2. Algebras important when studying the stochastical relaxation problem

For studying the one-dimensional stochastical relaxation problem related with the second order parabolic differential equation of the second kind [11]:

$$\frac{\partial}{\partial t}s = -\Gamma s. + \Lambda\left(\frac{\partial^2}{\partial x^2} - \alpha^2\frac{\partial^2}{\partial \bar{\tau}^2}\right)s$$

$$\text{or}\ \frac{\partial}{\partial \tau}s = -\Gamma s. + \Lambda\left(\frac{\partial^2}{\partial x^2} - \frac{\partial^2}{\partial \tilde{\tau}^2}\right)s,\quad \bar{\tau} = \alpha\tilde{\tau} \tag{1}$$

with real variables y, t, τ, given $\mathbb{C}^2$ – scalar functions Γ, Λ given real constant α and admissible function s, we need an algebra with generators $(\varepsilon, \varepsilon_0, \varepsilon_1)$ satisfying the relations

$$\varepsilon^2 = \varepsilon_1,\quad \varepsilon_0^2 = \varepsilon,\quad \varepsilon_1^2 = 0,\quad \varepsilon_0\varepsilon_1 + \varepsilon_1\varepsilon_0 = 0. \tag{2}$$

A physical meaning of the functions and constants involved is explained in [13]. Since $\bar{\tau}$ stands for temperature, entropy, or short-range order parameter, (1) describes a statistical problem. Because of (2) statistic description is put into the mathematical model, so the problem becomes stochastical.

The algebra governing (2) is called the *Clifford-Grassmann* $\mathcal{C}l^0_{1,0}(\mathbb{C})$ algebra [9]. As generators we may take

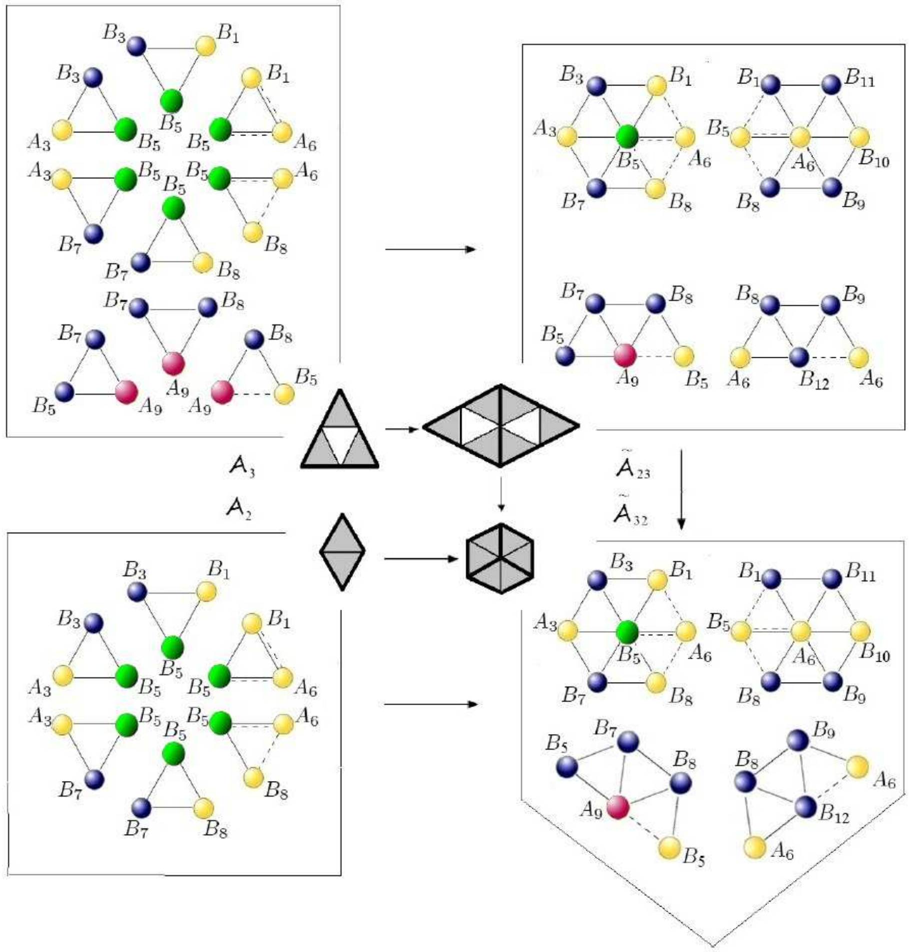

Fig. 3: Cumulative scheme $3 \cdot 2 \cdot 3\triangle \to 3 \cdot 3 \cdot 2\triangle$ of binary and ternary formal extensions (non-satisfactory for characterizing a quaternary structure).

$$\varepsilon = \begin{pmatrix} 1 & 0 \\ 0 & 1 \end{pmatrix}, \quad \varepsilon_0 = \begin{pmatrix} i & 0 \\ 0 & -i \end{pmatrix}, \quad \varepsilon_1 = \begin{pmatrix} 0 & i \\ 0 & 0 \end{pmatrix}, \tag{3}$$

i being the imaginary unit.

We can see that our algebra is closely related to the *Pauli algebra* with the familiar generators σ_1, σ_2, σ_3 namely: $\varepsilon_0 = i\sigma_3$, $\varepsilon_1 = \frac{1}{2}i(\sigma_1 + i\sigma_2)$, and to the quaternion algebra. Let us recall that, in analogy to the *complex algebra*, determined by the composition formula

$$(x_1^2+x_2^2)(y_1^2+y_2^2)=(x_1y_1-x_2y_2)^2+(x_2y_1+x_1y_2)^2,\quad x_1,\dots,y_2\ \text{real},$$

the quaternion algebra is determined by the composition formula

$$(x_1^2+\dots+x_4^2)(y_1^2+\dots+y_4^2)=(x_1y_1-x_2y_2-x_3y_3-x_4y_4)^2$$
$$+(x_2y_1+x_1y_2-x_4y_3+x_3y_4)^2+(x_3y_1+x_4y_2+x_1y_3-x_2y_4)^2$$
$$+(x_4y_1-x_3y_2+x_2y_3-x_1y_4),\quad x_1,\dots,y_4\ \text{real}, \tag{4}$$

and this leads to quaternions [29, 4-8]:

$$x=x_1+x_2i+x_3j+x_4k,$$

where

$$ij=k,\ \ jk=i,\ \ ki=j,\ \ i^2=j^2=k^2=-1,\ \ x_1,\dots,x_4\ \text{real}.$$

Instead, we may take four generators

$$I_3=\begin{pmatrix}1&0&0\\0&1&0\\0&0&1\end{pmatrix},\quad u=\begin{pmatrix}0&0&1\\\mathbf{j}&0&0\\0&\mathbf{j}^2&0\end{pmatrix},$$

$$v=\begin{pmatrix}0&0&1\\\mathbf{j}^2&0&0\\0&\mathbf{j}&0\end{pmatrix},\quad uv=\frac{1}{\mathbf{j}}vu=\mathbf{j}\begin{pmatrix}0&1&0\\0&0&1\\1&0&0\end{pmatrix},\quad \mathbf{j}^3=1,\ \mathbf{j}\neq 1,$$

and this leads to *quasi-quaternions* [22].

In analogy we take

$$x=x_1^*+x_2^*\tilde{i}+x_3^*\tilde{j}+x_4^*\tilde{k},$$

where

$$\tilde{i}\tilde{j}=\tilde{k},\quad \tilde{j}\tilde{k}=-\tilde{i},\quad \tilde{k}\tilde{i}=\tilde{j},\quad \tilde{i}^2=-\tilde{j}^2=-\tilde{k}^2=-1,\quad x_1^*,\dots,x_4^*$$

real, thus having *para-quaternions* [13, 11, 34, 10]. Instead, we may take for them four generators [22]:

$$I_3,\ \ u_{\perp\perp}=\begin{pmatrix}0&\mathbf{j}^2&0\\0&0&\mathbf{j}\\1&0&0\end{pmatrix},\quad v_{\perp\perp}=\begin{pmatrix}0&\mathbf{j}&0\\0&0&\mathbf{j}^2\\1&0&0\end{pmatrix},$$

$$(uv)_{\perp\perp}=\frac{1}{\mathbf{j}}(vu)_{\perp\perp}=\mathbf{j}\begin{pmatrix}0&0&1\\1&0&0\\0&1&0\end{pmatrix},\quad \mathbf{j}^3=1,\ \ \mathbf{j}\neq 1,$$

where $u_\perp^{\alpha\beta}=u^{\beta,4-\alpha}$, $\alpha,\beta=1,2,3$, and this leads to quasi-para-quaternions.

3. Background algebras involved in the linearization the Cayley-Dickson process

Let $\mathcal{A}$ be a finite-dimensional algebra over a field K equipped with an involution: $^* : \mathcal{A} \to \mathcal{A}$ such that $(ab)^* = b^*a^*$ for all $a, b \in \mathcal{A}$ and with norm $\| a \|^2 = aa^*$. Let

$$(a,b) + (c,d) = (a+c, b+d), \quad (a,b) \cdot (c,d) = (ac - db^*, da + bc^*)$$
$$\text{for} \ \ (a,b), (c,d) \in \mathcal{A} \times \mathcal{A}.$$

The set $\mathcal{A}' = \mathcal{A}^*$ with these operations is an algebra with involution: $(a,b)^* = (a,-b)^*$ and norm $\| S \|^2 = SS^*$, where $S = (a,b) \in \mathcal{A}$. Clearly, $\mathcal{A}$ is a subalgebra of $\mathcal{A}$ via the embedding $a \mapsto (a,0)$. The construction defined above is the so-called *Cayley-Dickson doubling process.*

With help of this process, from real algebra we can obtain the complex algebra, from complex algebra – the quaternion algebra, from quaternion algebra – the octonion algebra:

$$\mathbb{C} = \mathbb{R} \oplus \mathbb{R}i, \ \ \mathbb{H} = \mathbb{C} \oplus \mathbb{C}j, \ \ \mathbb{O} = \mathbb{H} \oplus \mathbb{H}\ell,$$

where i, j, ℓ are complex, resp. quaternionic, resp. octonionic units.

Because of (3) the complex multiplication is defined by

$$(x_1, x_1) \circ_{\mathbb{C}} (y_1, y_2) = (x_1 y_1 - x_2 y_2, \ x_2 y_1 + x_1 y_2).$$

Because of (4) the quaternional multiplication is defined by

$$(s_1, s_2) \circ_{\mathbb{H}} (w_1, w_2) = (s_1 w_1 - s_2 w_2, \ s_2 w_1 + s_1 w_2).$$

Coming from the complex to quaternion multiplication we loose the commutativity; coming from the quaterniome to octonionic multiplication, we loose the associativity.

4. The four- and two-sheeted Riemann surface approach to the algebras: 4 and 8 generators

Riemann surfaces are of great importance in the electromagnetic field theories [32, 33, 9, 10]. They are also important for our interest in algebras with 4 and 8 generators [22]. Following [30, 31, 26] consider the first quarter of the complex (3×3)-matrix plane uI_3v with origin I_3 and scaling (u, u^2), (v, v^2) as expressed in Fig. 4.

In analogy, we consider the third quarter of the same plane with scaling $(u_{\perp\perp}, u^2{}_{\perp\perp})$, $(v_{\perp\perp}, v^2{}_{\perp\perp})$ as expressed in Fig. 5.

In order to express in a similar way quasi-octonions we consider the first quarter as before, **together** with the second quarter [22], with origin $I_3^{\perp}$ and scaling $(u_{\perp}, u^2{}_{\perp})$, $(v_{\perp}, v^2{}_{\perp})$ as expressed in Fig. 6. In analogy, we consider the third quarter as before, **together** with the fourth quarter, with the origin $I_3^{\perp}$ and scaling $(u_{\perp\perp\perp}, u^2{}_{\perp\perp\perp})$, $(v_{\perp\perp\perp}, v^2{}_{\perp\perp\perp})$ as expressed in Fig. 7, arriving at para-octonions. The relationship between the both algebras will be determined in [20].

It is natural o construct from the quarter-planes in question a Riemann surface. Take two (yellow) planes Y_1, Y_2 and two (green) planes G_1, G_2 in the order

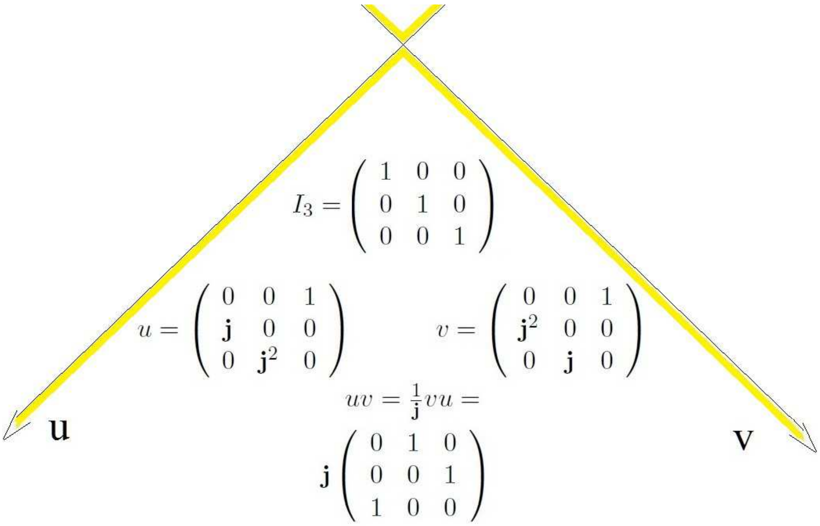

Fig. 4: The quasi-quaternion quarter-plane.

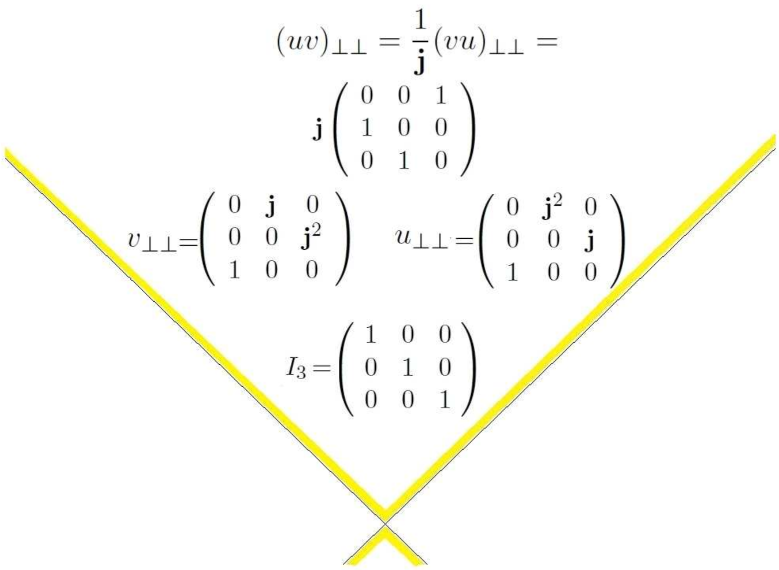

Fig. 5: The quasi-para-quaternion quarter-plane.

$Y_1 G_1 Y_2 G_2$, fix four origins as the critical point of the Riemann surface, cut Y_1, G_1 along positive v, $u_\perp$-half-axes, and glue the edge of the first Y_1-quarter to the edge of the second G_1-quarter. Next cut G_1, Y_2 along $\mathrm{v}_\perp$, $\mathrm{u}_{\perp\perp}$-half-axis and then glue the edge of second G_1-quarter to the edge of the third Y_2-quarter. In turn cut Y_2, G_2 along $\mathrm{v}_{\perp\perp}$, $\mathrm{u}_{\perp\perp\perp}$ half-axes, and glue the edge of the third Y_2-quarter to the edge of fourth G_2-quarter. Finally we cut G_2, Y_1 along $\mathrm{v}_{\perp\perp\perp}$, $\mathrm{u}_{\perp\perp\perp\perp}$ half-axis, and glue the edge of the fourth G_2-quarter to the edge of the first Y_1-quarter. Clearly, $\mathrm{u}_{\perp\perp\perp\perp}$ coincides with the positive u-half-axis. In order to do that we have to cut, in addition, G_1 and Y_2 along $\mathrm{v}_{\perp\perp\perp}$, $\mathrm{u}_{\perp\perp\perp\perp}$-axes (in the both cases) and the glued surface has to pierce the both cuts (Fig. 8).

Alternatively take one (yellow) plane Y and one (green) plane G in order YG (Fig. 9), fix two origins as one critical point of the Riemann surface, cut Y, G along positive v, $\mathrm{u}_\perp$- and $\mathrm{v}_\perp$ $\mathrm{u}_{\perp\perp}$-half-axes, and glue the edge of first Y-quarter to the edge of second G-quarter and the edge of third Y-quarter to the edge of fourth G-quarter. Next cut G, Y along $\mathrm{v}_{\perp\perp}$, $\mathrm{u}_{\perp\perp\perp}$ and $\mathrm{v}_{\perp\perp\perp}$, $\mathrm{u}_{\perp\perp\perp\perp}$ -half-axes and glue the edge of second G-quarter to the edge of third Y-quarter and the edge of fourth G-quarter to the edge of the first Y-quarter. As before, $\mathrm{u}_{\perp\perp\perp\perp}$ coincides with the positive u-half-axis. In order to do that we have to cut, in addition, G and Y along $\mathrm{v}_\perp$, $\mathrm{u}_{\perp\perp}$ and $\mathrm{v}_{\perp\perp\perp}$, $\mathrm{u}_{\perp\perp\perp\perp}$ axes and the glued surface has to pierce the both cuts.

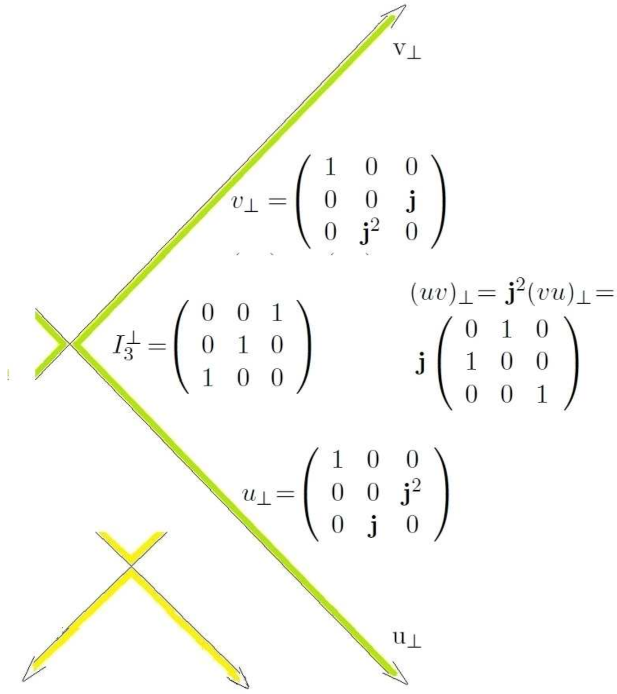

Fig. 6: The quasi-octonion half-plane.

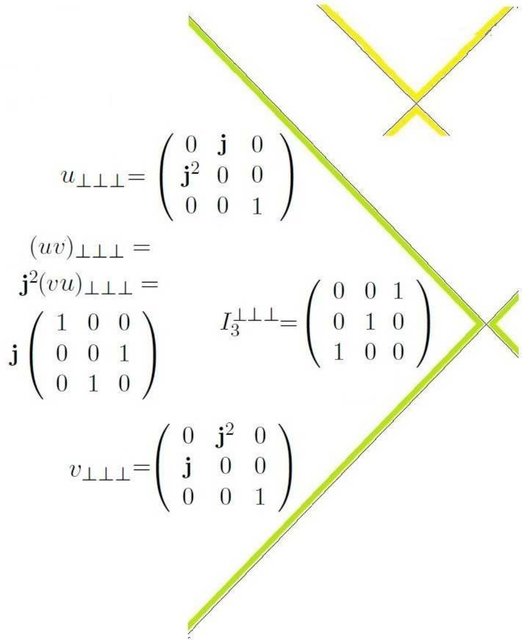

Fig. 7: The quasi-para-octonion half-plane.

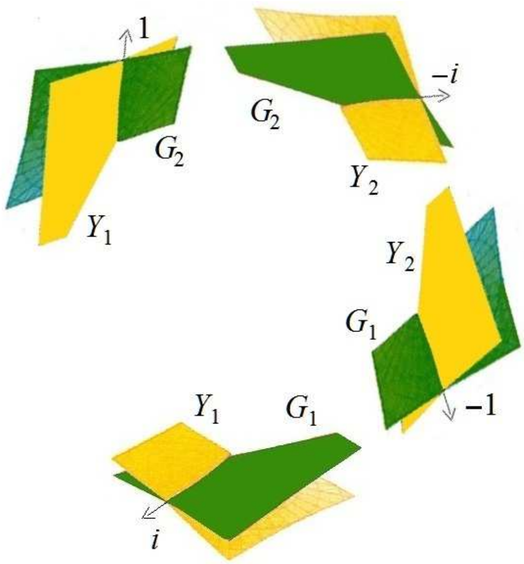

Fig. 8: A four-sheeted Riemann surface model for quasi-quaternion and quasi-octonion algebras.

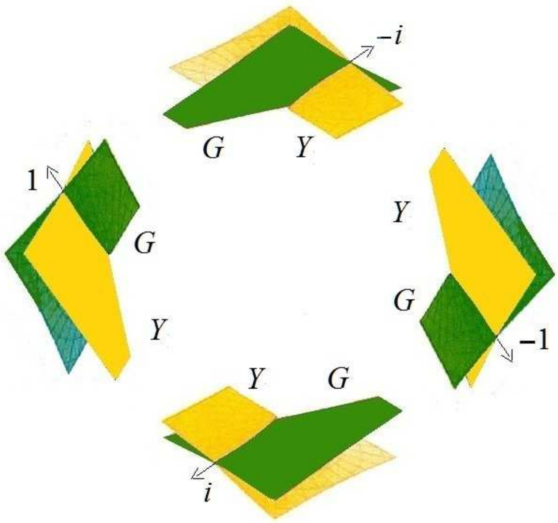

Fig. 9: A two-sheeted Riemann surface model of quasi-quaternion and quasi-octonion algebras.

5. The four-and two-sheeted Riemann surface approach to the algebras: 9 and 18 generators by bringing the scales to u^2v^α, $u^\alpha v^2$, $\alpha = 0, 1, 2$

In order to deal with ternary alloys we need the *nonion algebra* (with 9 complex 3×3 matrix generators); in order to deal with quaternary alloys we need the duodevicenion algebra (with 18 complex 3×3 matrix generators) – the constructions rely upon the cubic algebra (with 3 complex 3×3 matrix generators) [18–21, 4, 23, 17, 29–31].

To this end, we bridge the scales related to

$$u^2v^\alpha = \frac{1}{\mathbf{j}}v^\alpha u^2, \quad u^\alpha v^2 = \frac{1}{\mathbf{j}}v^2u^\alpha, \quad \alpha = 0, 1, 2$$

in Fig. 4 and in Figs 5–9 correspondingly. The results are shown in Figs 10–13.

Generators

$$I_3 = \begin{pmatrix} 1 & 0 & 0 \\ 0 & 1 & 0 \\ 0 & 0 & 1 \end{pmatrix}, \quad uv = \frac{1}{\mathbf{j}}vu = \mathbf{j}\begin{pmatrix} 0 & 1 & 0 \\ 0 & 0 & 1 \\ 1 & 0 & 0 \end{pmatrix},$$

$$u^2v^2 = \frac{1}{\mathbf{j}}v^2u^2 = \mathbf{j}^2\begin{pmatrix} 0 & 0 & 1 \\ 1 & 0 & 0 \\ 0 & 1 & 0 \end{pmatrix}, \quad \text{with } \mathbf{j}^3 = 1, \ \mathbf{j} \neq 1 \tag{5}$$

spread the so called *cubic algebra.*

We conclude that the para-nonion algebra coincides with the nonion algebra. However, different order of the generators allows a new geometrical interpreta-

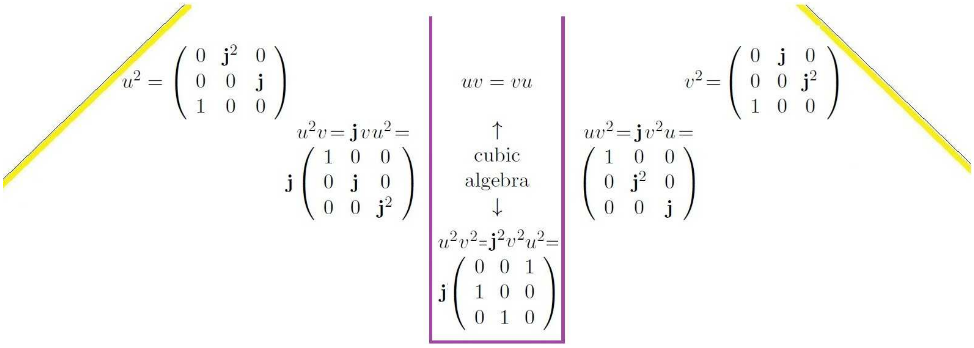

Fig. 10: Extension of the quasi-quaternion quarter-plane to nonion quarter-plane.

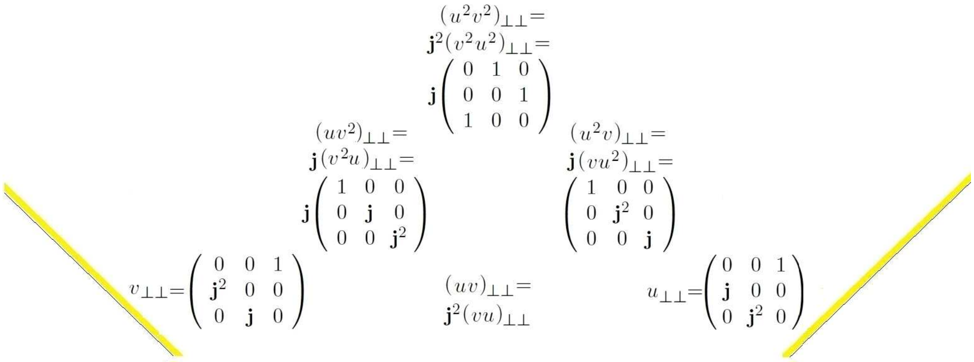

Fig. 11: Extension of the quasi-para-quaternion quarter-plane to para-nonion quarter-plane.

tion [20]. We can see that the generators of the duodevicenion algebra are the following:

three generators (5) of the cubic algebra and [16]:

$$\begin{pmatrix} 1 & 0 & 0 \\ 0 & \mathbf{j}^2 & 0 \\ 0 & 0 & \mathbf{j} \end{pmatrix}, \quad \begin{pmatrix} 0 & \mathbf{j}^2 & 0 \\ 0 & 0 & \mathbf{j} \\ 1 & 0 & 0 \end{pmatrix}, \quad \begin{pmatrix} 0 & 0 & 1 \\ \mathbf{j}^2 & 0 & 0 \\ 0 & \mathbf{j} & 0 \end{pmatrix},$$

$$\begin{pmatrix} 1 & 0 & 0 \\ 0 & \mathbf{j} & 0 \\ 0 & 0 & \mathbf{j}^2 \end{pmatrix}, \quad \begin{pmatrix} 0 & \mathbf{j} & 0 \\ 0 & 0 & \mathbf{j}^2 \\ 1 & 0 & 0 \end{pmatrix}, \quad \begin{pmatrix} 0 & 0 & 1 \\ \mathbf{j} & 0 & 0 \\ 0 & \mathbf{j}^2 & 0 \end{pmatrix},$$

$$\begin{pmatrix} 0 & 0 & 1 \\ 0 & 1 & 0 \\ 1 & 0 & 0 \end{pmatrix}, \quad \begin{pmatrix} 0 & 1 & 0 \\ 1 & 0 & 0 \\ 0 & 0 & 1 \end{pmatrix}, \quad \begin{pmatrix} 1 & 0 & 0 \\ 0 & 0 & 1 \\ 0 & 1 & 0 \end{pmatrix},$$

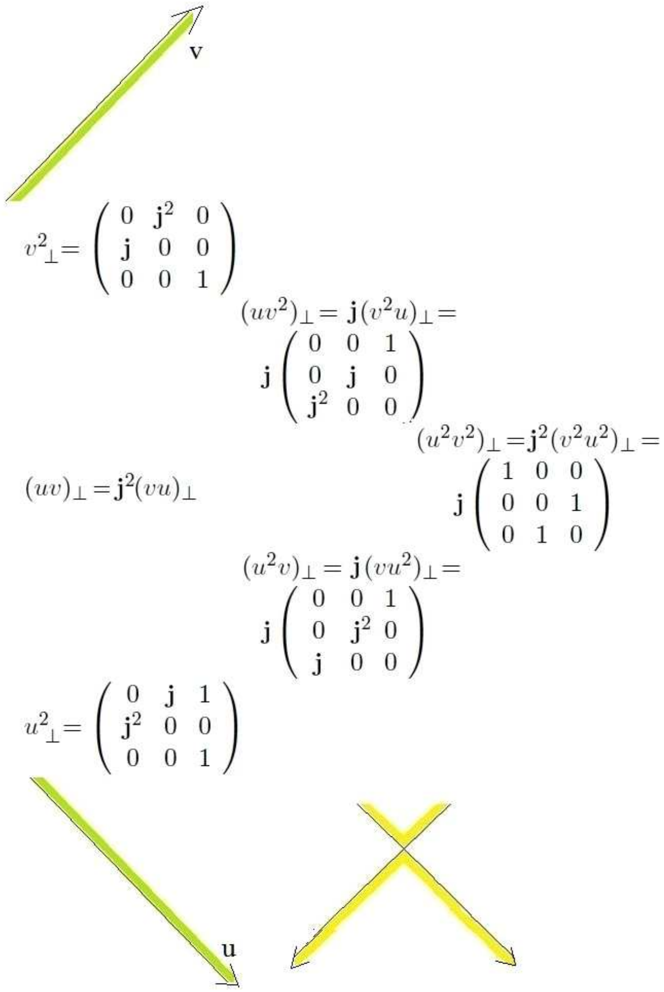

Fig. 12: Extension of the quasi-octonion half-plane to duodevicenion half-plane.

$$\begin{pmatrix} 0 & 0 & 1 \\ 0 & \mathbf{j}^2 & 0 \\ \mathbf{j} & 0 & 0 \end{pmatrix}, \quad \begin{pmatrix} 0 & \mathbf{j}^2 & 0 \\ \mathbf{j} & 0 & 0 \\ 0 & 0 & 1 \end{pmatrix}, \quad \begin{pmatrix} 1 & 0 & 0 \\ 0 & 0 & \mathbf{j}^2 \\ 0 & \mathbf{j} & 0 \end{pmatrix},$$

$$\begin{pmatrix} 0 & 0 & 1 \\ 0 & \mathbf{j} & 0 \\ \mathbf{j}^2 & 0 & 0 \end{pmatrix}, \quad \begin{pmatrix} 0 & \mathbf{j} & 0 \\ \mathbf{j}^2 & 0 & 0 \\ 0 & 0 & 1 \end{pmatrix}, \quad \begin{pmatrix} 1 & 0 & 0 \\ 0 & 0 & \mathbf{j} \\ 0 & \mathbf{j}^2 & 0 \end{pmatrix}.$$

We also conclude that the para-duodevicenion algebra coincides with the duodevicenion algebra. However, different order of the generators allows a new geometrical interpretation [20].

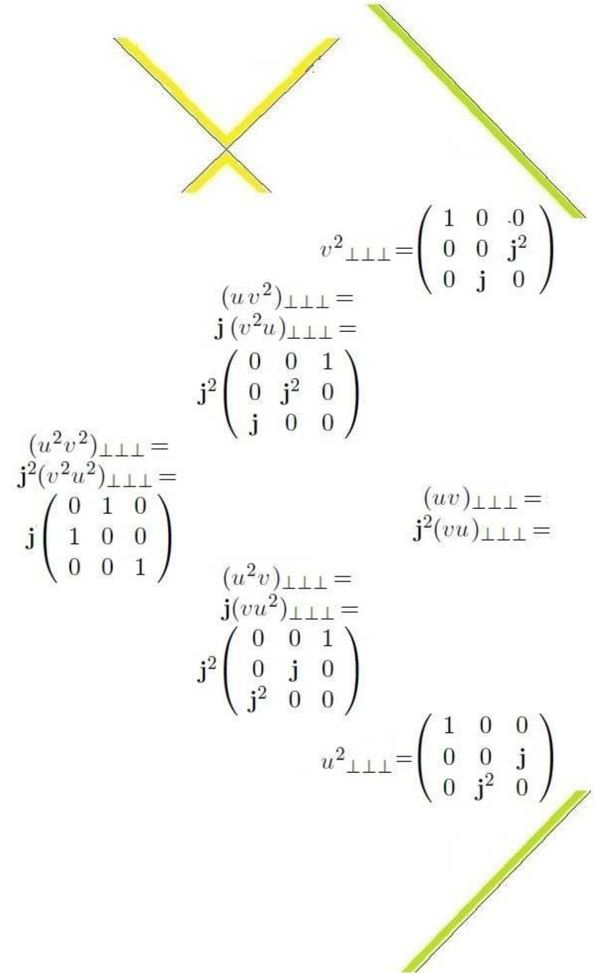

Fig. 13: Extension of the para-nonion half-plane to para-duodevicenion half-plane.

6. An analysis of linearization of the one-dimensional relaxation problem

We come back to the equation (1). Within the T. Oguchi theory of stochastical relaxation, $a = \hat{a}/\bar{a}$, where $\hat{a}$ is the amplitude of stochastical movement and $\bar{a}$ is the lattice constant. We may take the functions Γ and Λ as

$$\Gamma = \frac{1}{\hat{\tau}}\left[1 - \frac{1}{2}\left(1 - 4\,\langle s\rangle^2\,\frac{\hat{x}_1 \mathcal{J}}{k_{\mathrm{B}}T}\right)\right], \quad \Lambda = \frac{\bar{\alpha}^2}{\hat{\tau}} \cdot \frac{1}{\bar{\alpha}}\left(1 - 4\,\langle s\rangle^2\right)\frac{\hat{x}_1 \mathcal{J}}{k_{\mathrm{B}}T},$$

where $\hat{x}_1$ stands for the position of a fixed layer and $\hat{\tau} = x_2$ represents the stochastic variable (temperature, entropy, or short range order parameter) responsible for the stochastic behaviour of the lattice; it describes thermal oscillations of spin. Further, $\langle s \rangle$ stands for the canonical average of spin; we suppose that it does not depend on the position of a fixed layer $x_1 = \hat{x}_1$. The parameter $\mathcal{J}$ us due to the interaction between the neighbouring spins, k_{B} stands for the Boltzmann constant, and T is the absolute temperature. Following [11, 24, 25] we may take

$$s_* = s_0 \equiv -\int_0^t \int_{-\infty}^{+\infty} \int_{-\infty}^{+\infty} \exp\left[\frac{(x-x')^2 - (\tilde{\tau}-\tilde{\tau}')^2}{4\Lambda(x',\tilde{\tau}')(t-t')}\right]$$

$$(\Gamma s_0)\,(x-x', \tilde{\tau}-\tilde{\tau}', t-t')dx'd\tilde{\tau}'dt'. \tag{6}$$

The counterparts of the familiar ∂ and $\bar{\partial}$-operators known from the complex analysis have to satisfy the conditions

$$\begin{aligned} &\partial\bar{\partial}\mathbf{s} = \Lambda\left(\tfrac{\partial^2}{\partial x^2} - \tfrac{\partial^2}{\partial \tilde{\tau}^2}\right)\mathbf{s}, \quad \bar{\partial}\mathbf{s} = P\mathbf{s} = v, \quad \Lambda\partial(P\mathbf{s}) = \tfrac{\partial}{\partial t}\mathbf{s} \ \text{ with } \ \Lambda\partial\mathbf{v} = -\Gamma\mathbf{s}, \\ &\Lambda\partial(P\mathbf{s}) = \partial(Q\mathbf{s}), \quad Q\mathbf{s} = \mathbf{s}_{xt}\odot\varepsilon + \mathbf{s}_{yt}\odot\varepsilon_0 + \mathbf{s}_{xy}\odot\varepsilon\varepsilon_0 \end{aligned} \tag{7}$$

where $\odot$ is the multiplication in $\mathcal{C}\ell^{*0}_{1,0}(\mathbb{C})$:

$$\begin{aligned} &\mathbf{s} \equiv (s, s_0) = se + s_0e_0; \quad s, s_0 \in \mathbb{R}; \quad (x, \tilde{\tau}, t) = x\varepsilon + \tilde{\tau}\varepsilon_0 + t\varepsilon_1, \\ &e\odot\varepsilon = (e, e\odot\varepsilon)e + (e_0, e\odot\varepsilon)e_0 \\ &(e, e\odot e) = a_{\cdots}^{\cdot\cdot}e^2 + a_{\cdots}^{\cdot 0}ee_0 + a_{\cdots}^{0\cdot}e_0e + a_{\cdots}^{00}e_0^2 \ \text{ etc.,} \end{aligned} \tag{8}$$

(,) being scalar product.

The solution $\mathbf{s}$ may be expressed as

$$\mathbf{s} = c_1\mathbf{s}_1 + \ldots + c_6\mathbf{s}_6, \quad c_1, \ldots, c_6 \in \mathbb{C},$$

where $\mathbf{s}_1, \ldots, \mathbf{s}_6$ are fundamental solutions of (1):

$$\begin{aligned} &\mathbf{s}_1 = (\partial s_*)\varepsilon, \quad \mathbf{s}_4 = s_*\varepsilon + (\partial s_*)\varepsilon\varepsilon_1 \\ &\mathbf{s}_2 = (\partial s_*)\varepsilon_0, \quad \mathbf{s}_5 = s_*\varepsilon + (\partial s_*)\varepsilon_0\varepsilon_1 \\ &\mathbf{s}_3 = (\partial s_*)\varepsilon\varepsilon_0, \ \mathbf{s}_6 = -s_*\varepsilon\varepsilon_0 + (\partial s_*)\varepsilon\varepsilon_0\varepsilon_1. \end{aligned} \tag{9}$$

Setting $p = p(x, \tilde{\tau}, t) = \partial s_*$, $q = q(x, \tilde{\tau}, t) = s_*$, we finally obtain

$$\begin{aligned} \mathbf{s} \ &= \ p[c_1\varepsilon + c_2\varepsilon_0 + c_3\varepsilon_0\varepsilon_1 + (c_4\varepsilon + c_5\varepsilon_0 + c_6\varepsilon\varepsilon_0)\varepsilon_1] \\ &+ \ q(c_4\varepsilon + c_5\varepsilon_0 + c_6\varepsilon\varepsilon_0)\varepsilon_1. \end{aligned} \tag{10}$$

It is natural to suppose the initial conditions

$$\begin{aligned} &s(x, \tilde{\tau}, 0) = x_0, \quad s(x, \tilde{\tau}, t) \to 0 \ \text{ as } \ (x, t) \to (+\infty, t_0) \\ &s(x, \tilde{\tau}, t) \to 0 \ \text{ as } \ (x, \tilde{\tau}, t) \to (x_0, \tilde{\tau}, t) \ \text{ for some } \ x_0. \end{aligned} \tag{11}$$

Throughout the paper we also assume that

$$0.5 \cdot 10^{-12}\text{sec} \le t_0 \le 1.5 \cdot 10^{-12}\text{sec}, \;\; 2\mathring{A} \le a \le 3\mathring{A}.$$

7. Numerical procedure for calculating the six fundamental solutions with the example of solving effectively the boundary value problem

In order to calculate six fundamental solutions $s_1, \dots, s_6$ of (1) we choose the admissible function s^* so that the lines $s_1|_{t=\tilde{\tau}}$ etc. and $s_1|_{t=-\tilde{\tau}}$ etc. are singular [24, 11]. To this end we choose the values $(\partial s_*, \bar{\partial} s_*)$ satisfying (7) as shown in Fig. 14.

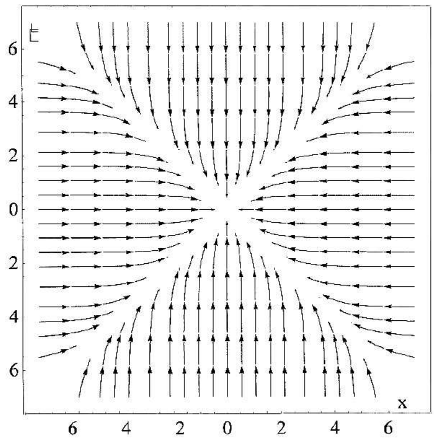

Fig. 14: The map of $(\partial, \bar{\partial})$ for the chosen admissible function s_*.

Taking into account the multiplication rules for $\odot$ given in Section 6 formulae (8), and the admitted there initial conditions (11), we arrive at the maps of $s_1, \dots, s_6$ (9). Since the differences between s_1, s_2, s_3 and between s_4, s_5 are mainly in the structure of singular lines, we show here the maps of s_1, s_5 and s_6 only. A mere detailed description including a study of singular lines is left to a future paper. It is worthwhile to describe shortly the numerical algorithm concerned [36, 37, 27] in the context of finding algorithm concerned has been presented in [27] in the context of finding the behaviour of superconducting unconventional Josephson junction described using the Ginsburg-Landau formalism. The authors of [27] assume that the general problem concerned with

$$\frac{\delta}{\delta X_i} F[X_i] = 0 \tag{12}$$

can be transformed into the schema

$$X_i(\zeta_{n+1}) = \frac{\zeta_{n+1} - \zeta_n}{\eta_i} \frac{\delta}{\delta X_i} F[X_i]\bigg|_{\zeta_n} + X_i(\zeta_n), \tag{13}$$

where F is a free energy functional, X_i is an unknown solution, ζ_n is an intensive independent variable parameter increased in each iteration step, $\delta F/\delta X_i$ is the Gâteaux derivative of F, and η_i is a constant. The first solution (X_i for $\zeta_0 = 0$) is obtained from the simplified problem description (e.g. linearized problem (12)). The proposed schema (13) is executed until the solution $X_i(\zeta_n)$ converge. The announced results are shown in Fig. 15.

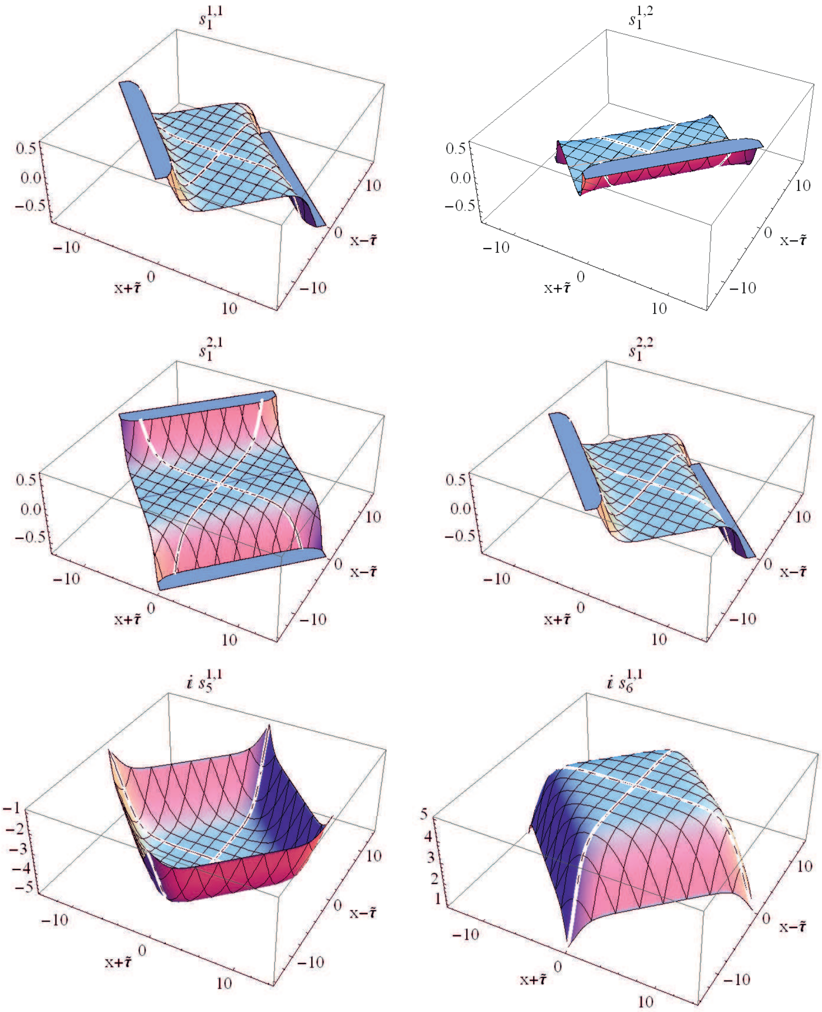

Fig. 15: The fundamental solutions $\underline{s}_1$, $s_5^{1,1}$, $s_6^{1,1}$ of equation (1). The upper index is used to the matrix elements numeration.

8. Calculation of total energy of an alloy

Physically and from the piont of view of possible technological applications, we consider the fundamental solutions s_1, s_5, s_6. We have

$$e_{s_1} = e_{s_2} = e_{s_3} << e_{s_4} = e_{s_5} = e_{s_6}$$

which may be calculated with the procedures [3, 2, 35] or, alternatively, by a the standard numerical finite-difference method.

More precisely, we can calculate the total energies e_{s_α} using the following expression

$$e_{s_\alpha} = \int\int |s_\alpha|^2 \, dx \, dy.$$

Following [24, 28] and (8) we can assume that

$$|s_\alpha s_{\alpha_0}| \leq \sqrt{2}|s_\alpha||s_{\alpha 0}|$$

therefore for

$$s_\alpha = \begin{pmatrix} a_\alpha & b_\alpha \\ c_\alpha & d_\alpha \end{pmatrix}$$

we have

$$s_\alpha = \frac{1}{4}|a_\alpha + d_\alpha|^2 + \frac{1}{4}|a_\alpha - d_\alpha|^2 + \frac{1}{4}|b_\alpha + c_\alpha|^2 + \frac{1}{4}|b_\alpha - c_\alpha|^2,$$

so that, finally,

$$e_{s_4} = e_{s_5} = e_{s_6} \approx 17.1874 e_{s_\alpha}, \quad \alpha = 1, 2, 3.$$

9. Conclusions concerning lines of force, equipotential lines, and physical and non-physical fundamental solutions

A map of lines of force and equipotential lines is formed in the plane (s, s_0). A careful analysis of magnetic fields generated by fundamental solutions $s_1, \ldots, s_6$ for s_* allows us to consider all of them as physical, i.e. physically realizable.

References

[1] F. L. Castillo Alvarado, J. Ławrynowicz, and Małgorzata Nowak-Kępczyk, *Fractal modelling of alloy thin films. Temperatures characteristic for local phase transitions*, in: Applied Complex and Quaternionic Approximation. Ed. by R. K. Kovacheva, J. Ławrynowicz, and S. Marchiafava, Ediz. Nuova Cultura, Univ. 'La Sapienza', Roma 2009, pp. 207-236.

[2] F. Ducastelle and F. Gauthier, *Generalized perturbation theory in disordered transitional alloys: Applications to the calculation of ordering energies,* J. Phys. F **6** (1976), 2039; doi: 10:1088/0305-4608/6/11/065.

[3] R. Kikuchi, *A theory of cooperative phenomena*, Phys. Rev. **81** (1951), 988–1003.

[4] J. Ławrynowicz, *On the coefficient problem for univalent polynomials*, Proc. Cambridge Philos. Soc. **64** (1968), 87–98.

[5] J. Ławrynowicz, *Variationsrechnung und Anwendungen* (Hochschltext), Springer-Verlag, Berlin-Heidelberg-New York-Tokyo 1986, xii+317pp.

[6] J. Ławrynowicz, *Quaternions and fractals vs. Finslerian geometry. A. Quaternions, noncommutativity, and C^*-algebras*, Bull. Soc. Sci. Lettres Łódź **55** Sér. Rech. Déform. **47** (2005), 55–66.

[7] J. Ławrynowicz, *Quaternions and fractals vs. Finslerian geometry. B. Algebraic possibilities (quaternions, octonions, sedenions)*, ibid. **55** Sér. Rech. Déform. **47** (2005), 67–82.

[8] J. Ławrynowicz, *Quaternions and fractals vs. Finslerian geometry. 1. Quaternion-based modifications of the Cayley-Dickson process*, ibid. **55** Sér. Rech. Déform. **47** (2005), 83–98.

[9] J. Ławrynowicz, in cooperation with J. Krzyż, *Quasiformal Mappings in the Plane. Parametrical Methods* (Lecture Notes in Mathematics 978), Springer-Verlag, Berlin-Heidelberg-New York-Tokyo 1983, vi+177pp.

[10] J. Ławrynowicz, S. Marchiafava, F. L. Castillo Alvarado, and Agnieszka Niemczynowicz, *(Para)quaternionic geometry, harmonic forms, and stochastical relaxation,* Publ. Math. Debrecen, **84**, no. 1-2 (2014), 205–220.

[11] J. Ławrynowicz, Agnieszka Niemczynowicz, Małgorzata Nowak-Kępczyk, and L. M. Tovar Sánchez, *On an extension of harmonicity and holomorphy*, Cont. Math., Contemporary Mathematics (2015), 8 pp., in print.

[12] J. Ławrynowicz, Małgorzata Nowak-Kępczyk, and O. Suzuki, *Fractals and chaos related to Ising-Onsager-Zhang lattices vs. the Jordan-von Neumann-Wigner procedures. Quaternary approach,* Internat. J. of Bifurcations and Chaos **22** no. 1 (2012) 1230003 (19 pages).

[13] J. Ławrynowicz, and H. M. Polatoglou, *The relaxation and stochastical relaxation problems in crystals in terms of para-quaternions*, Acta Physicae Superficierum **12** (2012), 97–107.

[14] J. Ławrynowicz, O. Suzuki, and Agnieszka Niemczynowicz, *Fractals and chaos related to Ising-Onsager-Zhang lattices vs. the Jordan-von Neumann-Wigner procedures. Ternary approach*, Internat. J. of Nonlinear Sci. and Numer. Simul. **14**, no. 3-4 (2013), 211–215.

[15] J. Ławrynowicz, O. Suzuki, Agnieszka Niemczynowicz, and Małgorzata Nowak-Kępczyk, *Fractals and chaos related to Ising-Onsager-Zhang lattices. Quaternary approach vs. ternary approach*, Ms. (2015) ca. 16 pp., to appear.

[16] J. Ławrynowicz, O. Suzuki, Agnieszka Niemczynowicz, and Małgorzata Nowak-Kępczyk, *Fractals and chaos related to Ising-Onsager-Zhang lattices. Ternary approach vs. binary approach*, Ms. (2015) ca. 16 pp., to appear.

[17] J. Ławrynowicz, O. Suzuki, Agnieszka Niemczynowicz, and Małgorzata Nowak-Kępczyk,*Fractals and chaos related to Ising-Onsager-Zhang lattices. Relations to the Onsager model*, Ms. (2015) ca. 12 pp., to appear.

[18] Małgorzata Nowak-Kępczyk, *An Algebra Governing Reduction of Quaternary Structures to Ternary Structures I, Reductions of Quaternary Structures to Ternary Structures*, Bull. Soc. Sci. Lettres Łódź Sér. Rech. Déform. **64** no. 2 (2014), 101–109.

[19] Małgorzata Nowak-Kępczyk, *An algebra governing reduction of quaternary structures to ternary structures II. A study of the multiplication table for the resulting algebra generators*, ibid. **64** no. 3 (2014), 81-90.

[20] Małgorzata Nowak-Kępczyk, *An algebra governing reduction of quaternary structures to ternary structures III. A study of generators of the resulting algebra*, ibid. **65**, no. 1 (2015), ca. 10 pp., to appear.

[21] Małgorzata Nowak-Kępczyk, *Riemann surface approach to duodevicenions,* ibid. **66**, no. 3 (2016), ca. 16 pp., to appear.

[22] Małgorzata Nowak-Kępczyk, *A Riemann surface approach to para-quaternions*, Ms. (2015), ca. 10 pp., in preparation.

[23] Małgorzata Nowak-Kępczyk, *From nonions to duodevicenions*, Ms. (2015), ca. 10 pp, in preparation.

[24] Elena Obolashvili, *Partial Differential Equations in Clifford Analysis* (Pitman Monographs and Surveys in Pure and Applied Mathematics 96), Addison-Wesley, Longman, Harlow 1998.

[25] Elena Obolashvili, *Higher Order Partial Differential Equations in Clifford Analysis. Effective Solutions to Problems* (Science Business Medicine 28), Birkhauser Verlag, Basel 2002; Springer, New York 2003.

[26] C. S. Peirce, *On Nonions*, in: Collected Papers of Charles Sanders Peirce, 3rd ed., vol. III, Harvard University Press, Cambridge Mass. 1967, pp. 411-416.

[27] K. Pomorski, M. Zubert, and P. Prokopow, *Numerical solutions of nearly time-independent Ginzburg-Landau equation for various superconductivity structures III. Analytical solutions and relaxation method,* Bull. Soc. Sci. Lettres Łódź Sér. Rech. Déform. **64**, no. 1 (2014), 109–119.

[28] I. R. Porteous, *Clifford Algebras and the Classical Groups* Cambridge Studies in Advanced Mathematics **50**, Cambridge Univ. Press, 1995, v+295 pp.

[29] T. Pusztai, G. Tegze, G. I. Tóth, L. Környei, G. Bansel, Z. Fan, and L. Gránásy, *Phase-field approach to polycristalline solidification including heterogenous and homogenous nucleation*, J. of Phys. Condensed Matter **20**, no. 40 (2008), 44205, 16 pp.

[30] J. J. Sylvester, *A word on nonions*, John Hopkins Univ. Circulars **1** (1882), 241–242 (1883), 46; in: The Collected Mathematical Papers of James Joseph Sylvester, vol. III, Cambridge Univ. Press, Cambridge 1909, pp. 647–650.

[31] J. J. Sylvester, *On quaternions, nonions, sedenions etc.*, Johns Hopkins Univ. Circulars **3** (1984), 7-9; in: The Collected Mathematical Papers of James Joseph Sylvester, vol. IV, Cambridge Univ. Press, Cambridge 1909, pp. 122–132.

[32] I. F. Tamm, *Foundations of the Theory of Electricity* [in Russian], 8th ed., Izdatelstvo "Nauka", Moskva 1966; English transl., “Mir” Publishers, Moscow 1979; German transl.: *Grundlagen der Elektrizitätstheorie*, ibid. 1969.

[33] I. F. Tamm, *Collected Works*, 2 volumes, Izdatelstvo “Nauka”, Moskva 1976.

[34] M. Vaccaro, *Subspaces of a paraquaternionic Hermitian vector space*, Internat. J. of Geom. Methods in Modern. Phys. **8**, no. 7 (2011), 1487–1506.

[35] M. Zubert, M. Janicki, T. Raszkowski, A. Samson, P. S. Nowak, and K. Pomorski, *The heat transport in nanoelectronic devices and PDEs translation into hardware description languages*, Bull. Soc. Sci. Lettres Łódź Sér. Rech. Déform. **64**, no. 3 (2014), 69–80.

[36] M. Zubert, Małgorzata Napieralska, and A. Napieralski, *RESCUER – the new solution in multidomain simulations*, Microelectronic J. **31** (2000), 945–954.

Department of Solid State Physics
University of Łódź
Pomorska 149/153, PL-90-236 Łódź;
Institute of Mathematics
Polish Academy of Sciences
Śniadeckich 8, P.O.Box 21
PL-00-956 Warszawa
Poland
e-mail: jlawryno@uni.lodz.pl

Physics Department
Aristotle University of Thessaloniki
GR-54-124 Thessaloniki
Greece
e-mail: anvalianti@gmail.com

Institute of Mathematics and Informatics
State School of Higher Education in Chełm
54 Pocztowa Street, PL-22-100 Chełm
Poland
e-mail: gosianmk@gmail.com

Department of Microelectronics
and Computer Science
Łódź University of Technology
Wólczańska 221/223, PL-90-924 Łódź
Poland
e-mail: mariuszz@dmcs.p.lodz.pl

Presented by Julian Ławrynowicz at the Session of the Mathematical-Physical Commission of the Łódź Society of Sciences and Arts on May 28, 2015

O FIZYCE ZŁOŻONYCH KRYSZTAŁÓW – JEDNOWYMIAROWY PROBLEM RELAKSACJI I ZNACZENIE OBLICZEŃ CAŁKOWITEJ ENERGII

S t r e s z c z e n i e

Dla badania złożonych stopów istotna jest linearyzacja równań różniczkowych przemieszczeń atomów w stopie, do czego niezbędne są pewne algebry o 4, 8, 9 i 18 generatorach, które omawiamy podając pewne nieznane dotąd własności (są to wyniki Małgorzaty N.-K.). Efektywne wyliczenie przeprowadzamy dla jednowymiarowej relaksacji stochastycznej, co wiąże się z wyliczeniem sześciu rozwiązań fundamentalnych i badaniem ich udziału w rozpatrywanych sytuacjach fizycznych. Pracę kończy przykład obliczenia całkowitej energii stopu.

Słowa kluczowe: materiał złożony, problem relaksacyjny, nieliniowe równanie paraboliczne, para-kwaterniony

PL ISSN 0459-6854

B U L L E T I N

DE LA SOCIÉTÉ DES SCIENCES ET DES LETTRES DE ŁÓDŹ

2015 Vol. LXV

Recherches sur les déformations no. 2

pp. 47–60

Arezki Touzaline

A VISCOELASTIC CONTACT PROBLEM WITH SLIP DEPENDENT FRICTION AND ADHESION

Summary

We consider a mathematical model which describes the equilibrium between a viscoelastic body in frictional contact with a foundation. The contact is modelled with a prescribed normal stress and adhesion, associated with a slip-dependent version of Coulomb's law of dry friction. The adhesion is modelled with a surface variable, the bonding field, whose evolution is described by a first-order differential equation. We establish a variational formulation of the mechanical problem and prove the existence and uniqueness result of the weak solution if either the slip weakening or the given normal stress on the contact surface are sufficiently small. The proof is based on arguments of time-dependent variational inequalities, differential equations and Banach fixed-point theorem.

Keywords and phrases: viscoelastic, adhesion, slip-dependent friction, fixed point, weak solution

1. Introduction

Contact problems involving deformable bodies are quite frequent in industry as well as in daily life and play an important role in structural and mechanical systems. Because of the importance of this process a considerable effort has been made in its modelling and numerical simulations. A first study of frictional contact problems within the framework of variational inequalities was made in [6]. The mathematical, mechanical and numerical state of the art can be found in [17]. The quasistatic contact problem with normal compliance and friction for viscoelastic materials was studied in [15]. In this paper we consider a mathematical model which describes a quasistatic contact between a viscoelastic body and a fondation. The contact is modelled with a prescribed normal stress, adhesion and slip-dependent friction. We recall that the assumption of slip-dependent friction is used by geological researchers in the study of the motion of tectonic plates; see [11, 13] and the references therein. The models for dynamic or quasistatic process of adhesive contact between a deformable body and a foundation have been studied by several authors, see for instance the references [2–5, 14, 16–21] and the references therein. Here, as in [8, 9] we use the bonding field as an additional state variable β, defined on the contact surface of the boundary. The variable is restricted to values $0 \leq \beta \leq 1$, when $\beta = 0$ all the bonds are severed and there are no active bonds; when $\beta = 1$ all the bonds are active; when $0 < \beta < 1$ it measures the fraction of active bonds and partial adhesion takes place. We refer the reader to the extensive bibliography on the subject in [10, 14, 16–20]. In this work we derive a variational formulation of the mechanical problem for which we prove the existence and uniqueness of a weak solution if either the slip weakening or the given normal stress on the contact surface are sufficiently small. The proof is based on arguments of time-dependent variational inequalities, differential equations and Banach fixed point theorem.

The paper is structured as follows. In section 2 we present some notations and give the variational formulation. In section 3 we state and prove our main existence and uniqueness result, Theorem 2.1.

2. Problem statement and variational formulation

We consider a viscoelastic body which occupies a domain $\Omega \subset \mathbb{R}^d$ $(d = 2, 3)$ and assume that its boundary Γ is regular and partitioned into three measurable and disjoint parts $\Gamma_1, \Gamma_2, \Gamma_3$ such that $meas\,(\Gamma_1) > 0$. The body is acted upon by a volume force of density f_1 in Ω and a surface traction of density f_2 on Γ_2. On Γ_3 the body is in adhesive contact with a foundation following a slip-dependent version of Coulomb's friction law.

Then, the classical formulation of the mechanical problem is written as follows.

Problem P_1. Find a displacement field $u : \Omega \times [0, T] \to \mathbb{R}^d$ and a bonding field $\beta : \Gamma_3 \times [0, T] \to [0, 1]$ such that

$$div\sigma\,(u, \dot{u}) = -f_1 \text{ in } \Omega \times (0, T)\,, \tag{2.1}$$

$$\sigma\,(u, \dot{u}) = A\varepsilon\,(\dot{u}) \ + B\varepsilon\,(u) \ \text{ in } \Omega \times (0, T)\,, \tag{2.2}$$

$$u = 0 \quad \text{on } \ \Gamma_1 \times (0, T)\,, \tag{2.3}$$

$$\sigma\nu = f_2 \quad \text{on } \Gamma_2 \times (0, T)\,, \tag{2.4}$$

$$-\sigma_\nu = S - c_\nu \beta^2 R_\nu\,(u_\nu) \quad \text{on } \Gamma_3 \times (0, T)\,, \tag{2.5}$$

$$(2.6)\qquad \begin{cases} \left|\sigma_\tau + c_\tau \beta^2 R_\tau\left(u_\tau\right)\right| \leq \mu\left(\left|u_\tau\right|\right) S \\ \left|\sigma_\tau + c_\tau \beta^2 R_\tau\left(u_\tau\right)\right| < \mu\left(\left|u_\tau\right|\right) S \Longrightarrow \dot{u}_\tau = 0 \\ \left|\sigma_\tau + c_\tau \beta^2 R_\tau\left(u_\tau\right)\right| = \mu\left(\left|u_\tau\right|\right) S \Longrightarrow \\ \exists \lambda \geq 0 \text{ s.t. } \dot{u}_\tau = -\lambda\left(\sigma_\tau + c_\tau \beta^2 R_\tau\left(u_\tau\right)\right) \end{cases} \quad \text{on } \Gamma_3 \times (0,T),$$

$$(2.7)\qquad \dot{\beta} = -[\beta(c_\nu \left|R_\nu\left(u_\nu\right)\right|^2 + c_\tau \left|R_\tau\left(u_\tau\right)\right|^2) - \varepsilon_a]_+ \text{ on } \Gamma_3 \times (0,T),$$

$$(2.8)\qquad u\left(0\right) = u_0 \text{ in } \Omega,$$

$$(2.9)\qquad \beta\left(0\right) = \beta_0 \text{ on } \Gamma_3.$$

Equation (2.1) represents the equilibrium equation where $\sigma = \sigma\left(u, \dot{u}\right)$ denotes the stress tensor. Equation (2.2) is the viscoelastic constitutive law of the material in which A and B are given nonlinear functions and $\varepsilon\left(u\right)$ is the small strain tensor. Here and below a dot above a variable represents a time derivative. Relations (2.3) and (2.4) are the displacement and traction boundary conditions, respectively, in which ν denotes the unit outward normal vector on Γ and $\sigma\nu$ represents the Cauchy stress vector. Condition (2.5) represents the prescribed normal stress S with adhesion and (2.6) is the associated Coulomb's law of dry friction on the contact surface Γ_3 where μ denotes the coefficient of friction. The parameters c_ν, c_τ and ε_a are adhesion coefficients which may depend on $x \in \Gamma_3$. Following [18], R_ν and R_τ are truncation operators defined by

$$R_\nu\left(s\right) = \begin{cases} L \text{ if } s < -L \\ -s \text{ if } -L \leq s \leq 0 \\ 0 \text{ if } s > 0 \end{cases}, \qquad R_\tau\left(v\right) = \begin{cases} v & \text{if } |v| \leq L \\ L\dfrac{v}{|v|} & \text{if } |v| > L \end{cases},$$

where $L > 0$ is a characteristic length of the bonds. Equation (2.7) represents the ordinary differential equation which describes the evolution of the bonding field and it was already used in several papers, see for example [21], where $[s]_+ = \max\left(s, 0\right)$ $\forall s \in \mathbb{R}$. Since $\dot{\beta} \leq 0$ on $\Gamma_3 \times (0,T)$, once debonding occurs, bonding cannot be reestablished. Also we wish to make it clear that from [12] it follows that the model does not allow for complete debonding field in finite time. Finally, (2.8) and (2.9) represent respectively the initial displacement field and the initial bonding field. We recall that the inner products and the corresponding norms on $\mathbb{R}^d$ and S_d are given by

$$u.v = u_i v_i, \quad |v| = (v.v)^{\frac{1}{2}} \quad \forall u, v \in \mathbb{R}^d,$$
$$\sigma.\tau = \sigma_{ij}\tau_{ij}, \; |\tau| = (\tau.\tau)^{\frac{1}{2}} \quad \forall \sigma, \tau \in S_d,$$

where S_d is the space of second order symmetric tensors on $\mathbb{R}^d$ $(d = 2, 3)$. Here and below, the indices i and j run between 1 and d and the summation convention over repeated indices is adopted. Now, to proceed with the variational formulation, we need the following function spaces:

$$H = \left(L^2(\Omega)\right)^d,\ H_1 = \left(H^1(\Omega)\right)^d,\ Q = \left\{\sigma = (\sigma_{ij}) : \sigma_{ij} = \sigma_{ji} \in L^2(\Omega)\right\},$$

$$Q_1 = \{\sigma \in Q : div\sigma \in H\}.$$

Note that H and Q are real Hilbert spaces endowed with the respective canonical inner products

$$(u,v)_H = \int_\Omega u_i v_i dx, \quad (\sigma,\tau)_Q = \int_\Omega \sigma_{ij}\tau_{ij} dx.$$

The strain tensor is

$$\varepsilon(u) = (\varepsilon_{ij}(u)),\ \text{where } \varepsilon_{ij}(u) = \frac{1}{2}(u_{i,j} + u_{j,i});$$

$div\sigma = (\sigma_{ij,j})$ is the divergence of σ. For every element $v \in H_1$ we denote by v_ν and v_τ the normal and the tangential components of v on the boundary Γ given by

$$v_\nu = v.\nu, \quad v_\tau = v - v_\nu \nu.$$

Similary, for a regular function $\sigma \in Q_1$, we define its normal and tangential components by

$$\sigma_\nu = (\sigma\nu).\nu, \quad \sigma_\tau = \sigma\nu - \sigma_\nu \nu$$

and we recall that the following Green's formula holds:

$$(\sigma, \varepsilon(v))_Q + (div\sigma, v)_H = \int_\Gamma \sigma\nu.v da \quad \forall v \in H_1,$$

where da is the surface measure element. Let V be the closed subspace of H_1 defined by

$$V = \{v \in H_1 : v = 0 \text{ on } \Gamma_1\}.$$

Since $meas(\Gamma_1) > 0$, the following Korn's inequality holds [6], where the constant $c_\Omega > 0$ depends only on Ω and Γ_1. We equip V with the inner product

$$\|\varepsilon(v)\|_Q \geq c_\Omega \|v\|_{H_1} \quad \forall v \in V, \tag{2.10}$$

$$(u,v)_V = (\varepsilon(u), \varepsilon(v))_Q$$

and $\|.\|_V$ is the associated norm. It follows from Korn's inequality (2.10) that the norms $\|.\|_{H_1}$ and $\|.\|_V$ are equivalent on V. Then $(V, \|.\|_V)$ is a real Hilbert space. Moreover by Sobolev's trace theorem, there exists $d_\Omega > 0$ which depends only on the domain Ω, Γ_1 and Γ_3 such that

$$\|v\|_{(L^2(\Gamma_3))^d} \leq d_\Omega \|v\|_V \quad \forall v \in V. \tag{2.11}$$

For $p \in [1,\infty]$, we use the standard norm of $L^p(0,T;V)$. We also use the Sobolev space $W^{1,\infty}(0,T;V)$ equipped with the norm

$$\|v\|_{W^{1,\infty}(0,T;V)} = \|v\|_{L^\infty(0,T;V)} + \|\dot{v}\|_{L^\infty(0,T;V)}.$$

For every real Banach space $(X, \|.\|_X)$ and $T > 0$ we use the notation $C([0,T];X)$ for the space of continuous functions from $[0,T]$ to X; recall that $C([0,T];X)$ is a real Banach space with the norm

$$\|x\|_{C([0,T];X)} = \max_{t\in[0,T]} \|x(t)\|_X .$$

We suppose that the body forces and surface tractions have the regularity

$$f_1 \in C([0,T];H), \qquad f_2 \in C\left([0,T];\left(L^2(\Gamma_2)\right)^d\right) \tag{2.12}$$

and, moreover, we use Riesz's representation to define a function

$$f : [0,T] \to V$$

by

$$(f(t),v)_V = \int_\Omega f_1(t).vdx + \int_{\Gamma_2} f_2(t).vda - \int_{\Gamma_3} Sv_\nu da \;\forall v\in V,\, t\in[0,T]. \tag{2.13}$$

(2.12) and (2.13) imply that

$$f \in C([0,T];V).$$

Also we define the functional $j_{fr} : V\times V \to \mathbb{R}$ by

$$j_{fr}(v,w) = \int_{\Gamma_3} \mu(|v_\tau|)\, S\,|w_\tau|\, da \quad \forall v,w\in V,$$

where the coefficient of friction μ and S are assumed to satisfy

$$\left.\begin{array}{l}
(a)\;\; \mu : \Gamma_3\times\mathbb{R}_+ \to \mathbb{R}_+;\\
(b)\;\; \text{there exists } L_\mu > 0 \text{ such that}\\
\qquad |\mu(x,r_1)-\mu(x,r_2)| \le L_\mu |r_1-r_2| \;\; \forall r_1,r_2\in\mathbb{R}_+,\ a.e.\ x\in\Gamma_3;\\
(c)\;\; \text{for any } r\in\mathbb{R}_+, \text{ the mapping } x\to\mu(x,r) \text{ is measurable on } \Gamma_3;\\
(d)\;\; \text{the mapping } x\to\mu(x,0)\in L^2(\Gamma_3).
\end{array}\right\} \tag{2.14}$$

$$S\in L^\infty(\Gamma_3) \text{ and } S\ge 0 \;\; a.e. \text{ on } \Gamma_3. \tag{2.15}$$

In the study of Problem P_1 we assume that the viscosity operator A satisfies

$$\left.\begin{array}{l}
(a)\;\; A : \Omega\times S_d \to S_d;\\
(b)\;\text{there exists } M_A>0 \text{ such that}\\
\qquad |A(x,\varepsilon_1)-A(x,\varepsilon_2)| \le M_A|\varepsilon_1-\varepsilon_2|,\\
\qquad \text{for all } \varepsilon_1,\varepsilon_2 \text{ in } S_d,\ a.e.\ x \text{ in } \Omega;\\
(c)\;\text{there exists } m_A>0 \text{ such that}\\
\qquad (A(x,\varepsilon_1)-A(x,\varepsilon_2)).(\varepsilon_1-\varepsilon_2) \ge m_A|\varepsilon_1-\varepsilon_2|^2,\\
\qquad \text{for all } \varepsilon_1,\varepsilon_2 \text{ in } S_d,\ a.e.\ x \text{ in } \Omega;\\
(d)\;\text{the mapping } x\to A(x,\varepsilon) \text{ is Lebesgue measurable on } \Omega,\\
\qquad \text{for any } \varepsilon \text{ in } S_d;\\
(e)\;\; x\to A(x,0)\in Q.
\end{array}\right\} \tag{2.16}$$

The elasticity operator B satisfies

$$
(2.17)\quad \left.\begin{array}{l}
(a)\ B:\Omega\times S_d\rightarrow S_d\\
(b)\ \text{there exists } M_B>0 \text{ such that}\\
\qquad |B(x,\varepsilon_1)-B(x,\varepsilon_2)|\leq M_B|\varepsilon_1-\varepsilon_2|,\\
\qquad \text{for all } \varepsilon_1,\varepsilon_2 \text{ in } S_d,\ a.e.\ x \text{ in } \Omega;\\
(c)\ \text{the mapping } x\rightarrow B(x,\varepsilon)\ \text{ is Lebesgue measurable on } \Omega,\\
\qquad \text{for any } \varepsilon \text{ in } S_d;\\
(e)\ x\rightarrow B(x,0)\in Q.
\end{array}\right\}
$$

As in [19] we suppose that the adhesion coefficients c_ν, c_τ and ε_a satisfy the conditions:

$$
(2.18)\qquad c_\nu, c_\tau\in L^\infty(\Gamma_3),\ \varepsilon_a\in L^2(\Gamma_3),\ \ c_\nu,\ c_\tau,\ \varepsilon_a\geq 0\ a.e.\ \text{on } \Gamma_3.
$$

We assume that the initial data satisfy

$$
2.19\qquad u_0\in V,
$$

$$
(2.20)\qquad \beta_0\in L^2(\Gamma_3):0\leq\beta_0\leq 1,\ \ a.e.\ \text{on } \Gamma_3.
$$

Next, we define the functional $j_{ad}:L^2(\Gamma_3)\times V\times V\rightarrow\mathbb{R}$ by

$$
j_{ad}(\beta,u,v)=\int_{\Gamma_3}(-c_\nu\beta^2R_\nu(u_\nu)v_\nu+c_\tau\beta^2R_\tau(u_\tau).v_\tau)da.
$$

Finally, we need to introduce the following set for the bonding field:

$$
\mathcal{B}=\left\{\theta:[0,T]\rightarrow L^2(\Gamma_3):0\leq\theta(t)\leq 1\ \forall t\in[0,T],\ a.e.\ \text{on } \Gamma_3\right\}.
$$

Now assuming the solution to be sufficiently regular, we obtain by using Green's formula that the problem P_1 has the following variational formulation.

Problem P_2. Find a displacement field $u:[0,T]\rightarrow V$ and a bonding field $\beta:[0,T]\rightarrow L^2(\Gamma_3)$ such that

(2.21)

$$
\begin{array}{l}
(A\varepsilon(\dot u(t)),\varepsilon(v)-\varepsilon(\dot u(t)))_Q+(B\varepsilon(u(t)),\varepsilon(v)-\varepsilon(\dot u(t)))_Q+j_{fr}(u(t),v)\\[2ex]
-j_{fr}(u(t),\dot u(t))+j_{ad}(\beta(t),u(t),v-\dot u(t))\geq(f(t),v-\dot u(t))_V\\[2ex]
\forall\ v\in V,\ t\in[0,T],
\end{array}
$$

$$
(2.22)\quad \dot\beta(t)=-[\beta(t)(c_\nu|R_\nu(u_\nu(t))|^2+c_\tau|R_\tau(u_\tau(t))|^2)-\varepsilon_a]_+\ a.e.\ t\in(0,T),
$$

$$
(2.23)\qquad u(0)=u_0,
$$

$$
(2.24)\qquad \beta(0)=\beta_0.
$$

Our main result of this section, which will be established in the next is the following theorem.

Theorem 2.1. *Assume* (2.12), (2.14), (2.15), (2.16), (2.17), (2.18), (2.19) *and* (2.20). *Then there exists a unique solution to Problem P_2 which satisfies*

$$u \in C^1([0,T];V),\ \beta \in W^{1,\infty}\left(0,T;L^2(\Gamma_3)\right) \cap \mathcal{B}$$

if

$$d_\Omega^2 L_\mu \|S\|_{L^\infty(\Gamma_3)} < m_A.$$

3. Existence of solution

The proof of Theorem 2.1 will be carried out in several steps. In the first step, for a given $\eta \in C([0,T];V)$ and $g \in C([0,T];V)$ we consider the following variational problem.

Problem $P_{\eta g}$. Find $v_{\eta g} : [0,T] \to V$ such that

$$\begin{aligned} &(A\varepsilon(v_{\eta g}(t)), \varepsilon(w) - \varepsilon(v_{\eta g}(t)))_Q + (\eta(t), w - v_{\eta g}(t))_V + j_{fr}(g(t), w) \\ &-j_{fr}(g(t), v_{\eta g}(t)) \geq (f(t), w - v_{\eta g}(t))_V \quad \forall w \in V,\ t \in [0,T]. \end{aligned} \tag{3.1}$$

We show the following result.

Lemma 3.1. *Problem $P_{\eta g}$ has a unique solution which satisfies $v_{\eta g} \in C([0,T];V)$.*

Proof. We define the operator $C : V \to V$ by

$$(Cv, w)_V = (A\varepsilon(v), \varepsilon(w))_Q \quad \forall v, w \in V.$$

It follows from assumption (2.16) that C is a strongly monotone and Lipschitz continuous operator. Next, let $t \in [0,T]$. The functional $j_{fr}(g(t), .)$ is a continuous semi-norm on V, then by a classical argument of elliptic variational inequalities [1], we deduce that there exists a unique element $v_{\eta g}(t) \in V$ such that

$$\begin{aligned} &(A\varepsilon(v_{\eta g}(t)), \varepsilon(w) - \varepsilon(v_{\eta g}(t)))_Q + j_{fr}(g(t), w) - j_{fr}(g(t), v_{\eta g}(t)) \\ &\geq (f(t) - \eta(t), w - v_{\eta g}(t))_V \quad \forall w \in V. \end{aligned} \tag{3.2}$$

Thus, we use (3.2) to see that $v_{\eta g}(t)$ is the unique element which solves (3.1), for each $t \in [0,T]$. Now, let $t_1, t_2 \in [0,T]$. We write (3.2) for $t = t_1$ and $w = v_{\eta g}(t_2)$, then for $t = t_2$ and $w = v_{\eta g}(t_1)$; by adding the resulting inequalities we obtain

$$\begin{aligned} &(A\varepsilon(v_{\eta g}(t_1)) - A\varepsilon(v_{\eta g}(t_2)), \varepsilon(v_{\eta g}(t_1)) - \varepsilon(v_{\eta g}(t_2)))_Q \\ &\leq (f(t_1) - f(t_2), v_{\eta g}(t_1) - v_{\eta g}(t_2))_V - (\eta(t_1) - \eta(t_2), v_{\eta g}(t_1) - v_{\eta g}(t_2))_V \\ &+j_{fr}(g(t_1), v_{\eta g}(t_2)) - j_{fr}(g(t_1), v_{\eta g}(t_1)) \\ &+j_{fr}(g(t_2), v_{\eta g}(t_1)) - j_{fr}(g(t_2), v_{\eta g}(t_2)). \end{aligned}$$

Using (2.16) (c), (2.14) (b), (2.18), and (2.11), we see that

$$m_A \left\| v_{\eta g}(t_1) - v_{\eta g}(t_2) \right\|_V^2 \leq d_\Omega^2 L_\mu \left\| S \right\|_{L^\infty(\Gamma_3)} \left\| v_{\eta g}(t_1) - v_{\eta g}(t_2) \right\|_V^2$$

$$+ \left\| \eta(t_1) - \eta(t_2) \right\|_V \left\| v_{\eta g}(t_1) - v_{\eta g}(t_2) \right\|_V$$

$$+ d_\Omega^2 \left\| g(t_1) - g(t_2) \right\|_V \left\| v_{\eta g}(t_1) - v_{\eta g}(t_2) \right\|_V$$

$$+ \left\| f(t_1) - f(t_2) \right\|_V \left\| v_{\eta g}(t_1) - v_{\eta g}(t_2) \right\|_V .$$

Then, it follows that if

$$d_\Omega^2 L_\mu \left\| S \right\|_{L^\infty(\Gamma_3)} < m_A,$$

there exists a constant $c_1 > 0$ such that

$$\left\| v_{\eta g}(t_1) - v_{\eta g}(t_2) \right\|_V \leq$$

$$c_1 \left(\left\| f(t_1) - f(t_2) \right\|_V + \left\| g(t_1) - g(t_2) \right\|_V + \left\| \eta(t_1) - \eta(t_2) \right\|_V \right).$$

As $f \in C([0,T];V)$, $g \in C([0,T];V)$ and $\eta \in C([0,T];V)$, we deduce that $v_{\eta g} \in C([0,T];V)$.
Now, let us consider the operator $\Lambda_\eta : C([0,T];V) \to C([0,T];V)$ defined by

$$\Lambda_\eta g = g_\eta, \quad g \in C([0,T];V), \tag{3.3}$$

where

$$g_\eta(t) = u_0 + \int_0^t v_{\eta g}(s)\, ds, \ t \in [0,T]. \tag{3.4}$$

We have the lemma below.

Lemma 3.2. *The operator Λ_η has a unique fixed point $g_\eta^* \in C([0,T];V)$.*

Proof. We refer the reader to [[15], Proposition 4.2].
Next, for $\eta \in C([0,T];V)$, we denote by g_η^* the fixed point given in Lemma 3.2 and we define the function $v_\eta \in C([0,T];V)$ by

$$v_\eta = v_{\eta g_\eta^*}. \tag{3.5}$$

By (3.3) and (3.4), let $u_\eta : [0,T] \to V$ be the function given by

$$u_\eta(t) = g_\eta^*(t) = u_0 + \int_0^t v_\eta(s)\, ds, \ t \in [0,T], \tag{3.6}$$

then, we consider the following problem. □

Problem $P_{\eta\beta}$. Find a bonding field $\beta_\eta : [0,T] \to L^2(\Gamma_3)$ such that

$$\dot{\beta}_\eta(t) = -[\beta_\eta(t)(c_\nu |R_\nu(u_{\eta\nu}(t))|^2 + c_\tau |R_\tau(u_{\eta\tau}(t))|^2) - \varepsilon_a]_+ \ a.e.\ t \in (0,T), \tag{3.7}$$

$$\beta_\eta(0) = \beta_0. \tag{3.8}$$

We have the following result.

Lemma 3.3. *There exists a unique solution to Problem $P_{\eta\beta}$ and it satisfies*

$$\beta_\eta \in W^{1,\infty}\left(0,T;L^2\left(\Gamma_3\right)\right) \cap \mathcal{B}.$$

Proof. Let $k > 0$ and consider the closed subset X of $C\left([0,T];L^2\left(\Gamma_3\right)\right)$ defined as

$$X = \left\{\theta \in C\left([0,T];L^2\left(\Gamma_3\right)\right),\ \theta\left(0\right) = \beta_0\right\},$$

where the Banach space $C\left([0,T];L^2\left(\Gamma_3\right)\right)$ is endowed with the norm

$$\left\|\theta\right\|_k = \max_{t\in[0,T]}\left[e^{-kt}\left\|\theta\left(t\right)\right\|_{L^2(\Gamma_3)}\right] \text{ for all } \theta \in C\left([0,T];L^2\left(\Gamma_3\right)\right).$$

We define the mapping $\Psi : X \to X$ by

$$\Psi\beta\left(t\right) = \beta_0 - \int_0^t\left[\beta\left(s\right)\left(c_\nu\left|R_\nu\left(u_{\eta\nu}\left(s\right)\right)\right|^2 + c_\tau\left|R_\tau\left(u_{\eta\tau}\left(s\right)\right)\right|^2\right) - \varepsilon_a\right]_+ da$$

and we will prove that Ψ has a unique fixed point, which is equally the solution of the problem $P_{\eta\beta}$. Indeed, using that $\left|R_r\left(u_{\eta r}\right)\right| \leq L$, $r = \nu, \tau$, it follows that for all β_1, $\beta_2 \in X$, there exists a constant $c_2 > 0$ such that

$$\begin{aligned}\left\|\Psi\beta_1\left(t\right) - \Psi\beta_2\left(t\right)\right\|_{L^2(\Gamma_3)} &\leq c_2 \textstyle\int_0^t \left\|\beta_1\left(s\right) - \beta_2\left(s\right)\right\|_{L^2(\Gamma_3)} ds \\ &= c_2 \textstyle\int_0^t e^{ks}(e^{-ks}\left\|\beta_1\left(s\right) - \beta_2\left(s\right)\right\|_{L^2(\Gamma_3)})ds \\ &\leq c_2\left\|\beta_1 - \beta_2\right\|_k e^{kt}/k.\end{aligned}$$

Then

$$\begin{aligned}\left\|\Psi\beta_1 - \Psi\beta_2\right\|_k &= \max_{t\in[0,T]}\left[e^{-kt}\left\|\Psi\beta_1\left(t\right) - \Psi\beta_2\left(t\right)\right\|_{L^2(\Gamma_3)}\right] \\ &\leq \frac{c_2}{k}\left\|\beta_1 - \beta_2\right\|_k.\end{aligned}$$

Hence, for all β_1, $\beta_2 \in X$

$$\left\|\Psi\beta_1 - \Psi\beta_2\right\|_k \leq \frac{c_2}{k}\left\|\beta_1 - \beta_2\right\|_k, \tag{3.9}$$

so that the inequality (3.9) shows that for k sufficiently large, Ψ is a contraction. Then we deduce, by Banach fixed-point theorem that Ψ has a unique fixed point β_η which satisfies (3.7) and (3.8). To show that $\beta_\eta \in \mathcal{B}$, it suffices to use (3.7), (3.8) and (2.20), see [18] for details. □

Next, using Riesz's representation theorem we define the function

$$\Lambda : [0,T] \to V$$

by

$$\begin{aligned}&\left(\Lambda\eta\left(t\right), w\right)_V = \left(B\varepsilon\left(u_\eta\left(t\right)\right), \varepsilon\left(w\right)\right)_Q + j_{ad}\left(\beta_\eta\left(t\right), u_\eta\left(t\right), w\right), \\ &\forall w \in V,\ t \in [0,T].\end{aligned} \tag{3.10}$$

We have the lemma below.

Lemma 3.4. *For each $\eta \in C([0,T];V)$ the function $\Lambda\eta : [0,T] \to V$ belongs to $C([0,T];V)$. Moreover, there exists a unique $\eta^* \in C([0,T];V)$ such that $\Lambda\eta^* = \eta^*$.*

Proof. Let $\eta \in C([0,T];V)$, t_1, $t_2 \in [0,T]$. Using (3.10), it follows that there exists a constant $c_3 > 0$ such that

$$\|\Lambda\eta(t_1) - \Lambda\eta(t_2)\|_V \le \|B\varepsilon(u_\eta(t_1)) - B\varepsilon(u_\eta(t_2))\|_Q$$
$$+c_3(\left\|\beta_\eta^2(t_1) R_\tau(u_{\eta\tau}(t_1)) - \beta_\eta^2(t_2) R_\tau(u_{\eta\tau}(t_2))\right\|_{L^2(\Gamma_3)}$$
$$+\|\mu(|u_{\eta\tau}(t_1)|) - \mu(|u_{\eta\tau}(t_2)|)\|_{L^2(\Gamma_3)}$$
$$+\left\|\beta_\eta^2(t_1) R_\nu(u_{\eta\nu}(t_1)) - \beta_\eta^2(t_2) R_\nu(u_{\eta\nu}(t_2))\right\|_{L^2(\Gamma_3)}).$$

Now we use the properties (see [18]) of the operators R_ν, R_τ such that

$$|R_r(u_{\eta r})| \le L, r = \nu, \tau, \ |R_\nu(a) - R_\nu(b)| \le |a-b| \ \forall a, b \in \mathbb{R},$$
$$|R_\tau(a) - R_\tau(b)| \le |a-b| \quad \forall a, b \in \mathbb{R}^d,$$

$(2.14)(b)$, (2.17), and $0 \le \beta_\eta(t) \le 1$, $\forall t \in [0,T]$. Then it follows that there exists a constant $c_4 > 0$ such that

$$\|\Lambda\eta(t_1) - \Lambda\eta(t_2)\|_V$$
$$\le c_4(\|u_\eta(t_1) - u_\eta(t_2)\|_V + \|\beta_\eta(t_1) - \beta_\eta(t_2)\|_{L^2(\Gamma_3)}). \tag{3.11}$$

Since $u_\eta \in C^1([0,T];V)$ and $\beta_\eta \in W^{1,\infty}(0,T;V)$, we deduce from inequality (3.11) that $\Lambda\eta \in C([0,T];V)$.

Let now $\eta_1, \eta_2 \in C([0,T];V)$. For $t \in [0,T]$ we integrate (3.7) with the initial condition (3.8) to obtain that

$$\beta_{\eta_i}(t) = \beta_0 - \int_0^t [\beta_{\eta_i}(s)(c_\nu |R_\nu(u_{\eta_i\nu}(s))|^2 + c_\tau |R_\tau(u_{\eta_i\tau}(s))|^2) - \varepsilon_a]_+ da.$$

Then there exists a constant $c_5 > 0$ such that

$$\|\beta_{\eta_1}(t) - \beta_{\eta_2}(t)\|_{L^2(\Gamma_3)} \le$$
$$c_5(\textstyle\int_0^t \left\|\beta_{\eta_1}(s)|R_\nu(u_{\eta_1\nu}(s))|^2 - \beta_{\eta_2}(s)|R_\nu(u_{\eta_2\nu}(s))|^2\right\|_{L^2(\Gamma_3)} ds$$
$$+\textstyle\int_0^t \left\|\beta_{\eta_1}(s)|R_\tau(u_{\eta_1\tau}(s))|^2 - \beta_{\eta_2}(s)|R_\tau(u_{\eta_2\tau}(s))|^2\right\|_{L^2(\Gamma_3)} ds)$$

and after some elementary calculus we find that there exists a constant $c_6 > 0$ such that

$$\|\beta_{\eta_1}(t) - \beta_{\eta_2}(t)\|_{L^2(\Gamma_3)} \le c_6(\textstyle\int_0^t \|\beta_{\eta_1}(s) - \beta_{\eta_2}(s)\|_{L^2(\Gamma_3)}$$
$$+\textstyle\int_0^t \|u_{\eta_1\nu}(s) - u_{\eta_2\nu}(s)\|_{L^2(\Gamma_3)} ds + \int_0^t \|u_{\eta_1\tau}(s) - u_{\eta_2\tau}(s)\|_{(L^2(\Gamma_3))^d} ds).$$

Then by (2.11), it follows that

$$\begin{aligned}&\|\beta_{\eta_1}(t)-\beta_{\eta_2}(t)\|_{L^2(\Gamma_3)}\\&\le c_6\big(\textstyle\int_0^t\|\beta_{\eta_1}(s)-\beta_{\eta_2}(s)\|_{L^2(\Gamma_3)}+2d_\Omega\int_0^t\|u_{\eta_1}(s)-u_{\eta_2}(s)\|_V\,ds\big)\end{aligned}$$

and using a Gronwall-type inequality, we deduce that there exists a constant $c_7>0$ such that

$$\|\beta_{\eta_1}(t)-\beta_{\eta_2}(t)\|_{L^2(\Gamma_3)}\le c_7\int_0^t\|u_{\eta_1}(s)-u_{\eta_2}(s)\|_V\,ds. \tag{3.12}$$

On the other hand, using arguments similar to those in the proof of (3.12), we find that there exists a constant $c_8>0$ such that

$$\begin{aligned}&\|\Lambda\eta_1(t)-\Lambda\eta_2(t)\|_V\\&\le c_8(\|u_{\eta_1}(t)-u_{\eta_2}(t)\|_V+\|\beta_{\eta_1}(t)-\beta_{\eta_2}(t)\|_{L^2(\Gamma_3)}).\end{aligned}$$

Then, by (3.12) we have

$$\begin{aligned}&\|\Lambda\eta_1(t)-\Lambda\eta_2(t)\|_V\\&\le c_8(\|u_{\eta_1}(t)-u_{\eta_2}(t)\|_V+c_7\textstyle\int_0^t\|u_{\eta_1}(s)-u_{\eta_2}(s)\|_V\,ds).\end{aligned} \tag{3.13}$$

On the other hand, the function u_{η_i} satisfies the inequality

$$\begin{aligned}&(A\varepsilon(v_{\eta i}(t)),\varepsilon(w-v_{\eta i}(t)))_Q+(\eta_i(t),w-v_{\eta i}(t))_V+j_{fr}(u_{\eta i}(t),w)\\&-j_{fr}(u_{\eta i}(t),v_{\eta i}(t))\ge(f(t),w-v_{\eta i}(t))_V\quad\forall w\in V,\end{aligned} \tag{3.14}$$

$i=1,2$. It follows from (3.14) and the estimate in the proof of Lemma 3.1 that there exists a constant $c_9>0$ such that

$$\begin{aligned}&\|u_{\eta_1}(t)-u_{\eta_2}(t)\|_V\le\textstyle\int_0^t\|v_{\eta_1}(s)-v_{\eta_2}(s)\|_V\,ds\\&\le c_9(\textstyle\int_0^t\|\eta_1(s)-\eta_2(s)\|_V\,ds+\int_0^t\|u_{\eta_1}(s)-u_{\eta_2}(s)\|_V\,ds).\end{aligned}$$

Using now a Gronwall-type inequality we get

$$\|u_{\eta_1}(t)-u_{\eta_2}(t)\|_V\le c_{10}\int_0^t\|\eta_1(s)-\eta_2(s)\|_V\,ds, \tag{3.15}$$

where $c_{10}>0$. Then by (3.13) and (3.15), it follows that there exists a constant $c_{11}>0$ such that

$$\|\Lambda\eta_1(t)-\Lambda\eta_2(t)\|_V\le c_{11}\int_0^t\|\eta_1(s)-\eta_2(s)\|_V\,ds. \tag{3.16}$$

Let now $\alpha>0$, and denote

$$\|\eta\|_\alpha=\sup_{t\in[0,T]}\left[e^{-\alpha t}\|\eta(t)\|_V\right]\quad\forall\eta\in C([0,T];V).$$

Clearly $\|.\|_\alpha$ defines a norm on the space $C([0,T];V)$ which is equivalent to the standard norm $\|.\|_{C([0,T];V)}$. Using (3.16) and arguments similar to those in the proof of (3.9), we have

$$\|\Lambda\eta_1 - \Lambda\eta_2\|_\alpha \leq \frac{c_{11}}{\alpha}\|\eta_1 - \eta_2\|_\alpha, \ \forall \eta_1, \ \eta_2 \in C([0,T];V).$$

So for α sufficiently large, the operator Λ is a contraction on the space $C([0,T];V)$ endowed with the norm $\|.\|_k$. Then by Banach-fixed point theorem it follows that Λ has a unique fixed point $\eta^* \in C([0,T];V)$, which concludes the proof.

Now, we have all the ingredients to prove Theorem 2.1.

Proof of Theorem 2.1. Existence. Let $\eta^* \in C([0,T];V)$ be the fixed point of Λ and let v_{η^*}, and u_{η^*} be the functions given by (3.5) and (3.6) for $\eta = \eta^*$. Let β_{η^*} the solution of Problem $P_{\eta\beta}$ for $\eta = \eta^*$. We show that $(u_{\eta^*}, \beta_{\eta^*})$ is a solution of Problem P_2 . To this end, choosing $\eta = \eta^*$, $g = g^*_{\eta^*}$ in (3.1) and using (3.5), we obtain
(3.17)

$$(A\varepsilon(v_{\eta^*}(t)), \varepsilon(w) - \varepsilon(v_{\eta^*}(t)))_Q + (\eta^*(t), w - v_{\eta^*}(t))_V + j_{fr}\left(g^*_{\eta^*}(t), w\right)$$

$$-j_{fr}\left(g^*_{\eta^*}(t), v_{\eta^*}(t)\right) \geq (f(t), w - v_{\eta^*}(t))_V \quad \forall w \in V, \ t \in [0,T].$$

Let β denote the solution of Problem $P_{\eta\beta}$ for $\eta = \eta^*$, i.e., $\beta = \beta_{\eta^*}$. As $\eta^* = \Lambda\eta^*$, the inequality (2.21) follows from (3.4), (3.6) and (3.17), since $v_{\eta^*} = \dot{u}_{\eta^*}$ and $g^*_{\eta^*} = u_{\eta^*}$. The equality (2.23) follows from (3.6), and the regularity $u_{\eta^*} \in C^1([0,T];V)$ is a consequence of Lemma 3.1, (2.19) and (3.6). Clearly, equalities (2.22) and (2.24) hold by Problem $P_{\eta\beta}$. Also the regularity of the bonding field $\beta \in W^{1,\infty}\left(0,T;L^2(\Gamma_3)\right) \cap \mathcal{B}$ follows from Lemma 3.3. □

Uniqueness. Let $(u,\beta) \in C^1([0,T];V) \times W^{1,\infty}\left(0,T;L^2(\Gamma_3)\right) \cap \mathcal{B}$ be a solution of Problem P_2 and denote by $\eta \in C([0,T];V)$ the function defined by
(3.18)

$$(\eta(t), w)_V = (B\varepsilon(u(t)), \varepsilon(w))_Q + j_{ad}(\beta(t), u(t), w), \ \forall w \in V, \ t \in [0,T],$$

and let

$$v = \dot{u}. \tag{3.19}$$

Using (2.21) we obtain that v is a solution of the variational problem $P_{\eta u}$ and since this problem has a unique solution $v_{\eta u} \in C([0,T];V)$, we conclude that

$$v = v_{\eta u}. \tag{3.20}$$

Hence, from (2.23), (3.19) and (3.20) we obtain

$$u(t) = u_0 + \int_0^t v_{\eta u}(s)\,ds, \ t \in [0,T],$$

i.e., u is a fixed point of Λ_η, defined by $\Lambda_\eta u = u$. It follows from Lemma 3.1 that $u = g^*_\eta$ and by (3.20) we have

$$v = v_{\eta g^*_\eta}. \tag{3.21}$$

Then, (3.5) and (3.21) imply

(3.22) $$v = v_\eta.$$

So, it follows from (2.23), (3.6), (3.19) and (3.22) that

(3.23) $$u = u_\eta.$$

Next, (2.22) and the initial condition $\beta(0) = \beta_0$ imply that β is a solution of Problem $P_{\eta\beta}$ and, since this problem admits a unique solution β_η, we conclude that

(3.24) $$\beta = \beta_\eta.$$

Using now (3.10), (3.18), (3.23) , and (3.24) we obtain that $\Lambda\eta = \eta$ and as the operator Λ admits a unique fixed point guaranteed by Lemma 3.4, it follows that

(3.25) $$\eta = \eta^*.$$

The uniqueness of the solution is now a consequence of (3.23)–(3.25).

References

[1] H. Brezis, *Equations et inéquations non linéaires dans les espaces vectoriels en dualité*, Annales Inst. Fourier **18** (1968), 115–175.

[2] L. Cangémi, *Frottement et adhérence: modèle, traitement numérique et application à l'interface fibre/matrice,* Ph. D. Thesis, Univ. Méditerranée, Aix Marseille I, 1997.

[3] O. Chau, J. R. Fernandez, M. Shillor, and M. Sofonea, *Variational and numerical analysis of a quasistatic viscoelastic contact problem with adhesion*, Journal of Computational and Applied Mathematics **159** (2003), 431–465.

[4] O. Chau, M. Shillor, and M. Sofonea, *Dynamic frictionless contact with adhesion,* J. Appl. Math. Phys. (ZAMP) **55** (2004), 32–47.

[5] M. Cocou and R. Rocca, *Existence results for unilateral quasistatic contact problems with friction and adhesion,* Math. Model. Num. Anal. **34** (2000), 981–1001.

[6] G. Duvaut and J.-L. Lions, *Les inéquations en mécanique et en physique*, Dunod, Paris 1972.

[7] J. R. Fernandez, M. Shillor, and M. Sofonea, *Analysis and numerical simulations of a dynamic contact problem with adhesion,* Math. Comput. Modelling **37** (2003), 1317–1333.

[8] M. Frémond, *Adhérence des solides,* J. Mécanique Théorique et Appliquée **6** (1987), 383–407.

[9] M. Frémond, *Equilibre des structures qui adhèrent à leur support,* C. R. Acad. Sci. Paris, **295**, série II (1982), 913–916.

[10] M. Frémond, *Non Smooth Thermomechanics*, Springer, Berlin 2002.

[11] I. R. Ionescu and Q.-L. Nguyen, *Dynamic contact problems with slip dependent friction in viscoelasticity*, Int. J. Appl. Math. Comput. Sci. **12** (2002), 71–80.

[12] S. A. Nassar, T. Andrews, S. Kruk, and M. Shillor, *Modelling and simulations of a bonded rod,* Math. Comput. Modelling **42** (2005), 553–572.

[13] G. J. Perrin, J. R. Rice, and G. Zheng, *Self-healing slip pulse on a frictional surface*, J. Mech. Phys. Solids **43** (1995), 1461–1495.

[14] M. Raous, L. Cangémi, and M. Cocu, *A consistent model coupling adhesion, friction, and unilateral contact,* Comput. Meth. Appl. Mech. Engng. **177** (1999), 383–399.

[15] R. Rochdi, M. Shillor, and M. Sofonea, *Quasistatic viscoelastic contact with normal compliance and friction*, Journal of Elasticity **51** (1998), 105–126.

[16] J. Rojek and J. J. Telega, *Contact problems with friction, adhesion and wear in orthopeadic biomechanics. I: General developements,* J. Theor. Appl. Mech. **39** (2001), 655–677.

[17] M. Sofonea, W. Han, and M. Shillor, *Analysis and Approximation of Contact Problems with Adhesion or Damage*, Pure and Applied Mathematics 276, Chapman & Hall / CRC Press, Boca Raton, Florida, 2006.

[18] M. Sofonea and T. V. Hoarau-Mantel, *Elastic frictionless contact problems with adhesion*, Adv. Math. Sci. Appl. **15**, no. 1 (2005), 49–68.

[19] M. Sofonea, R. Arhab, and R. Tarraf, *Analysis of electroelastic frictionless contact problems with adhesion*, Journal of Applied Mathematics, **64217** (2006), 1–25.

[20] A. Touzaline, *A quasistatic contact problem with friction and adhesion for viscoelastic maerials*, Appl. Math. (Warsaw) **37** (2010), 39–52.

[21] A. Touzaline, *A study of a unilateral and adhesive contact problem with normal compliance,* Appl. Math. (Warsaw) **41** (2014), 385–402.

Laboratoire de Systèmes Dynamiques
Faculté de Mathématiques, USTHB
BP 32 El Alia, Bab-Ezzouar, 16111
Algérie
e-mail: ttouzaline@yahoo.fr

Presented by Ilona Zasada at the Session of the Mathematical-Physical Commission of the Łódź Society of Sciences and Arts on May 28, 2015

O ZAGADNIENIU ELASTYCZNEGO KONTAKTU Z UWZGLĘDNIENIEM LEPKOŚCI PRZY TARCIU ZALEŻNYM OD POŚLIZGU I ADHEZJI

S t r e s z c z e n i e

Przedstawiony jest matematyczny model zagadnienia sformułowanego w tytule pracy.

Słowa kluczowe: elastyczność, lepkość, przyleganie, adhezja, tarcie, ślizg, poślizg, stały punkt, słabe rozwiązanie

PL ISSN 0459-6854

B U L L E T I N

DE LA SOCIÉTÉ DES SCIENCES ET DES LETTRES DE ŁÓDŹ

2015 Vol. LXV

Recherches sur les déformations no. 2

pp. 61–69

Mohamed Arif, Jacek Dziok, and Mohamed Raza

ON SOME VARIATIONS OF JANOWSKI FUNCTIONS

Summary

The aim of this paper is to define the classes of analytic functions related to functions with bounded boundary rotations. Some remarkable properties of these classes are investigated. Newly introduced classes generalize the classes of Janowski functions and the class of functions with bounded boundary rotation.

Keywords and phrases: Janowski functions, bounded variation, bounded radius rotation, bounded boundary rotation

1. Introduction

Let A denote the class of functions which are analytic in $E = \{z : |z| < 1\}$ and let A_p $(p \in \mathbb{N}_0 := \{0, 1, 2, ...\})$ denote the class of functions $f \in A$ of the form

$$f(z) = z^p + \sum_{n=p+1}^{\infty} a_n z^n \quad (z \in E). \tag{1.1}$$

A function $f \in A$ is said to be *subordinated* to a function $g \in A$ with notation $f \prec g$, if there exists a Schawarz function $w \in A$ with $w(0) = 0$ and $|w(z)| < 1$ $(z \in E)$ and such that $f(z) = g(w(z))$ $(z \in E)$. In particular, if g is univalent in E, then $f \prec g$ if and only if $f(0) = g(0)$ and $f(E) \subset g(E)$.

Let $-1 \leq b < a \leq 1,\ 0 \leq \alpha < 1, 0 < \beta \leq 1,\ m \leq 2$.

Definition 1.1. A function $h \in A_0$ is said to belong to the class $P_\beta(a, b, \alpha)$, if

$$h(z) \prec h_\beta(p, a, b, \alpha) := (1 - \alpha)\left(\frac{1 + az}{1 + bz}\right)^\beta + \alpha = 1 + a_1 z + \dots. \tag{1.2}$$

Moreover, let $P_\beta(a,b) := P_\beta(a,b,0)$.

The class $P(a,b) := P_1(a,b)$ was introduced by Janowski [11,12] (see also [6,9, 10,20]) and $P := P(1,-1)$ is the class of analytic functions with positive real part. It is easy to show that

$$h \in P_\beta(a,b) \Longleftrightarrow q = (1-\alpha)h + \alpha \in P_\beta(a,b,\alpha) \tag{1.3}$$

We note, that the Herglotz representation for a function $h \in P_\beta(a,b,\alpha)$ is given as

$$h(z) = \alpha + \frac{1-\alpha}{2}\int_0^{2\pi}\left(\frac{1+aze^{-i\phi}}{1+bze^{-i\phi}}\right)^\beta d\mu(\phi) \quad (z \in E), \tag{1.4}$$

where μ is a non-decreasing function in $[0,2\pi]$ such that $\int_0^{2\pi} d\mu(\phi) = 2$; see for details [7] and [8].

Definition 1.2. A function $h \in A_0$ is said to the class $P_{m,\beta}(a,b,\alpha)$, if there exists a function $\mu(\phi)$ which is non-decreasing in $[0,2\pi]$ with

$$\int_0^{2\pi} d\mu(\phi) = 2 \quad\text{and}\quad \int_0^{2\pi} |d\mu(\phi)| \leq m$$

such that h is given by (1.4).

Now we define the following classes of functions:

$$R_{m,\beta}(p,a,b,\alpha) = \left\{ f \in A_p : \frac{zf'(z)}{pf(z)} \in P_{m,\beta}(a,b,\alpha) \right\},$$
$$V_{m,\beta}(p,a,b,\alpha) = \left\{ f \in A_p : \frac{(zf'(z))'}{pf'(z)} \in P_{m,\beta}(a,b,\alpha) \right\},$$
$$(p \in \mathbb{N} := \mathbb{N}_0 \diagdown \{0\},\ f(z)z^{-1} \neq 0,\ f'(z) \neq 0,\ z \in E).$$

Special cases:

For $p=1, \beta=1, \alpha=0$, we obtain the classes studied by Noor and Yousaf [15] and Noor and Arif [14].

For $p=1, a=1, b=-1, \beta=1, \alpha=0$, the classes introduced by Paatero [16] and Pinchuk [18].

For $p=1, a=1, b=-1, \beta=1, 0 \leq \alpha < 1$, we obtain the classes defined by Padmanabhan and Parvatham [17].

For $p=1, a=1, b=-1, \beta=1, \alpha = 1 - e^{-i\lambda}(1-\rho)\cos\lambda$, the classes studied by Moulis [13], see also [1,2].

For $a=1, b=-1$ or $\alpha=0, a=2\rho-1, b=-1$ we have the classes studied by Dziok [3,5].

It can easily be seen that

$$f \in V_{m,\beta}(p,a,b,\alpha) \Longleftrightarrow \frac{zf'(z)}{p} \in R_{m,\beta}(p,a,b,\alpha)\,. \tag{1.5}$$

Some remarkable properties of defined classes are investigated.

2. Main results

The function $\varphi := h_\beta(p,a,b,0)$ defined by (1.2) is univalent and convex in E. Moreover, the domain $\varphi(E)$ is symetric with respect the real axis. Therefore, by using properties of subordination we have the following lemma.

Lemma 2.1. *Let $h \in P_\beta(a,b)$, $|z| = r < 1$. Then*

$$\left(\frac{1-ar}{1-br}\right)^\beta \le \mathrm{Re}\ h(z) \le |h(z)| \le \left(\frac{1+ar}{1+br}\right)^\beta.$$

The result is sharp with extremal function $h_\beta(p,a,b,0)$ defined by (1.2).

Lemma 2.2. [19] *Let $f \in A$ be a function of the form:*

$$f(z) = \sum_{n=1}^{\infty} a_n z^n \quad (z \in E)\,.$$

If $g \in A_1$ is a function univalent and convex in E and $f \prec g$, then

$$|a_n| \le 1 \qquad (n \in \mathbb{N})\,.$$

Lemma 2.3. *Let $h \in P_\beta(a,b,\alpha)$ be of the form*

$$h(z) = 1 + \sum_{n=1}^{\infty} h_n z^n \quad (z \in E)\,. \tag{2.1}$$

Then

$$|h_n| \le \beta(a-b)(1-\alpha) \quad (n \in \mathbb{N})\,.$$

Proof. Let $h \in P_\beta(a,b,\alpha)$. Then from Definition 1.2 we have

$$\frac{h(z)-1}{\beta(a-b)(1-\alpha)} \prec g(z),$$

where

$$g(z) = \frac{1}{\beta(a-b)}\left\{\left(\frac{1+az}{1+bz}\right)^\beta - 1\right\} = z + ... \quad (z \in E)\,.$$

Thus, by (2.1), we get

$$\sum_{n=1}^{\infty} \frac{h_n}{\beta(a-b)(1-\alpha)} z^n \prec g(z)\,.$$

Since the function g is univalent and convex in E, by Lemma 2.2 we obtain the required result. $\square$

Lemma 2.4. [4] *If $h \in P_{m,\beta}(a,b,\alpha)$, then there exist $h_1, h_2 \in P_\beta(a,b,\alpha)$ such that*

$$h = \left(\frac{m}{4}+\frac{1}{2}\right)h_1 - \left(\frac{m}{4}-\frac{1}{2}\right)h_2. \tag{2.2}$$

Theorem 2.5. *Let $h \in P_{m,\beta}(a,b,\alpha)$ be of the form* (2.1)*. Then*

$$|h_n| \le \frac{m}{2}\beta(a-b)(1-\alpha) \quad (n \in \mathbb{N}).$$

Proof. Let $h \in P_{m,\beta}(a,b,\alpha)$. Then, by Lemma 2.4 there exist $h_1, h_2 \in P_\beta(a,b,\alpha)$ such that

$$h = \left(\frac{m}{4}+\frac{1}{2}\right)h_1 - \left(\frac{m}{4}-\frac{1}{2}\right)h_2.$$

Let

$$h_1(z) = 1 + \sum_{n=1}^{\infty} c_n z^n, \ h_2(z) = 1 + \sum_{n=1}^{\infty} d_n z^n \quad (z \in E).$$

Then

$$1 + \sum_{n=1}^{\infty} h_n z^n = \left(\frac{m}{4}+\frac{1}{2}\right)\left(1 + \sum_{n=1}^{\infty} c_n z^n\right) - \left(\frac{m}{4}-\frac{1}{2}\right)\left(1 + \sum_{n=1}^{\infty} d_n z^n\right).$$

Comparing the coefficients at z^n, we obtain

$$h_n = \left(\frac{m}{4}+\frac{1}{2}\right)c_n - \left(\frac{m}{4}-\frac{1}{2}\right)d_n.$$

Now using the triangle inequality with Lemma 2.3, we get the required result. $\square$

Theorem 2.6. *Let $h \in P_{m,\beta}(a,b,\alpha)$, $|z| = r < 1$, $0 \le \alpha < 1$. Then*

$$(1-\alpha)\left(\left(\frac{m}{4}+\frac{1}{2}\right)\left(\frac{1-ar}{1-br}\right)^{\beta} - \left(\frac{m}{4}-\frac{1}{2}\right)\left(\frac{1+ar}{1+br}\right)^{\beta}\right) + \alpha \le$$

$$\operatorname{Re} h(z) \le (1-\alpha)\left(\left(\frac{m}{4}+\frac{1}{2}\right)\left(\frac{1+ar}{1+br}\right)^{\beta} - \left(\frac{m}{4}-\frac{1}{2}\right)\left(\frac{1-ar}{1-br}\right)^{\beta}\right) + \alpha.$$

The result is sharp.

Proof. Let $h \in P_{m,\beta}(a,b,\alpha)$. Then there exist $h_1, h_2 \in P_\beta(a,b)$, such that

$$h = \left(\frac{m}{4}+\frac{1}{2}\right)((1-\alpha)h_1 + \alpha) - \left(\frac{m}{4}-\frac{1}{2}\right)((1-\alpha)h_2 + \alpha).$$

Thus, by Lemma 2.1 we have

$$\begin{aligned}\mathrm{Re}h\left(z\right) &\geq \left(\frac{m}{4}+\frac{1}{2}\right)\left((1-\alpha)\left(\frac{1-ar}{1-br}\right)^{\beta}+\alpha\right)\\ &\quad-\left(\frac{m}{4}-\frac{1}{2}\right)\left((1-\alpha)\left(\frac{1+ar}{1+br}\right)^{\beta}+\alpha\right).\end{aligned}$$

For the upper bound, we note that

$$\begin{aligned}&\mathrm{Re}h\left(z\right)\leq\left(\frac{m}{4}+\frac{1}{2}\right)\max_{h_1\in P_\beta(a,b)}\left\{(1-\alpha)\,\mathrm{Re}h_1\left(z\right)+\alpha\right\}-\\ &\left(\frac{m}{4}-\frac{1}{2}\right)\min_{h_1\in P_\beta(a,b)}\left\{(1-\alpha)\,\mathrm{Re}h_2\left(z\right)+\alpha\right\},\\ &\leq\left(\frac{m}{4}+\frac{1}{2}\right)\left((1-\alpha)\left(\frac{1+ar}{1+br}\right)^{\beta}+\alpha\right)\\ &-\left(\frac{m}{4}-\frac{1}{2}\right)\left((1-\alpha)\left(\frac{1-ar}{1-br}\right)^{\beta}+\alpha\right).\end{aligned}$$

By taking

$$h_1=\left(\frac{1+az}{1+bz}\right)^{\beta},\ h_2=\left(\frac{1-az}{1-bz}\right)^{\beta},\ z=r,$$

it can easily shown that this result is sharp. □

Theorem 2.7. *The class $P_{m,\beta}\left(a,b,\alpha\right)$ is a convex set.*

Proof. Let $h,q\in P_{m,\beta}\left(a,b,\alpha\right)$. Then there exist $h_1,h_2,q_1,q_2\in P_\beta\left(a,b,\alpha\right)$ such that

$$\begin{aligned}h&=\left(\frac{m}{4}+\frac{1}{2}\right)h_1-\left(\frac{m}{4}-\frac{1}{2}\right)h_2,\\ q&=\left(\frac{m}{4}+\frac{1}{2}\right)q_1-\left(\frac{m}{4}-\frac{1}{2}\right)q_2.\end{aligned}$$

Now for $0\leq\gamma\leq1$, we consider

$$\begin{aligned}&(1-\gamma)\,h+\gamma q=(1-\gamma)\left\{\left(\frac{m}{4}+\frac{1}{2}\right)h_1-\left(\frac{m}{4}-\frac{1}{2}\right)h_2\right\}\\ &+\gamma\left\{\left(\frac{m}{4}+\frac{1}{2}\right)q_1-\left(\frac{m}{4}-\frac{1}{2}\right)q_2\right\}\\ &=\left(\frac{m}{4}+\frac{1}{2}\right)\varphi_1-\left(\frac{m}{4}-\frac{1}{2}\right)\varphi_2,\end{aligned}$$

where

$$\varphi_1=(1-\gamma)\,h_1+\gamma q_1,\ \varphi_2=(1-\gamma)\,h_2+\gamma q_2$$

both belong to $P_\beta\left(a,b,\alpha\right)$ being a convex set. Hence $P_{m,\beta}\left(a,b,\alpha\right)$ is a convex set. □

Theorem 2.8. *Let $h \in P_{m,\beta}(a,b,\alpha)$, $z = re^{i\theta} \in E$. Then*

$$\frac{1}{2\pi}\int_0^{2\pi} \left|h\left(re^{i\theta}\right)\right|^2 d\theta \leq \frac{4 + \left[\{m\beta(1-\alpha)(a-b)\}^2 - 4\right]r^2}{4(1-r^2)}. \tag{2.3}$$

Proof. Using the Parseval identity, we have

$$\frac{1}{2\pi}\int_0^{2\pi} \left|h\left(re^{i\theta}\right)\right|^2 d\theta = \sum_{n=0}^{\infty} |h_n|^2 r^{2n}$$

by using Theorem 2.5. Thus we have

$$\frac{1}{2\pi}\int_0^{2\pi} \left|h\left(re^{i\theta}\right)\right|^2 d\theta \leq 1 + \left(\frac{m}{2}\beta(a-b)(1-\alpha)\right)^2 \sum_{n=1}^{\infty} r^{2n}.$$

Hence (2.3) follows easily. □

Theorem 2.9. *Let $f \in A_p$. Then $f \in R_{m,\beta}(p,a,b,\alpha)$ if and only if*

$$f(z) = z^p \exp \int_0^{2\pi}\int_0^{z} \frac{p(1-\alpha)}{2s}\left[\left(\frac{1+ase^{-i\phi}}{1+bse^{-i\phi}}\right)^{\beta} - 1\right] ds d\mu(\phi).$$

Proof. Let $f \in R_{m,\beta}(p,a,b,\alpha)$. Then

$$\frac{zf'(z)}{pf(z)} = \alpha + \frac{1-\alpha}{2}\int_0^{2\pi}\left(\frac{1+aze^{-i\phi}}{1+bze^{-i\phi}}\right)^{\beta} d\mu(\phi).$$

This implies that

$$\left(\log\frac{f(z)}{z^p}\right)' = \frac{p(1-\alpha)}{2z}\int_0^{2\pi}\left[\left(\frac{1+aze^{-i\phi}}{1+bze^{-i\phi}}\right)^{\beta} - 1\right] d\mu(\phi).$$

Hence,

$$\left(\log\frac{f(z)}{z^p}\right) = \int_0^{2\pi}\int_0^{z} \frac{p(1-\alpha)}{2s}\left[\left(\frac{1+ase^{-i\phi}}{1+bse^{-i\phi}}\right)^{\beta} - 1\right] ds d\mu(\phi).$$

Therefore,

$$f(z) = z^p \exp \int_0^{2\pi}\int_0^{z} \frac{p(1-\alpha)}{2s}\left[\left(\frac{1+ase^{-i\phi}}{1+bse^{-i\phi}}\right)^{\beta} - 1\right] ds d\mu(\phi)$$

and the proof is completed. □

Corollary 2.10. *Let $f \in A_p$. Then $f \in R_{m,1}(p,a,b,\alpha)$, if and only if*

$$f(z) = \begin{cases} z^p \exp\left\{ p(1-\alpha)\left(\frac{a-b}{2b}\right) \int\limits_0^{2\pi} \log\left(1+bze^{-i\phi}\right) d\mu(\phi) \right\}, & b \neq 0, \\ z^p \exp\left\{ p(1-\alpha)\frac{a}{2} \int\limits_0^{2\pi} ze^{-i\phi} d\mu(\phi) \right\}, & b = 0. \end{cases}$$

Theorem 2.11. *Let $f \in R_{m,\beta}(p,a,b,\alpha)$. Then there exist $f_1,\ f_2 \in R_{2,\beta}(p,a,b,\alpha)$ such that*

$$f = \frac{f_1^{\left(\frac{m+2}{4}\right)}}{f_2^{\left(\frac{m-2}{4}\right)}}. \tag{2.4}$$

Proof. Let $f \in R_{m,\beta}(p,a,b,\alpha)$. Then there exist $h_1, h_2 \in P_{m,\beta}(a,b,\alpha)$ such that

$$\frac{zf'(z)}{pf(z)} = \left(\frac{m}{4}+\frac{1}{2}\right) h_1(z) - \left(\frac{m}{4}-\frac{1}{2}\right) h_2(z).$$

Thus, there exist $f_1, f_2 \in R_{2,\beta}(p,a,b,\alpha)$ such that

$$\frac{zf'(z)}{pf(z)} = \left(\frac{m}{4}+\frac{1}{2}\right) \frac{zf_1'(z)}{pf_1(z)} - \left(\frac{m}{4}-\frac{1}{2}\right) \frac{zf_2'(z)}{pf_2(z)},$$

$$\frac{f'(z)}{f(z)} = \left(\frac{m}{4}+\frac{1}{2}\right) \frac{f_1'(z)}{f_1(z)} - \left(\frac{m}{4}-\frac{1}{2}\right) \frac{f_2'(z)}{f_2(z)},$$

and the integration gives

$$\log f(z) = \left(\frac{m}{4}+\frac{1}{2}\right) \log f_1(z) - \left(\frac{m}{4}-\frac{1}{2}\right) \log f_2(z).$$

Thus we get (2.4). □

By (1.5), Theorems 2.9 and 2.11 with Corollary 2.10 we have the following results.

Corollary 2.12. *Let $f \in A_p$. Then $f \in V_{m,\beta}(p,a,b,\alpha)$, if and only if*

$$f'(z) = pz^{p-1} \exp \int\limits_0^{2\pi} \int\limits_0^{z} \frac{p(1-\alpha)}{2s} \left[\left(\frac{1+ase^{-i\phi}}{1+bse^{-i\phi}} \right)^{\beta} - 1 \right] ds d\mu(\phi).$$

Corollary 2.13. *Let* $f \in A_p$. *Then* $f \in V_{m,1}(p,a,b,\alpha)$, *if and only if*

$$f'(z) = \begin{cases} pz^{p-1} \exp\left\{ p(1-\alpha)\left(\frac{a-b}{2b}\right) \int\limits_0^{2\pi} \log\left(1 + bze^{-i\phi}\right) d\mu(\phi) \right\}, & b \neq 0, \\ pz^{p-1} \exp\left\{ p(1-\alpha)\frac{a}{2} \int\limits_0^{2\pi} ze^{-i\phi} d\mu(\phi) \right\}, & b = 0. \end{cases}$$

Corollary 2.14. *Let* $f \in V_{m,\beta}(p,a,b,\alpha)$. *Then there exist* $f_1, f_2 \in V_{2,\beta}(p,a,b,\alpha)$ *such that*

$$f' = \frac{(f_1')^{\frac{m+2}{4}}}{(f_2')^{\frac{m-2}{4}}}.$$

Acknowledgement

This paper is partially supported by the Centre for Innovation and Transfer of Natural Sciences and Engineering Knowledge, University of Rzeszów.

References

[1] M. Arif, K. I. Noor, and M. Raza, *On a class of analytic functions related with generalized Bazilevic type functions*, Comp. Math. Appl. **61** (2011), 2456–2462.

[2] M. Arif, M. Raza, K. I. Noor, and S. N. Malik, *On strongly Bazilevic functions associated with generalized Robertson functions*, Math. Comput. Model. **54** (2011), 1608–1612.

[3] J. Dziok, *Characterizations of analytic functions associated with functions of bounded variation*, Ann. Polon. Math. **109** (2013), 199–207.

[4] J. Dziok, *Classes of functions associated with the bounded Mocanu variation*, J. Inequal. Appl. **2013** (2013), 349.

[5] J. Dziok, *Meromorphic functions with bounded boundary rotation*, Acta Math. Sci. Ser. B Engl. Ed. **34 B**(2014), 1–7.

[6] R. M. Goel, *A class of clos-to-convex functions*, Czechosl. Math. J. **18** (1968), 104–116.

[7] A. W. Goodman, *Univalent functions, polygonal publishing house*, Washington, New Jersey 1983.

[8] D. J. Hallenbeck and T. H. MacGregor, *Linear problems and convexity techniques in geometric function theory*, Pitman Advanced Publishing Program, Boston 1984.

[9] Z. J. Jakubowski, *On the coefficients of Carathéodory functions*, Bull. Acad. Polon. Sci. Sér. Sci. Math. Astronom. Phys. **19**, no. 9 (1971), 805–809.

[10] Z. J. Jakubowski and J. Kamiński, *On some properties of Mocanu-Janowski functions*, Rev. Roumaine Math. Pures Appl. **23**, no. 10 (1978), 1523–1532.

[11] W. Janowski, *Some extremal problems for certain families of analytic functions. I*, Ann. Polon. Math. **28** (1973), 297–326.

[12] W. Janowski, *Some extremal problems for certain families of analytic functions. I*, Bull. Acad. Polon. Sci. **21** (1973), 17–25 (presented on July 5, 1972).

[13] E. J. Moulis, *Generalizations of the Robertson functions*, Pacific J. Math. **81**, no. 1 (1979), 167–174.

[14] K. I. Noor and M. Arif, *Mapping properties of an integral operator*, Applied Math. Lett. **25** (2012), 1826–1829.

[15] K. I. Noor and K. Yousaf, *On classes of analytic functions related with generalized Janowski functions*, W Appl. Sci. J. **13** (2011), 40–47.

[16] V. Paatero, *Uber die konforme Abbildung von Gebieten, deren Ränder von beschränkter Drehung sind*, Ann. Acad. Sci. Fenn. Ser. A **33**, no. 9(1931), 77.

[17] K. S. Padmanabhan and R. Parvatham, *Properties of a class of functions with bounded boundary rotation*, Ann. Polon. Math. **31** (1975), 311–323.

[18] B. Pinchuk, *Functions with bounded boundary rotation*, Isr. J. Math. **10** (1971), 7–16.

[19] W. Rogosiński, *On the coefficients of subordinate functions*, Proc. Lond. Math. Soc. **48** (1943), 48–82.

[20] J. Stankiewicz and J. Waniurski, *Some classes of functions subordinate to linear transformation and their applications*, Ann. UMCS **28**, no. 9(1974), 85–94.

Department of Mathematics
Abdul Wali Khan University Mardan
Pakistan
e-mail: marifmaths@yahoo.com

Department of Mathematics
GC University Faisalabad
Pakistan
e-mail: mohsan976@yahoo.com

Faculty of Mathematics
and Natural Sciences
University of Rzeszów
Poland
e-mail: jdziok@ur.edu.pl

Presented by Zbigniew Jakubowski at the Session of the Mathematical-Physical Commission of the Łódź Society of Sciences and Arts on July 13, 2015

O PEWNYCH WARIACJACH FUNKCJI JANOWSKIEGO

S t r e s z c z e n i e

W pracy zdefiniowane zostały klasy powiązane z funkcjami Janowskiego i funkcjami o ograniczonej rotacji brzegowej. W klasach tych rozwazane są podstawowe problemy ekstremalne takie jak oszacowania współczynników, oszacowania modulu funkcjii części rzeczywistej funkcji oraz nierówności związane ze średnią całkową. Zostały także wyznaczone wzory strukturalne w omawianych klasach funkcji.

Słowa kluczowe: funkcje Janowskiego, funkcje o ograniczonej wariacji, funkcje o ograniczonej rotacji

PL ISSN 0459-6854

B U L L E T I N

DE LA SOCIÉTÉ DES SCIENCES ET DES LETTRES DE ŁÓDŹ

2015 Vol. LXV

Recherches sur les déformations no. 2

pp. 71–82

Kinga Cudna and Adam Lecko

SOME SCHWARZ INEQUALITY ON THE BOUNDARY FOR ANALYTIC FUNCTIONS WITH PRESCRIBED ZEROS

Summary

In this paper we slightly generalize the recent result due to Dubinin [2] which concerns the classical Schwarz inequality on the boundary connected with zeros of the function.

Keywords and phrases: Schwarz inequality, analytic function with prescribed zeros

1. Introduction

1. For $r > 0$ let $\mathbf{D}_r := \{z \in \mathbf{C} : |z| < r\}$, $\overline{\mathbf{D}}_r := \{z \in \mathbf{C} : |z| \leq r\}$ and $\mathbf{T}_r := \{z \in \mathbf{C} : |z| = r\}$. Let $\mathbf{D} := \mathbf{D}_1$ and $\mathbf{T} := \mathbf{T}_1$.

For a set $A \subset \mathbf{C}$ with $0 \in A$ let $A^0 := A \setminus \{0\}$. Particularly, $\mathbf{D}^0 = \mathbf{D} \setminus \{0\}$ and $\overline{\mathbf{D}}^0 = \overline{\mathbf{D}} \setminus \{0\}$.

For a set A^0 let $\mathbf{\Omega}(A)$ be the family of all finite subsets of A^0 including the empty set. Let $\mathbf{\Omega} := \mathbf{\Omega}(\mathbf{D})$.

2. Let G be a domain in $\mathbf{C}$ and let $\mathcal{H}(G)$ be the set of all analytic functions in G. Let $\mathcal{H} := \mathcal{H}(\mathbf{D})$.

For $r > 0$, $a \in \mathbf{C}$ and $n \in \mathbf{N}$ let $\mathcal{H}_a[r, n]$ be the class of functions $f \in \mathcal{H}(\mathbf{D}_r)$ such that

$$f(0) = a, \quad f'(0) = \ldots = f^{(n-1)}(0) = 0, \quad f^{(n)}(0) \neq 0,$$

i.e., of the form

$$f(z) = a + \sum_{k=n}^{\infty} a_n z^n, \quad z \in \mathbf{D}_r, \tag{1.1}$$

with $a_n \neq 0$, and let $\mathcal{H}_a[n] := \mathcal{H}_a[1,n]$.

Let $\mathcal{B}$ be the subset of $\mathcal{H}$ of all self-mappings of $\mathbf{D}$. Let $\mathcal{B}_0$ be the subset of $\mathcal{B}$ of all functions keeping the origin fixed, i.e., the set of Schwarz functions. For $n \in \mathbf{N}$ let $\mathcal{B}_0[n] := \mathcal{B}_0 \cap \mathcal{H}_0[n]$.

3. Let $f \in \mathcal{H}$, $D \subset \mathbf{D}$ and $w_0 \in f(D)$. Let

$$Z_{f,w_0}(D) := \left\{ z \in D^0 : f(z) = w_0 \right\},$$
$$Z_f(D) := Z_{f,0}(D), \quad Z_{f,w_0} := Z_{f,w_0}(\mathbf{D}), \quad Z_f := Z_{f,0}.$$

Let

$$n_f : Z_f(D) \ni z \mapsto \inf \left\{ k \in \mathbf{N} : f^{(k)}(z) \neq 0 \right\}.$$

Thus

$$n_f(z) = \inf \left\{ k \in \mathbf{N} : f^{(k)}(z) \neq 0 \right\}, \quad z \in D.$$

For $w_0 \in f(\mathbf{D})$ let

$$n_{f,w_0} := n_{f-w_0}.$$

2. Notation

Now we introduce some constants required in further considerations.

Definition 2.1. Let $\zeta \in \mathbf{C}^0$, $r := |\zeta|$, $\emptyset \neq \Omega \in \mathbf{\Omega}(\mathbf{D}_r)$, $\lambda : \Omega \to \mathbf{N}$, a, $b > 0$ and $n \in \mathbf{N}$. Let

$$M(\Omega, \lambda; \zeta) := \sum_{\alpha \in \Omega} \lambda(\alpha) \frac{|\zeta|^2 - |\alpha|^2}{|\zeta - \alpha|^2},$$
$$K(\Omega, \lambda; a, b, r, n) := \frac{a \prod_{\alpha \in \Omega} |\alpha|^{\lambda(\alpha)} - b r^{n + \sum_{\alpha \in \Omega} \lambda(\alpha)}}{a \prod_{\alpha \in \Omega} |\alpha|^{\lambda(\alpha)} + b r^{n + \sum_{\alpha \in \Omega} \lambda(\alpha)}},$$
$$L(\Omega, \lambda; a, b, r, n) := -\frac{1}{2} \log \frac{b r^{n + \sum_{\alpha \in \Omega} \lambda(\alpha)}}{a \prod_{\alpha \in \Omega} |\alpha|^{\lambda(\alpha)}},$$
$$K(\Omega, \lambda; a, b) := K(\Omega, \lambda; a, b, 1, n) = \frac{a \prod_{\alpha \in \Omega} |\alpha|^{\lambda(\alpha)} - b}{a \prod_{\alpha \in \Omega} |\alpha|^{\lambda(\alpha)} + b},$$
$$L(\Omega, \lambda; a, b) := L(\Omega, \lambda; a, b, 1, n) = -\frac{1}{2} \log \frac{b}{a \prod_{\alpha \in \Omega} |\alpha|^{\lambda(\alpha)}}.$$

Lemma 2.2. *Let $\Omega_1, \Omega_2 \in \mathbf{\Omega}$, $\Omega_1 \subset \Omega_2$, $\Omega_1 \neq \emptyset$, $\lambda : \Omega_2 \to \mathbf{N}$, $r \in (0,1]$, a, $b > 0$ and $n \in \mathbf{N}$. Then*

$$K(\Omega_1, \lambda; a, b, r, n) \geq K(\Omega_2, \lambda; a, b) \tag{2.1}$$

and

$$L(\Omega_1, \lambda; a, b, r, n) \geq L(\Omega_2, \lambda; a, b). \tag{2.2}$$

Proof. Let $\Omega_1, \Omega_2 \in \mathbf{\Omega}$, $\Omega_1 \subset \Omega_2$, $\Omega_1 \neq \emptyset$, $\lambda : \Omega_2 \to \mathbf{N}$, $r \in (0,1]$, a, $b > 0$ and $n \in \mathbf{N}$. Since $0 < |\alpha| < 1$ for $\alpha \in \Omega_2$, and $\Omega_1 \subset \Omega_2$, so

$$\prod_{\alpha\in\Omega_1} |\alpha|^{\lambda(\alpha)} \geq \prod_{\alpha\in\Omega_2} |\alpha|^{\lambda(\alpha)}. \tag{2.3}$$

Hence and by the fact that the function

$$[0,1] \ni x \mapsto \frac{ax-c}{ax+c}, \quad a, c > 0,$$

is strictly increasing it follows that

$$K(\Omega_1, \lambda; a, b, r, n) = \frac{a\prod_{\alpha\in\Omega_1} |\alpha|^{\lambda(\alpha)} - br^{n+\sum_{\alpha\in\Omega_1}\lambda(\alpha)}}{a\prod_{\alpha\in\Omega_1} |\alpha|^{\lambda(\alpha)} + br^{n+\sum_{\alpha\in\Omega_1}\lambda(\alpha)}} \tag{2.4}$$

$$\geq \frac{a\prod_{\alpha\in\Omega_2} |\alpha|^{\lambda(\alpha)} - br^{n+\sum_{\alpha\in\Omega_2}\lambda(\alpha)}}{a\prod_{\alpha\in\Omega_2} |\alpha|^{\lambda(\alpha)} + br^{n+\sum_{\alpha\in\Omega_2}\lambda(\alpha)}} = K(\Omega_2, \lambda; a, b, r, n).$$

Since the function

$$[0,1] \ni x \mapsto \frac{d-bx}{d+bx}, \quad d, b > 0,$$

is strictly decreasing so

$$K(\Omega_2, \lambda; a, b, r, n) = \frac{a\prod_{\alpha\in\Omega_2} |\alpha|^{\lambda(\alpha)} - br^{n+\sum_{\alpha\in\Omega_2}\lambda(\alpha)}}{a\prod_{\alpha\in\Omega_2} |\alpha|^{\lambda(\alpha)} + br^{n+\sum_{\alpha\in\Omega_2}\lambda(\alpha)}}$$

$$\geq \frac{a\prod_{\alpha\in\Omega_2} |\alpha|^{\lambda(\alpha)} - b}{a\prod_{\alpha\in\Omega_2} |\alpha|^{\lambda(\alpha)} + b} = K(\Omega_2, \lambda; a, b).$$

Hence and from the inequality (2.4) we get the inequality (2.1).

Since $r \in (0,1]$, so

$$L(\Omega_1, \lambda; a, b, r, n) = -\frac{1}{2}\log\frac{br^{n+\sum_{\alpha\in\Omega_1}\lambda(\alpha)}}{a\prod_{\alpha\in\Omega_1} |\alpha|^{\lambda(\alpha)}} \tag{2.5}$$

$$\geq -\frac{1}{2}\log\frac{b}{a\prod_{\alpha\in\Omega_1} |\alpha|^{\lambda(\alpha)}} = L(\Omega_1, \lambda; a, b).$$

Using the inequality (2.3) we have

$$L(\Omega_1, \lambda; a, b) = -\frac{1}{2}\log\frac{b}{a\prod_{\alpha\in\Omega_1} |\alpha|^{\lambda(\alpha)}}$$

$$\geq -\frac{1}{2}\log\frac{b}{a\prod_{\alpha\in\Omega_2} |\alpha|^{\lambda(\alpha)}} = L(\Omega_2, \lambda; a, b).$$

Hence and from the inequality (2.5) we get the inequality (2.2). □

Definition 2.3. Let $r > 0$, $f \in \mathcal{H}(\mathbf{D}_r)$, $w_0 \in f(\mathbf{D}_r)$, $\zeta \in \mathbf{T}_r$, a, $b > 0$ and $n \in \mathbf{N}$. Let

$$M_{f,w_0}(\zeta) := M(Z_{f,w_0}(\mathbf{D}_r), n_{f,w_0}; \zeta) = \sum_{\alpha \in Z_{f,w_0}(\mathbf{D}_r)} n_{f,w_0}(\alpha) \frac{|\zeta|^2 - |\alpha|^2}{|\zeta - \alpha|^2},$$

$$M_f(\zeta) := M_{f,0}(\zeta) = \sum_{\alpha \in Z_f(\mathbf{D}_r)} n_f(\alpha) \frac{|\zeta|^2 - |\alpha|^2}{|\zeta - \alpha|^2},$$

$$K_{f,w_0}(a,b,r,n) := K\left(Z_{f,w_0}(\mathbf{D}_r), n_{f;w_0}; a, b, r, n\right) =$$

$$= \frac{a \prod_{\alpha \in Z_{f,w_0}(\mathbf{D}_r)} |\alpha|^{n_{f,w_0}(\alpha)} - b r^{n + \sum_{\alpha \in Z_{f,w_0}(\mathbf{D}_r)} n_{f,w_0}(\alpha)}}{a \prod_{\alpha \in Z_{f,w_0}(\mathbf{D}_r)} |\alpha|^{n_{f,w_0}(\alpha)} + b r^{n + \sum_{\alpha \in Z_{f,w_0}(\mathbf{D}_r)} n_{f,w_0}(\alpha)}},$$

$$K_f(a,b,r,n) := K_{f,0}(a,b,r,n) =$$

$$= \frac{a \prod_{\alpha \in Z_f(\mathbf{D}_r)} |\alpha|^{n_f(\alpha)} - b r^{n + \sum_{\alpha \in Z_f(\mathbf{D}_r)} n_f(\alpha)}}{a \prod_{\alpha \in Z_f(\mathbf{D}_r)} |\alpha|^{n_f(\alpha)} + b r^{n + \sum_{\alpha \in Z_f(\mathbf{D}_r)} n_f(\alpha)}},$$

$$K_f(a,b) := K_f(a,b,1,n) = \frac{a \prod_{\alpha \in Z_f} |\alpha|^{n_f(\alpha)} - b}{a \prod_{\alpha \in Z_f} |\alpha|^{n_f(\alpha)} + b},$$

$$L_{f,w_0}(a,b,r,n) := L\left(Z_{f,w_0}(\mathbf{D}_r), n_{f;w_0}; a, b, r, n\right) =$$

$$= -\frac{1}{2} \log \frac{b r^{n + \sum_{\alpha \in Z_{f,w_0}(\mathbf{D}_r)} n_{f,w_0}(\alpha)}}{a \prod_{\alpha \in Z_{f,w_0}(\mathbf{D}_r)} |\alpha|^{n_{f,w_0}(\alpha)}},$$

$$L_f(a,b,r,n) := L_{f,0}(a,b,r,n) =$$

$$= -\frac{1}{2} \log \frac{b r^{n + \sum_{\alpha \in Z_f(\mathbf{D}_r)} n_f(\alpha)}}{a \prod_{\alpha \in Z_f(\mathbf{D}_r)} |\alpha|^{n_f(\alpha)}},$$

$$L_f(a,b) := L_f(a,b,1,n) = -\frac{1}{2} \log \frac{b}{a \prod_{\alpha \in Z_f} |\alpha|^{n_f(\alpha)}}.$$

3. Main results

Let us start with the definition.

Definition 3.1. Let $f \in \mathcal{H}(\mathbf{D}_r),\ r > 0$, be a function such that at the point $\zeta \in \overline{\mathbf{D}}_r$ the limit $f(\zeta) \neq 0$ and the derivative $f'(\zeta)$ exist. Define

$$I(f;\zeta) := \frac{\zeta f'(\zeta)}{f(\zeta)}.$$

The lemma below follows directly from Julia-Wolff-Carathéodory Theorem (see [5, Proposition 4.13, p. 82], [1, pp. 53-57]).

Theorem 3.2. *If* $\omega \in \mathcal{B}$ *and at* $\zeta_0 \in \mathbf{T}$

(a) *the limit* $\omega(\zeta_0)$ *exists and* $\omega(\zeta_0) \in \mathbf{T}$,

(b) *the derivative* $\omega'(\zeta_0)$ *exists,*

then

$$I(\omega; \zeta_0) > 0. \tag{3.1}$$

The inequality (3.2) in the theorem below is a part of Lemma 2.2a [3] (c.f. [4, Remark 3]). The inequality (3.3) was proved by Osserman [4, Remark 3] (c.f. [2, p. 3624]).

Theorem 3.3. *If* $n \in \mathbf{N}$, $\omega \in \mathcal{B}_0[n]$ *and the assumptions* (a) *and* (b) *of Theorem 3.2 hold, then*

$$I(\omega; \zeta_0) \geq n. \tag{3.2}$$

Moreover, if $b_n := \omega^{(n)}(0)/n!$, *then*

$$I(\omega; \zeta_0) \geq n + \frac{1 - |b_n|}{1 + |b_n|}. \tag{3.3}$$

The equality in (3.2) *holds for the function*

$$\omega(z) := z^n, \quad z \in \mathbf{D}, \tag{3.4}$$

and in (3.3) *for the function*

$$\omega(z) := \left(\frac{z}{\zeta_0}\right)^n \frac{z + x\zeta_0}{\zeta_0 + xz}, \quad z \in \mathbf{D}, \tag{3.5}$$

with any $x \in (0, 1)$.

The case $n := 1$ was shown by Unkelbach [6, p. 741].

Theorem 3.4. *If* $\omega \in \mathcal{B}_0[1]$ *and the conditions* (a) *and* (b) *of Theorem 3.2 hold, then*

$$I(\omega; \zeta_0) \geq \frac{2}{1 + |b_1|}. \tag{3.6}$$

The equality in (3.6) *holds for the function* (3.4) *with* $n := 1$.

The next two theorems was proved by Dubinin [2, p. 3623]. In the original paper Dubinin formulated both theorems as a unique one (Theorem 1).

Theorem 3.5. *If* $n \in \mathbf{N}$, $\omega \in \mathcal{B}_0[n]$,

$$Z_\omega \neq \emptyset, \quad b_n := \omega^{(n)}(0)/n!,$$

and the conditions (a) *and* (b) *of Theorem 3.2 hold, then for every subset* $A \subset Z_\omega$ *and every function* $\lambda : A \to \mathbf{N}$ *such that*

$$\lambda(\alpha) \leq n_\omega(\alpha), \quad \alpha \in A, \tag{3.7}$$

the following inequality holds

$$
\begin{aligned}
\text{(3.8)} \qquad I(\omega;\zeta_0) &\geq n + M(A,\lambda;\zeta_0) + K(A,\lambda_A;1,|b_n|)\\
&= n + \sum_{\alpha\in A}\lambda(\alpha)\frac{1-|\alpha|^2}{|\zeta_0-\alpha|^2} + \frac{\prod_{\alpha\in A}|\alpha|^{\lambda(\alpha)}-|b_n|}{\prod_{\alpha\in A}|\alpha|^{\lambda(\alpha)}+|b_n|}.
\end{aligned}
$$

Particularly,

$$
\begin{aligned}
\text{(3.9)} \qquad I(\omega;\zeta_0) &\geq n + M_\omega(\zeta_0) + K_\omega(1,|b_n|)\\
&= n + \sum_{\alpha\in Z_\omega} n_\omega(\alpha)\frac{1-|\alpha|^2}{|\zeta_0-\alpha|^2} + \frac{\prod_{\alpha\in Z_\omega}|\alpha|^{n_\omega(\alpha)}-|b_n|}{\prod_{\alpha\in Z_\omega}|\alpha|^{n_\omega(\alpha)}+|b_n|},
\end{aligned}
$$

The equality in (3.8) *holds for the function*

$$
\text{(3.10)} \qquad \omega(z) := z^n \prod_{\alpha\in A}\left(\frac{-\overline{\alpha}}{|\alpha|}\cdot\frac{z-\alpha}{1-\overline{\alpha}z}\right)^{\lambda(\alpha)}, \quad z\in\mathbf{D},
$$

and in (3.9) *for the function* (3.10) *with* $A := Z_\omega$ *and* $\lambda := n_\omega$.

Theorem 3.6. *If* $n\in\mathbf{N}$, $\omega\in\mathcal{B}_0[n]$, $b_n := \omega^{(n)}(0)/n!$, *and the conditions* (a) *and* (b) *of Theorem 3.2 hold, and if*

1. $Z_\omega \neq \emptyset$, *then*

$$
\begin{aligned}
\text{(3.11)} \qquad I(\omega;\zeta_0) &\geq n + M_\omega(\zeta_0) + L_\omega(1,|b_n|)\\
&= n + \sum_{\alpha\in Z_\omega} n_\omega(\alpha)\frac{1-|\alpha|^2}{|\zeta_0-\alpha|^2} - \frac{1}{2}\log\frac{|b_n|}{\prod_{\alpha\in Z_\omega}|\alpha|^{n_\omega(\alpha)}};
\end{aligned}
$$

2. $Z_\omega = \emptyset$, *then*

$$
\text{(3.12)} \qquad I(\omega;\zeta_0) \geq n - \frac{1}{2}\log|b_n|.
$$

The equality in (3.11) *holds for the function* (3.10) *with* $A := Z_\omega$ *and* $\lambda := n_\omega$, *and in* (3.12) *for the function* (3.4).

In the following theorem we consider an arbitrary disk centered at the origin instead of the unit disk $\mathbf{D}$. The inequality (3.13) is as the inequality (3.2). This theorem is a version of Lemma 2.2a of [3, p. 19] completed with the inequality (3.14).

Theorem 3.7. *Let* $r_0 > 0$, $z_0 \in \mathbf{T}_{r_0}$, $n\in\mathbf{N}$ *and* $\varphi\in\mathcal{H}_0[r_0,n]$ *be a function such that*

(a) $\varphi(\mathbf{D}_{r_0})\subset\mathbf{D}$,
(b) *at* z_0 *the limit* $\varphi(z_0)$ *exists and* $\varphi(z_0)\in\mathbf{T}$,
(c) *at* z_0 *the derivative* $\varphi'(z_0)$ *exists.*

Then

$$I(\varphi; z_0) \geq n. \tag{3.13}$$

Moreover, if

$$c_n := \varphi^{(n)}(0)/n!,$$

then

$$I(\varphi; z_0) \geq n + \frac{1 - |c_n| r_0^n}{1 + |c_n| r_0^n}. \tag{3.14}$$

Proof. We will show the inequality (3.13) by applying the inequality (3.2). Since $\varphi \in \mathcal{H}_0[r_0, n]$, so by (1.1) we have

$$\varphi(z) = \sum_{k=n}^{\infty} c_k z^k, \quad z \in \mathbf{D}_{r_0}, \tag{3.15}$$

with $c_n \neq 0$. Define

$$\omega(z) := \varphi(z_0 z), \quad z \in \mathbf{D}. \tag{3.16}$$

Hence and by (3.15)we have

$$\omega(z) = \sum_{k=n}^{\infty} b_k z^k, \quad z \in \mathbf{D}, \tag{3.17}$$

where

$$b_k := c_k z_0^k, \quad k = n, n+1, \ldots \tag{3.18}$$

Thus $\omega \in \mathcal{H}_0[n]$. Since $\varphi(\mathbf{D}_{r_0}) \subset \mathbf{D}$, so $\omega(\mathbf{D}) \subset \mathbf{D}$. Therefore $\omega \in \mathcal{B}_0[n]$. As at $z_0 \in \mathbf{T}_{r_0}$ the limit $\varphi(z_0) \in \mathbf{T}$ exists, so at 1 the limit $\omega(1) = \varphi(z_0) \in \mathbf{T}$ exists. Since at z_0 the derivative $\varphi'(z_0)$ exists, so at 1 the derivative $\omega'(1)$ exists and

$$\omega'(1) = z_0 \varphi'(z_0). \tag{3.19}$$

Thus the function ω satisfies the assumptions of Theorem 3.3 with $\zeta_0 := 1$. Using the fact that $\omega(1) = \varphi(z_0)$ and the condition (3.19) by the inequality (3.2) we have

$$I(\varphi; z_0) = \frac{z_0 \varphi'(z_0)}{\varphi(z_0)} = \frac{\omega'(1)}{\omega(1)} = I(\omega; 1) \geq n. \tag{3.20}$$

Thus the inequality (3.13) was shown.

Using the left-hand side of the inequality (3.20), the inequality (3.3) and (3.18) with $k := n$, we get

$$I(\varphi; z_0) = I(\omega; 1) \geq n + \frac{1 - |b_n|}{1 + |b_n|} = n + \frac{1 - |c_n| r_0^n}{1 + |c_n| r_0^n}, \tag{3.21}$$

which shows the inequality (3.14). □

The next two theorems slightly generalize Dubinin Theorem by replacing the unit disk as by an arbitrary one.

Theorem 3.8. *If the assumptions of Theorem 3.7 are satisfied, $c_n := \varphi^{(n)}(0)/n!$ and $Z_\varphi(\mathbf{D}_{r_0}) \neq \emptyset$, then for every subset $B \subset Z_\varphi(\mathbf{D}_{r_0})$ and every function $\mu : B \to \mathbf{N}$ such that*

$$\mu(\alpha) \leq n_\varphi(\alpha), \quad \alpha \in B, \tag{3.22}$$

the following inequality holds

$$\begin{aligned} I(\varphi; z_0) &\geq n + M(B, \mu; z_0) + K(B, \mu; 1, |c_n|, r_0, n) \\ &= n + \sum_{\alpha \in B} \mu(\alpha) \frac{|z_0|^2 - |\alpha|^2}{|z_0 - \alpha|^2} + \frac{\prod_{\alpha \in B} |\alpha|^{\mu(\alpha)} - |c_n| r_0^{n + \sum_{\alpha \in B} \mu(\alpha)}}{\prod_{\alpha \in B} |\alpha|^{\mu(\alpha)} + |c_n| r_0^{n + \sum_{\alpha \in B} \mu(\alpha)}}. \end{aligned} \tag{3.23}$$

Particularly,

$$\begin{aligned} I(\varphi; z_0) &\geq n + M_\varphi(z_0) + K_\varphi(1, |c_n|, r_0, n) \\ &= n + \sum_{\alpha \in Z_\varphi(\mathbf{D}_{r_0})} n_\varphi(\alpha) \frac{|z_0|^2 - |\alpha|^2}{|z_0 - \alpha|^2} + \\ &\quad + \frac{\prod_{\alpha \in Z_\varphi(\mathbf{D}_{r_0})} |\alpha|^{n_\varphi(\alpha)} - |c_n| r_0^{n + \sum_{\alpha \in Z_\varphi(\mathbf{D}_{r_0})} n_\varphi(\alpha)}}{\prod_{\alpha \in Z_\varphi(\mathbf{D}_{r_0})} |\alpha|^{n_\varphi(\alpha)} + |c_n| r_0^{n + \sum_{\alpha \in Z_\varphi(\mathbf{D}_{r_0})} n_\varphi(\alpha)}}. \end{aligned} \tag{3.24}$$

Proof. Under the assumptions of Theorem 3.7 we define the function ω as in (3.16). Then the properties (3.16)-(3.19) hold. Let $\alpha \in Z_\varphi(\mathbf{D}_{r_0})$. Since $\alpha \neq 0$ and

$$\left| \frac{\alpha}{z_0} \right| \leq \frac{|\alpha|}{r_0} < 1,$$

so $\alpha/z_0 \in \mathbf{D}^0$. From the fact that

$$\omega\left(\frac{\alpha}{z_0}\right) = \varphi\left(z_0 \frac{\alpha}{z_0}\right) = \varphi(\alpha) = 0,$$

it follows that $\alpha/z_0 \in Z_\omega$. Let $\beta \in Z_\omega$. Thus

$$\omega(\beta) = \varphi(z_0\beta) = \varphi(\alpha) = 0,$$

where $\alpha := z_0\beta$. Hence $\alpha \in Z_\varphi(\mathbf{D}_{r_0})$ and $\beta = \alpha/z_0 \in Z_\omega$. In this way we shown that

$$Z_\omega = \{\alpha/z_0 : \alpha \in Z_\varphi(\mathbf{D}_{r_0})\}. \tag{3.25}$$

Observe also that from (3.15), (3.17) and (3.18) it follows that

$$n_\omega(\alpha/z_0) = n_\varphi(\alpha). \tag{3.26}$$

Let

$$A := \{\alpha/z_0 : \alpha \in B\}. \tag{3.27}$$

In view of (3.25) we have $A \subset Z_\omega$. Define $\lambda : A \to \mathbf{N}$ s follows:

$$\lambda(\alpha/z_0) := \mu(\alpha), \quad \alpha \in B. \tag{3.28}$$

Hence, by (3.26) and (3.22) we get

$$\lambda(\alpha/z_0) = \mu(\alpha) \le n_\varphi(\alpha) = n_\omega(\alpha/z_0), \quad \alpha \in B. \tag{3.29}$$

Thus the inequality (3.7) holds for the set A and the function λ.

By (3.27) and (3.28) we have

$$\begin{aligned} M(A,\lambda;1) &:= \sum_{\alpha//z_0\in A} \lambda(\alpha/z_0)\frac{1-\left|\dfrac{\alpha}{z_0}\right|^2}{\left|1-\dfrac{\alpha}{z_0}\right|^2} \\ &= \sum_{\alpha\in B}\mu(\alpha)\frac{|z_0|^2-|\alpha|^2}{|z_0-\alpha|^2} = M(B,\mu;z_0). \end{aligned} \tag{3.30}$$

Using (3.18) for $k := n$ we have

$$\begin{aligned} K(A,\lambda;1,|b_n|) &= \frac{\prod_{\alpha/z_0\in A}\left|\dfrac{\alpha}{z_0}\right|^{\lambda(\alpha/z_0)} - |b_n|^n}{\prod_{\alpha/z_0\in A}\left|\dfrac{\alpha}{z_0}\right|^{\lambda(\alpha/z_0)} + |b_n|^n} \\ &= \frac{\prod_{\alpha\in B}\dfrac{|\alpha|^{\mu(\alpha)}}{|z_0|^{\mu(\alpha)}} - |c_n||z_0|^n}{\prod_{\alpha\in B}\dfrac{|\alpha|^{\mu(\alpha)}}{|z_0|^{\mu(\alpha)}} + |c_n||z_0|^n} \\ &= \frac{\prod_{\alpha\in A}|\alpha|^{\mu(\alpha)} - |c_n|r_0^{n+\sum_{\alpha\in B}\mu(\alpha)}}{\prod_{\alpha\in B}|\alpha|^{\mu(\alpha)} + |c_n|r_0^{n+\sum_{\alpha\in B}\mu(\alpha)}} = K(B,\mu;1,|c_n|,r_0,n). \end{aligned} \tag{3.31}$$

Taking into account (3.30), (3.31), and using the inequality (3.8) for $\zeta_0 := 1$ we obtain

$$\begin{aligned} I(\varphi;z_0) = \frac{z_0\varphi'(z_0)}{\varphi(z_0)} &= \frac{\omega'(1)}{\omega(1)} = I(\omega;1) \\ &\ge n + M(A,\lambda;1) + K(A,\lambda;1,|b_n|) \\ &= n + M(B,\mu;z_0) + K(B,\mu;1,|c_n|,r_0,n). \end{aligned}$$

In this way the inequality (3.23) was proved.

In view of (3.25) and (3.26) we have

$$\begin{aligned} M_\omega(1) &= \sum_{\alpha/z_0\in Z_\omega} n_\omega(\alpha/z_0)\frac{1-\left|\dfrac{\alpha}{z_0}\right|^2}{\left|1-\dfrac{\alpha}{z_0}\right|^2} \\ &= \sum_{\alpha\in Z_\varphi(\mathbf{D}_{r_0})} n_\varphi(\alpha)\frac{|z_0|^2-|\alpha|^2}{|z_0-\alpha|^2} = M_\varphi(z_0). \end{aligned} \tag{3.32}$$

By (3.25), (3.26) and (3.18) for $k := n$ we have

$$K_\omega(1,|b_n|) = \frac{\prod_{\alpha/z_0\in Z_\omega}\left|\dfrac{\alpha}{z_0}\right|^{n_\omega(\alpha//z_0)} - |b_n|}{\prod_{\alpha/z_0\in Z_\omega}\left|\dfrac{\alpha}{z_0}\right|^{n_\omega(\alpha/z_0)} + |b_n|} \tag{3.33}$$

$$= \frac{\prod_{\alpha\in Z_\varphi(\mathbf{D}_{r_0})}|\alpha|^{n_\varphi(\alpha)} - |c_n| r_0^{n+\sum_{\alpha\in Z_\varphi(\mathbf{D}_{r_0})} n_\varphi(\alpha)}}{\prod_{\alpha\in Z_\varphi(\mathbf{D}_{r_0})}|\alpha|^{n_\varphi(\alpha)} + |c_n| r_0^{n+\sum_{\alpha\in Z_\varphi(\mathbf{D}_{r_0})} n_\varphi(\alpha)}}$$

$$= K_\varphi(1,|c_n|,r_0,n).$$

Taking into account (3.32) and (3.33), and using (3.9) for $\zeta_0 := 1$ we get

$$I(\varphi;z_0) = \frac{z_0\varphi'(z_0)}{\varphi(z_0)} = \frac{\omega'(1)}{\omega(1)} = I(\omega;1)$$

$$\geq n + M_\omega(1) + K_\omega(1,|b_n|) = n + M_\varphi(z_0) + K_\varphi(1,|c_n|,r_0,n).$$

In this way the inequality (3.24) was proved. □

Theorem 3.9. *If the assumptions of Theorem 3.7 are satisfied,* $c_n := \varphi^{(n)}(0)/n!$ *and*

1. $Z_\varphi(\mathbf{D}_{r_0}) \neq \emptyset$, *then*

$$I(\varphi;z_0) \geq n + M_\varphi(z_0) + L_\varphi(1,|c_n|,r_0,n) = \tag{3.34}$$

$$= n + \sum_{\alpha\in Z_\varphi(\mathbf{D}_{r_0})} n_\varphi(\alpha)\frac{|z_0|^2-|\alpha|^2}{|z_0-\alpha|^2} +$$

$$-\frac{1}{2}\log\frac{|c_n| r_0^{n+\sum_{\alpha\in Z_\varphi(\mathbf{D}_{r_0})} n_\varphi(\alpha)}}{\prod_{\alpha\in Z_\varphi(\mathbf{D}_{r_0})}|\alpha|^{n_\varphi(\alpha)}};$$

2. $Z_\varphi(\mathbf{D}_{r_0}) = \emptyset$, *then*

$$I(\varphi;z_0) \geq n - \frac{1}{2}\log|c_n r_0^n|. \tag{3.35}$$

Proof. We define the function ω as in (3.16).

1. Suppose that $Z_\varphi(\mathbf{D}_{r_0}) \neq \emptyset$. Then the properties (3.16)–(3.19), (3.26), (3.27) and (3.30) hold. By (3.25), (3.26) and (3.18) for $k := n$ we have

$$
\begin{aligned}
(3.36) \qquad L_\omega(1,|b_n|) &= -\frac{1}{2}\log \frac{|b_n|}{\prod_{\alpha/z_0\in Z_\omega}\left|\dfrac{\alpha}{z_0}\right|^{n_\omega(\alpha/z_0)}} \\
&= -\frac{1}{2}\log \frac{|b_n|}{\prod_{\alpha\in Z_\varphi(\mathbf{D}_{r_0})}\dfrac{|\alpha|^{n_\varphi(\alpha)}}{|z_0|^{n_\varphi(\alpha)}}} \\
&= -\frac{1}{2}\log \frac{|c_n| r_0^{n+\sum_{\alpha\in Z_\varphi(\mathbf{D}_{r_0})} n_\varphi(\alpha)}}{\prod_{\alpha\in Z_\varphi(\mathbf{D}_{r_0})}|\alpha|^{n_\varphi(\alpha)}} = L_\varphi(1,|c_n|,r_0,n).
\end{aligned}
$$

Taking into account (3.28) and (3.36), and using the inequality (3.11) for $\zeta_0 := 1$ we have

$$
\begin{aligned}
I(\varphi; z_0) &= \frac{z_0\varphi'(z_0)}{\varphi(z_0)} = \frac{\omega'(1)}{\omega(1)} = I(\omega;1) \\
&\geq n + M_\omega(1) + L_\omega(1,|b_n|) = n + M_\varphi(z_0) + L_\varphi(1,|c_n|,r_0,n).
\end{aligned}
$$

In this way the inequality (3.34) was proved.

2. Suppose that $Z_\varphi(\mathbf{D}_{r_0}) = \emptyset$. Then $Z_\omega = \emptyset$. By the inequality (3.12) for $\zeta_0 := 1$ and (3.18) for $k := n$ we get

$$
I(\varphi; z_0) = I(\omega;1) \geq n - \frac{1}{2}\log|b_n| = n - \frac{1}{2}\log|c_n r_0^n|.
$$

In this way the inequality (3.35) was proved. □

References

[1] C. Carathéodory, *Conformal representation*, Cambridge University Press, Cambridge 1963.

[2] V. N. Dubinin, *The Schwarz inequality on the boundary for functions regular in the disk*, J. Math. Sci. **122**, no. 6 (2004), 3623–3629.

[3] S. S. Miller and P. T. Mocanu, *Differential Subordinations. Theory and Appli- cations*, Marcel Dekker, Inc., New York-Basel 2000.

[4] R. Osserman, *A sharp Schwarz inequality on the boundary*, Proc. Amer. Math. Soc. **128**, no. 12 (2000), 3513–3517.

[5] Ch. Pommerenke, *Boundary Behaviour of Conformal Maps*, Springer-Verlag, Berlin-Heidelberg-New York 1992.

[6] H. Unkelbach, *Über die Randenverzerrung bei konformer Abbildung*, Math. Z. **43** (1938), 739–742.

Department of Analysis and Differential Equations
University of Warmia and Mazury
Słoneczna 54, 10-710 Olsztyn
Poland
e-mail: alecko@matman.uwm.edu.pl

Presented by Zbigniew Jakubowski at the Session of the Mathematical-Physical Commission of the Łódź Society of Sciences and Arts on September 10, 2015

PEWNA NIERÓWNOŚĆ SCHWARZA NA BRZEGU DLA FUNKCJI ANALITYCZNYCH Z WYRÓŻNIONYMI ZERAMI

S t r e s z c z e n i e

W pracy tej podane jest pewne uogólnienie wyniku Dubinina z roku 2004 dotyczącego brzegowej wersji klasycznego lematu Schwarza z uwzględnieniem zer funkcji analitycznej.

Słowa kluczowe: nierówność Schwarza, funkcja analityczna z wyróżnionymi zerami

PL ISSN 0459-6854

B U L L E T I N

DE LA SOCIÉTÉ DES SCIENCES ET DES LETTRES DE ŁÓDŹ

2015 Vol. LXV

Recherches sur les déformations no. 2

pp. 83–91

Stanisław Bednarek

COUPLING BETWEEN ROTATION AND AXIAL OSCILLATIONS IN A UNIPOLAR MOTOR

Summary

This article describes a unipolar motor which is an altered version of one of the very first electric motors invented by M. Faraday. A modification consists of applying a rotor in a helix shape winded on a cylinder surface. The rotor is located on an alkaline cylindrical battery which was placed on a cylindrical neodymium magnet. One can observe that, despite the rotor's rotation, a relaxation oscillations occur directed alongside its axis. That new effect was explained and conditions of its occurrence were discussed.

Keywords and phrases: unipolar motor, electrodynamics force, rotation, oscillation, coupling

1. Introduction

The very first electric motor was invented by Michael Faraday in 1821. It was a unipolar motor. Within this motor, a conductor, in which there is a flow of electric current, rotates around one pole of a permanent magnet [1]. Motion of the rotor is caused by an electrodynamic force. In another model of Faraday's motor, the magnet rotated around the final part of the conductor with a current flow. Electric motors, constructed in the next few years, e.g. Barlov's wheel, were unipolar motors as well [2]. Later there were developed and created various types of electric motors applied in machines propel them. Although unipolar motors are rarely used these days, the principle of their operation still remains the subject of great interest. Also new kinds of these motors are being constructed. The article is about an interesting effect which was observed after a change of unipolar motors' construction.

2. Faraday's unipolar motor with a rotating frame

Nowadays, wide access to strong neodymium magnets and alkaline batteries makes the construction of the unipolar motor easier. An example of the contemporary unipolar motor, which uses mentioned elements, was described by H. J. Schlichting and C. Ucke [3]. The structure of the motor, described in their paper, is based on the very first unipolar motor, invented by M. Faraday [4]. Its outlook and operation principle are presented in the Fig. 1.

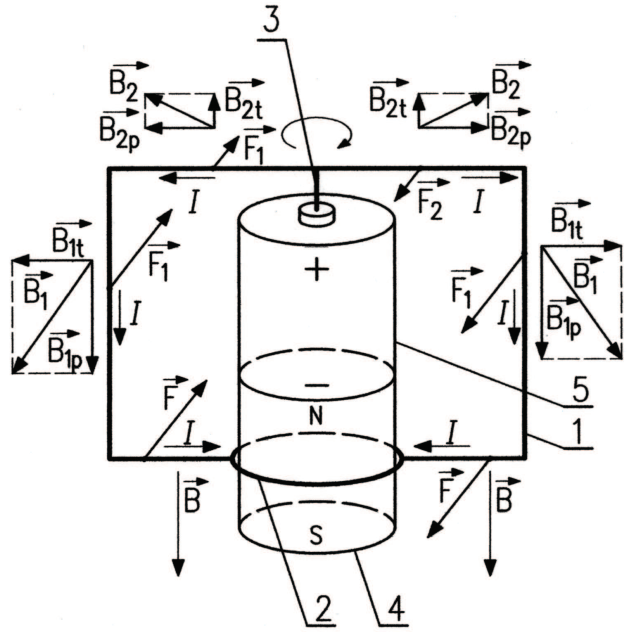

Fig. 1: The construction and operation principle of the unipolar motor based on the Faraday's motor; 1 – frame made of nonferromagnetic wire, 2 – a contact ring, 3 – a tip, 4 – a cylindrical neodymium magnet, 5 – a cylindrical battery, 6 – N, S – the magnet poles, I – the current intensity, $\mathbf{B}$, $\mathbf{B}_1$, $\mathbf{B}_2$ – the vectors of magnetic field induction on the side surface of a frame, B1t, B2t – the components of the induction vectors perpendicular to the sides of the frame, $\mathbf{B}_{1p}$, $\mathbf{B}_{2p}$ – the components of the induction vectors parallel to the sides of the frame, $\mathbf{F}$, $\mathbf{F}_1$, $\mathbf{F}_2$ – the electrodynamics forces applied to the frame's sides.

This motor is composed of a single rectangular frame consisting of a copper wire without isolation. In its lower part, the frame is equipped with a contact ring touching the side surface of the cylinder shaped neodymium magnet. In the upper part, the frame includes a tip based on one pole of cylindrical battery, located on the magnet. Electric current flows through the blade, then through all sides of the frame and the ring, as well as through the magnet's surface. If a positive pole of the battery is turned upwards, then the directions of electric current flow within a frame are as those presented in the Fig. 1. The frame is located in the magnetic field, produced by the cylinder magnet. Components of a magnetic induction vector, which are perpendicular towards the frame sides, cause electrodynamics forces. The momentum of those forces causes a rotation of the frame. The unipolar motor discussed in the paper allows us to present the basic laws of electromagnetism in an attractive way. Other advantages of the unipolar motor also encompass a very simple structure and an uncomplicated method of construction.

3. Construction of a unipolar motor with a helical rotor

The frame, within the described motor, may be of different than the rectangular shape, for example of a trapezoid or another polygon. On the Internet there are videos which show unipolar motors' operation principles and there are presented some the frames, e.g. in shape of a heart or dragonfly wings [5]. An interesting and surprising effect occurs when a wire forming sides of the frame is winded into a helix. The helix will not only rotate, but also oscillate in a vertical direction.

The purpose of this article is to present a description of such a motor, as well as an explanation of the phenomena appearing within it. The structure of the unipolar motor with a helical rotor is presented in the Fig. 2. Helix 1 is made of nonferromagnetic wire, which has also some elastic properties. The lower part of the wire creates a contact ring 2 touching the side surface of the cylindrical neodymium magnet 3. The upper end of the wire is directed towards the side of the helix axis and then curved downwards and filed in a form of a cone. As a result, the upper end of the wire creates a tip 4 which touches the pole of the cylindrical battery 5, located on the neodymium magnet.

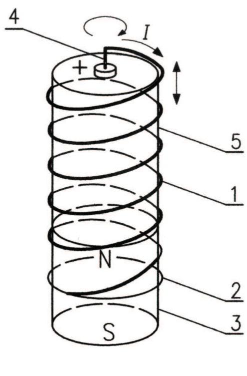

Fig. 2: The construction of the unipolar motor with a helical rotor; 1 – the helix winded with a nonferromagnetic wire, 2 – a contact ring, 3 – a cylindrical neodymium magnet, 4 – a tip, 5 – a cylindrical battery, N, S – the poles of magnet, I – the electric current intensity.

An appropriate material to construct a helix is a cooper wire without isolation, with a diameter of approximately 0.5–1 mm, coated with tin or silver and used to create connections in electric networks. The wire with that a diameter is accurate for hand winding and it can also be bent with universal pliers. The isolated wire can be used and applied to roll windings, but isolation enamel needs to be removed from the parts that compose the contact ring and the tip. In order to enable easy laying of helix, the magnet diameter should be the same or grater than that of the battery. If these diameters are equal to each other, then the helix may be properly winded on the battery. While winding, each wire convolution should be placed precisely next to the previous and the following ones. After hand winding and releasing the wire, helix diameter, as well as a distance between the coils will slightly increase which is caused by the wire elasticity. The increase in internal diameter of the helix makes its movement easier after placing it on the battery. The contact ring is composed of 2–3 wire coils which adhere to each other and are soldered together. This ring's inner diameter should be about 0.5 mm grater than the neodymium magnet diameter. Then it enables a good contact between the ring and magnet, and there is little friction during the rotation. The number of helix coils may vary from only a few to even several dozens. A direction of winding (left-handed or right-handed) is arbitrary.

In the constructed motors, there were applied cylindrical neodymium magnets: one with the diameter 14 mm and height 10 mm and the other one with the diameter 33 mm and 30 mm in height. In both cases, cylindrical alkaline batteries with the electromotive force 1.5 V were used. Batteries had steel shield enabling their coaxial positioning and connection with the magnet. For smaller magnets, there were used batteries LR6 (AA) with the diameter 14 mm, and for bigger ones LR20 batteries with the diameter 33 mm. The number of convolutions used in helix ranged from 5 to 20. In order to start the motor, the batteries ought to be placed on the magnet in a coaxial position, and then the helix should be put on the battery. In order to ensure better contact between the helix and the battery, a slight cavity can be made inside the battery's pole. To do this one should take a tip of nail, place it on the battery pole and gently it with a hammer. If orientation of the magnets poles and the battery, as well as direction of the helix winding is the same as in Fig. 2, then the vertical helix oscillations will appear. Moreover, the helix will revolve, similarly as frame in Faraday's motor. The motors constructed are presented on photos 1–3.

4. Operation of the unipolar motor with a helical rotor

The reason of the observed helix movements will be explained and discussed below. To do this, we shall consider forces which are applied to an element of helix that is located on the battery. According to a generally accepted convention, magnetic field lines are oriented from the north to south pole; cf. Fig. 3.

Spatial distribution of field lines has an axis symmetry and these lines are located within surfaces which go through the magnet axis. The magnetic induction

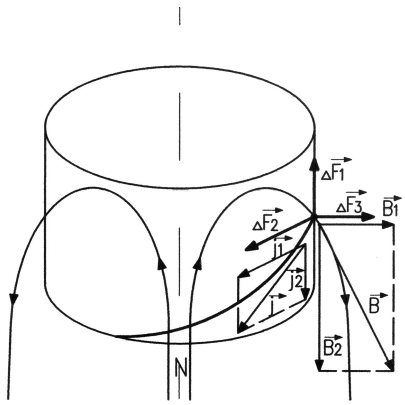

Fig. 3: Explanation of the electrodynamics forces origins in the unipolar motor with a helical rotor; $\Delta\mathbf{F}_1,\ \Delta\mathbf{F}_2,\ \Delta\mathbf{F}_3$ – the components of electrodynamic forces applied to the helix element respectively: vertical, tangent and radial, $\mathbf{B}$ – a vector of magnetic field induction, $\mathbf{B}_1,\ \mathbf{B}_2$ – the components of the field induction respectively: horizontal and vertical, $\mathbf{j}$ – a current density vector, $\mathbf{j}_1,\ \mathbf{j}_2$ – the components of the current density respectively: horizontal and vertical.

vector $\mathbf{B}$ occurs at every point of the magnetic field, and is tangent to those lines. Within points on the helix, the induction vector $\mathbf{B}$ is inclined downwards. It can be decomposed into a horizontal element $\mathbf{B}_1$, and a vertical element $\mathbf{B}_2$ directed alongside radius, which is tangent to helix. Similarly, the current density $\mathbf{j}$, flowing in the helix, is inclined and tangent to the direction of convolution. This vector will be also decomposed into a horizontal component $\mathbf{j}_1$ and a vertical component $\mathbf{j}_2$. Both components, $\mathbf{j}_1$ and $\mathbf{j}_2$ are located within a plane tangent to the helix side surface. Vectors $\mathbf{j}_1$ and $\mathbf{B}_1$ are perpendicular to each other. Therefore there is an electrodynamics force $\Delta\mathbf{F}_1$, applied to an element of helix wire of length Δl, and the force $\Delta\mathbf{F}_1$ is located vertically upwards. Using generally accepted signs, the force $\Delta\mathbf{F}_1$ may be expressed by

$$\Delta\mathbf{F}_1 = S\Delta l\,(\mathbf{j}_1 \times \mathbf{B}_1) \tag{1}$$

where S means the area of wire cross section. Similarly, vectors $\mathbf{j}_2$ and $\mathbf{B}_1$ are also mutually perpendicular, thus the electrodynamics force $\Delta\mathbf{F}_2$ occurs, oriented horizontally and perpendicularly to the helix radius. This force can be expressed as:

$$\Delta\mathbf{F}_2 = S\Delta l\,(\mathbf{j}_2 \times \mathbf{B}_1)\,. \tag{2}$$

The force $\Delta\mathbf{F}_2$ creates a momentum which turns the helix around. However, if a resulting force $\Delta\mathbf{F}_1$ is high enough, it will lift of helix convolutions. As a result, the helix tip stops touching the upper pole of the battery and the electric circuit becomes opened. The force $\Delta\mathbf{F}_1$ will become zero and the helix convolutions will fall down because of their own weight. That situation will cause another close of circuit which generates the force $\Delta\mathbf{F}_1$. Afterwards, these processes will repeat, and cause the helix oscillation motion. The oscillations, developed in such a manner, have a relaxation character. These oscillations are possible only in case of the above orientation of the magnet and battery, as well as for the direction of the helix winding, in which the force $\Delta\mathbf{F}_1$ is directed upwards. In addition the horizontal component $\mathbf{j}_1$ of the current density vector is also perpendicular to the vertical component of the magnetic induction $\mathbf{B}_2$ and then, the electrodynamics force $\Delta\mathbf{F}_3$ which is produced in such a method is oriented along the helix radius. As the result the force $\Delta\mathbf{F}_3$ cannot trigger the helix motion, and only causes its radial tension. Moreover, within the helix convolutions, there is a flow of electric current in the same direction. Because of this, the convolutions attract each other. However the force occurring in this process may not be taken into consideration, as it is significantly lower than the interaction force between the wires and the magnetic field, which is developed by the magnet. It is derived from both the measurements and the calculations. Such a research indicates that area average magnetic induction, generated by the magnet within the helix zone, equals to a few dozens m T. In comparison the average induction of the area, generated by the adjacent helix convolutions is about a few μT (for a typical electric current intensity of about 2 A which can be averagely obtained from a cylindrical battery).

5. Alternative unipolar motors with a helical rotor

The unipolar motor described above allows to make alterations in its construction, and an investigation of its influence on the helix actions. The battery can be easily placed on a magnet conversely, this means to direct its positive pole downwards. The magnet can also be inverted around, as to place its north pole downwards. The inversion of the batteries poles only or the magnet poles orientation causes an inversion of the force $\Delta\mathbf{F}_1$, and an oscillation of the helix will not appear. Then there will be a downwards extension of the helix, and a tension of its tip exerted on the battery will increase. Senses of the forces $\Delta\mathbf{F}_2$ and $\Delta\mathbf{F}_3$ will become also inverted. In such a situation, the helix can only turn around in an opposite direction. The angular velocity will be lower because of an increase within a friction force and its momentum. If the friction force is too high, then the rotation will not occur, and the helix will only remain extended. In this case, the experiments should not be prolonged because the battery is in a state of short circuit by the helix, and it results in heating of both elements.

Simultaneous change of the poles of the battery and the magnet orientation will not cause a change in the helix motion. Further experiments may be performed in the field of application of the helix, winded in an opposite direction, and may investigate influence of this change on the direction of the rotation and the oscillation occurrence. The others thorough examinations may investigate how is the influence of the helix convolutions number, their diameters, pitch of convolution and the diameter of the applied wire on a frequency and the amplitude of oscillation within the helix, as well as its angular velocity. What is more, the described unipolar motor is easy to build, powered by two or more batteries, located one on the top of another. When using a greater number of batteries, the attraction force of the higher placed batteries towards the magnet will be less. Hence, in order to ensure good stability of the system and an electric contact, the batteries should be connected towards each other, and their side surface should be secured with an adhesive tape.

It is also worth applying the helix in a popular version of the unipolar motor with the neodymium magnet suspended on a nail attraction to the battery [3]. Such a motor is presented in Fig. 4.

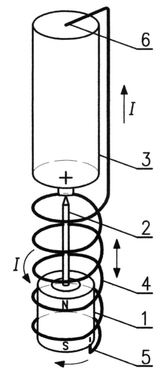

Fig. 4: The application of helix in the unipolar motor with a suspended magnet; 1 – a cylindrical neodymium magnet, 2 – a nail, 3 – a cylindrical battery, 4 – the helix winded with the nonferromagnetic wire, 5 – the lower end of the wire, 6 – the upper end of the wire, N, S – the poles of the magnet, I – the electric current intensity.

This figure presents that the battery LR6 (AA) and the helix winded from a thin, nonferromagnetic wire with 0.3 mm diameter were applied. The lower end of the helix should touch a flat surface of the magnet (the upper or the lower one), near its edge, in order to enable a current flow through the magnet in a radial direction. In such version of the motor, a battery is held with a thumb and a middle finger of one hand, and index finger presses the upper end of the helix towards the battery pole. For a respective orientation of the magnet and battery poles in that version of the motor, both the magnet rotation and the helix oscillation can be observed. Such a system is, in a way, similar to the Roget's helix, called "the dancing spring" [6, 7]. Summing up, it can be stated that the above described unipolar motor with the helical rotor, is adequate for various display experiments, as well as for more advanced quantitative research. Its substantial advantages encompass the uncomplicated construction and the low costs of the applied materials.

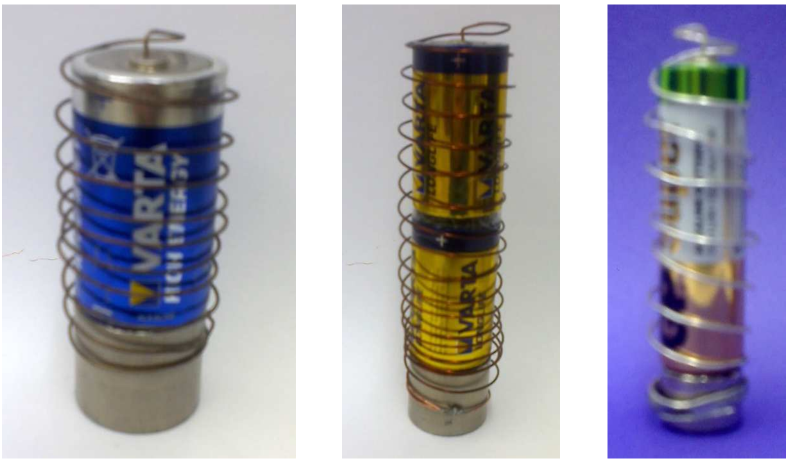

a) b) c)

Photo 1: The external view of the three unipolar motors with the helix rotor selected from a constructed series; a) a motor with LR6 (AA) battery, b) a motor with R20 battery, c) a motor with two batteries R20 connected in series.

References

[1] www.sparkmuseum.com/Early Electric Motor.

[2] N. Sugimoto and H. Kawada, *The unipolar motor and its evolution*, The Physics Teacher **44** (2006), 313.

[3] H. J. Schlichting and C. Ucke, *Der einfachste Electromotor der Welt: Spielweise*, Physik in unserer Zeitschrift **35**, no. 6 (2004), 272.

[4] A. K. T. Assis and J. P. M. C. Chaiba, *Ampêre's motor: Its history and the controversies surrounding its working mechanism*, American Journal of Physics **80**, no. 11 (2012), 990.

[5] https://www.youtube.com/Unipolar Dragonfly.

[6] G. D. Freier and F. J. Anderson, *A demonstration handbook for physics*, American Association of Physics Teachers, College Park Madison (1996) E-28.

[7] R. M. Sutton, *Demonstration experiments in physics*, McGraw-Hill Book Company Inc. New York-London 1938, 311.

Chair of Informatics
University of Łódź
Pomorska 149/153, PL-90-236 Łódź
Poland
e-mail: bedastan@uni.lodz.pl

Presented by Leszek Wojtczak at the Session of the Mathematical-Physical Commission of the Łódź Society of Sciences and Arts on May 28, 2015

SPRZĘŻENIE MIĘDZY OBROTEM I DRGANIAMI PODŁUŻNYMI W SILNIKU JEDNOBIEGUNOWYM

S t r e s z c z e n i e

W artykule opisano silnik, który jest zmienioną wersją jednego z najwcześniejszych silników wynalezionych przez M. Faraday'a. Zmiana polega na zastosowaniu wirnika w kształcie spirali nawiniętej na powierzchni cylindrycznej. Wirnik ten nałożony został na walcową baterię alkaliczną, ustawiona na również walcowym magnesie neodymowym. Zaobserwowano wówczas, że oprócz obrotu wirnik wykonuje również drgania w kierunku osiowym. Ten nowy efekt został wyjaśniony oraz przedyskutowano warunki jego występowania.

Słowa kluczowe: silnik jednobiegunowy, siła elektrodynamiczna, obrót, drgania osiowe, sprzężenie

PL ISSN 0459-6854

BULLETIN

DE LA SOCIÉTÉ DES SCIENCES ET DES LETTRES DE ŁÓDŹ

2015 Vol. LXV

Recherches sur les déformations no. 2

pp. 93–103

Stanisław Bednarek and Paweł Tyran

THE MICROWAVES ABSORPTION IN FERROFLUID CONTROLLED BY THE MAGNETIC FIELD

Summary

The construction of the system for research of microwaves interaction with ferrofluid located in the magnetic field produced by Helmholtz coils is described. The microwaves frequency equals 6.5 GHz. The magnetic field induction directed alongside of microwaves beam were changed in range of 0–80 mT. The ferrofluid's samples of thickness 0–15 mm consist of magnetite nanoparticles coated by oleic acid and dispersed in mineral oil were tested in this system. The most important result of this investigation is detection that intensity of microwaves transmitted by ferrofluid depends on the applied magnetic field induction. Technological application of this dependence in microwave absorber controlled by the magnetic field is possible.

Keywords and phrases: ferrofluid, microwave, magnetic field, absorption

1. Introduction

In recent years an increasing interest in electromagnetic weapon, called the E-weapon, has been observed [1]. The principle of operation of this weapon consists in emission of high power microwave pulses [2]. While reaching objects prepared from conductive materials, such pulses induce electromotive forces and electric current of high intensity. In case of encountering electrical and electronic equipment, the induced currents destroy or damage them [3]. The main targets of the E-weapons are posed by power and information networks, serving-receiving apparatus and hardware [4].

Since the listed objects of fire are of considerable significance for operation of contemporary states and societies, effective means of protection against the E-weapon are sought for [5]. For that purpose, there are various studies performed over material that absorb the energy of microwaves, e.g. metamaterials, cavity and porous structures, composites, paints, pastes and suspensions. A material serviceable for that purpose may be constituted by ferrofluids. This assumption arises from the fact that ferrofluids are particle suspensions with high magnetic permeability, which triggers an increase of the absorption coefficient of electromagnetic waves [6]. Furthermore, spatial distribution of those particles is altered upon application of the magnetic field. This may allow to control the absorbing properties of those materials. The discussed premises caused investigation into the interactions between the microwaves and the ferrofluid. Results of the mentioned investigation are included in the article.

2. The experimental system

The experimental system presented in Fig. 1 and Photo 1. has been applied in the investigation over the microwaves absorption by ferrofluids . Samples of the ferrofluid were closed in a cylindrical container 1 with an internal diameter of 32 mm, prepared from polymethylacrylate, Fig. 2 and Photo 2. Structure of the container allowed to increase the contained amount of the ferrofluid easily. The container was place horizontally on the support 2 with an opening. There was a diaphragm 3 beneath the opening, prepared from aluminum plate, which limited the widths of the microwave beam to the container's internal diameter. The source of the microwaves was posed by a transmitter 4, equipped with a $k-19$ reflex klystron [7]. Voltages necessary for the klystron to operate were produced by a supplier P. Microwaves frequency amounted 6.5 GHz, and the emitted beam power equaled 35 mW.

The outgoing beam was directed vertically from the bottom, to the ferrofluid container through a horn of the transmitter 5. It was an incident beam 7. Magnetic field was applied to the ferrofluid, produced by the system of Helmholtz's coils 12, 14, arranged symmetrically towards the container, on the supports 13, 14. Direction of induction of the magnetic field $\mathbf{B}$ was parallel to the axis of microwaves beam and of the ferrofluid container. The magnetic field induction was altered in the range 0–80 mT, through changing the power source voltage U of the Helmholtz's coils. Thanks to application of the system of these coils, homogeneity of the magnetic field induction inside the ferrofluid container did not exceed $\pm 4\,\%$. Measurements of the magnetic field induction were carried out with a teslameter with Hall sensor. Having been transmitted through the ferrofluid container, the incident beam 7 was converted into the transmitting beam 8, and entered into the receiver's horn 9. Intensity of the beam was measured by the receiver 10. The microwaves detector in the receiver was a microwave diode D, biased in reverse direction. The reverse bias caused no current to flow through the diode, where the microwaves did not descend on it [8].

When the microwaves descended on the diode, current carriers were generated and current flow was triggered with intensity directly proportional to that beam's intensity. The current was amplified by an amplifier A and measured through a micro

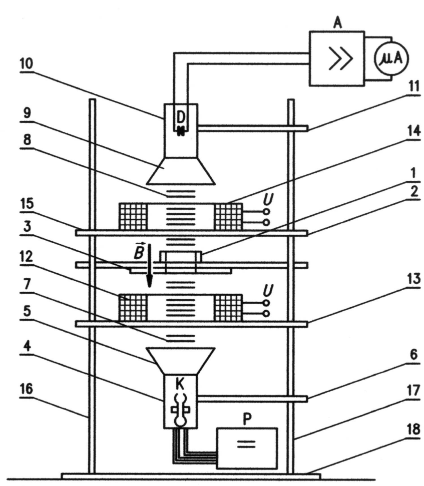

Fig. 1: Scheme of the system for investigation of microwaves absorption in ferrofluids; 1 – a container with ferrofluid, 2 – base of the container, 3 – cover, 4 – microwaves transmitter, 5 – horn of the transmitter, 6 – holder of the receiver, 7 – the incident beam of microwaves, 8 – the transmitted beam of microwaves, 9 – horn of the receiver, 10 – receiver of the microwaves, 11 – holder of the receiver, 12 – lower Helmholtz's coil, 13 – support of the lower coil, 14 – upper Helmholtz's coil, 15 – support of the upper coil, 16, 17 – brackets, 18 – base of the system, K – reflective klystron, P – power supply of the klystron, D – microwave diode, A – amplifier, μA – microammeter, U – power voltage of the coils, B – magnetic field induction.

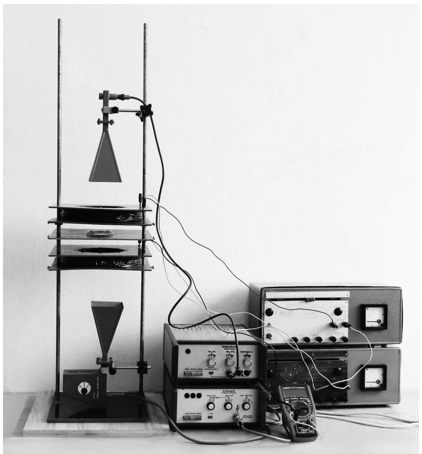

Photo 1: External view of the system,
where absorption of waves in ferrofluids was investigated.

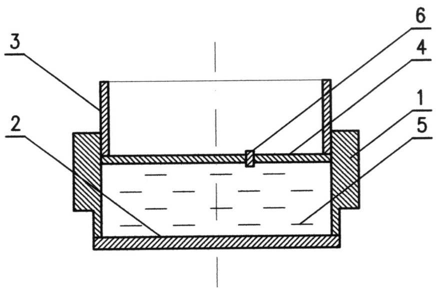

Fig. 2: Structure of the ferrofluid container; 1 – lower part of the container, 2 – bottom of the lower part, 3 – upper part of the container, 4 – bottom of the upper part, 5 – ferrofluid, 6 – venting cork.

Photo 2: External view of the ferrofluid container.

ammeter μA. Based on the indications of the ammeter, a proportion of intensity of the beam transmitted through the ferrofluid towards the incident beam. A ferrofluid with magnetite nanoparticles – 10–40 nm in size, coated with a mononuclear layer of oleic acid, dispersed in mineral oil – was applied, The layer of oleic acid protected against agglomeration and sedimentation of particles. The magnetite content constituted 6.15 % of the ferrofluid mass, and was estimated with an X-ray microanalyzer. No diluted and diluted ferrofluids were applied. A mixture of toluene and acetone in a volume ration 7 : 3 was applied as a diluent. An addition of the diluent was 30 % or 60 % of the ferrofluid volume. The whole investigation was performed in the temperature 24°C.

In the first part of the experiment, the transmission ability of the incident beam of constant intensity through a layer of ferrofluid in dependence on its thickness was investigated. In this part of the experiment, there was no magnetic field applied to the ferrofluid. At first, the empty container 1 was placed in the experimental system, and the microwaves beam was directed towards it. The intensity of the current respective to the beam intensity I_0, which was transmitted through the empty container, was measure with the ammeter. Afterwards, the ferrofluid was poured into the container, generating layers with increasing thickness h, which the beam was transmitted through. Thickness of this layer was altered in the range of 0 mm to 15 mm with spacing of 1 mm. The respective current intensity – directly proportional to the microwaves intensity, transmitted through the layer I – was measured for each thickness of the layer. On the basis of achieved results, the ratio of intensity of the beam transmitted through the ferrofluid layer towards the incident beam I/I_0 was calculated. The obtained results served preparation of the charts presented in Fig. 3.

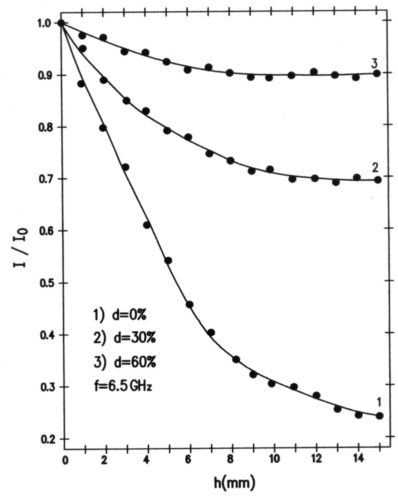

Fig. 3: Relation between the transmitted beam intensity ratio to the incident beam intensity I/I_0, and the thickness of the ferrofluid layer h for various degrees of dilution d.

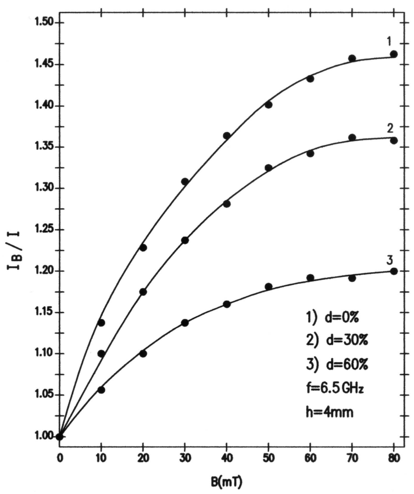

Fig. 4: Relation between the transmitted beam intensity ratio with the applied magnetic field to the transmitted beam intensity without the magnetic field I_B/I and the field induction B for a ferrofluid layer $h = 4$ mm thick with various degrees of dilution d.

In the second part of experiment, transmission of the incident beam with intensity specified by a ferrofluid layer of selected thickness from induction of the applied magnetic field B was investigated. The investigation was performed in case of three chosen thicknesses – 4 mm, 8 mm and 12 mm. For that purpose, a layer of ferrofluid of selected thickness was placed inside the container and a microwave beam was directed on it. In such conditions, current intensity I, corresponding to the beam transmitted through the magnetic field was measured. Afterwards, the magnetic field of induction B – change in the range 0–80 mT with interval 10 mT – was applied to the ferrofluid, and current intensity I_B, corresponding to the transmitted beam intensity was measured. While applying the obtained values, the I_B/I ratio was calculated. Results of the calculations was used to draw charts presented in Figs. 4–6.

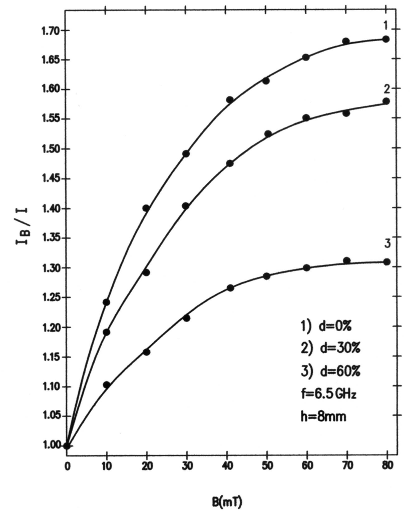

Fig. 5: Relation between the transmitted beam intensity ratio with the applied magnetic field to the transmitted beam intensity without the magnetic field I_B/I and the field induction B for a ferrofluid layer $h = 8\,\text{mm}$ thick with various degrees of dilution d.

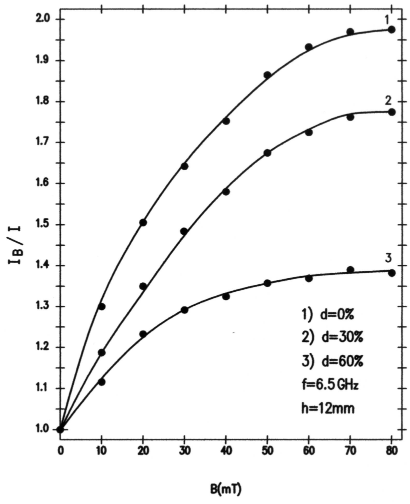

Fig. 6: Relation between the transmitted beam intensity ratio with the applied magnetic field to the transmitted beam intensity without the magnetic field I_B/I and the field induction B for a ferrofluid layer $h = 12\,\text{mm}$ thick with various degrees of dilution d.

3. Discussion on the results

The performed investigation proved that before applying the magnetic field to the ferrofluid, intensity of the transmitted beam I decreases together with thickness of its layer h, Fig. 3. A layer of not-diluted ferrofluid, 15 mm thick, causes reduction in the transmitted beam by 3.9 times. The ferrofluid layers of the same thickness, with 30 % and 60 % of the diluent provide attenuation of the beam 1.5 and 1.1 times respectively. Dependencies of intensity of the transmitted beam I on thickness of the ferrofluid h is of nonlinear character. For lower thicknesses of the ferrofluid, reaching several millimeters, reduction of intensity of the transmitted beam takes place faster than for higher thickness. Furthermore, this effect is considerably weaker for diluted ferrofluids. For an non-diluted ferrofluid, an increase in the layer thickness h from 0 mm to 4 mm, caused reduction of the transmitted beam intensity by 1.9 times. After adding 60 % diluent, the reduction reached only 1.05 times. For the sake of comparison, an increase in thickness of the non-diluted ferrofluid from 10 mm to 15 mm resulted in reduction of the transmitted beam intensity only by 1.4 times, and for the ferrofluid with 60 % diluent, this reduction was non-measurable (see curve 3 in Fig. 3).

Having placed the ferrofluid in the magnetic field, the transmitted beam intensity I_B increased together with a rise of the magnetic field induction B. This increase took place for all three layers selected for investigation, with thicknesses 4 mm, 8 mm and 12 mm, both for non-diluted and diluted ferrofluids. The speed of this increase depended on the thickness of the ferrofluid layer and on the degree of its dilution. Furthermore, in all of the mentioned cases, the dependency of the transmitted beam intensity I_B, on the magnetic field B was non-linear. If the ferrofluid layer was thicker, the ratio of the transmitted beam intensity I_B, in the magnetic field of maximal induction 80 mT to the transmitted beam induction I before application of the field was higher. For example, for a layer $h = 4$ mm, the ratio was 1.47, and for $h = 12$ mm, equaled 1.97 (compare Fig. 5 and 7). These values are related to the non-diluted ferrofluic

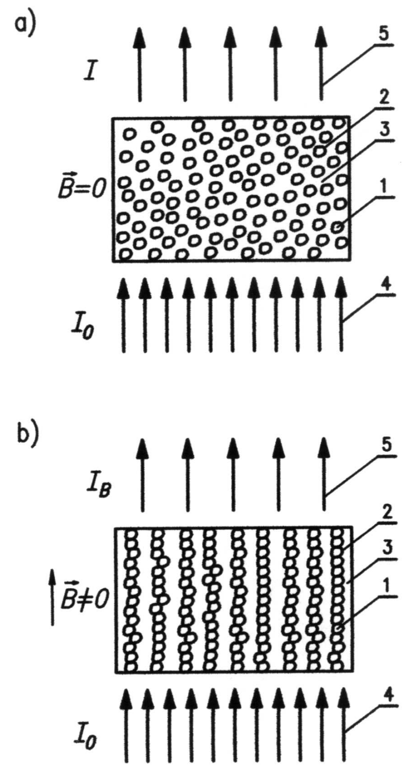

Fig. 7: Schematic presentation of microwaves beam transmission in a ferrofluid: a) before application of the magnetic field, b) after application of the field; 1 – magnetite particle, 2 – surface–active substance, 3 – dispersion fluid, 4 – incident beam, 5 – transmitted beam, I_0 – intensity of the incident beam, I – intensity of the transmitted beam without magnetic field, I_B – intensity of the transmitted beam after application, without magnetic field, B – field induction.

Ferrofluid dilution caused a reduction in I_B/I. In case of 8 mm thickness, addition of 60 % diluent caused a reduction I_B/I from 1.69 to 1.31 (cf. Fig. 6). The nonlinear dependency of the transmitted beam intensity I_B on the magnetic field induction B is shown through a quick increase of this intensity in the initial part of the range of induction changes (0–30 mT) in comparison with the final part of this range (50–80 mT). This regularity is more considerable for diluted ferrofluids, where stabilization of the transmitted beam intensity was observed in the final part of the range of induction changes (compare curves 3 and 1 in Fig. 5–7).

A reason for the observed changes in the microwaves intensity while transmitting through the ferrofluid is its interaction with the magnetite particles, where the spatial distribution is changed after application of the magnetic field, Fig. 7. If the electromagnetic waves incident on the material of high electric conductivity σ and relative magnetic permeability close to $\mu_r \approx 1$, e.g. aluminum or copper, they are reflected. What is more, the waves penetrate the medium to rather shallowly. The penetrating waves are strongly dumped. Intensity of the penetrating wave I_w on the level x, measured from the material surface, is expressed by the following formula [6].

$$I_w = I_0 e^{-\frac{x}{u}}, \tag{1}$$

where: I_0 – intensity of the incident wave, u – conventional depth of penetration, for which intensity of the wave in the medium is reduced by e times.

The depth of penetration u is calculated from the formula

$$u = \sqrt{\frac{1}{\pi f \sigma \mu_0 \mu_r}}\,, \tag{2}$$

where: f – wave frequency, μ_0 – magnetic permeability of vacuum.

For the discussed materials and frequencies from the microwave range, the conventional depth of penetration is very small, reaching $10^{-5} - 10^{-6}$ m. Even smaller depth of penetration is proved by conductive ferromagnets, e.g. iron or steel, for which $\mu_r \gg 1$. In case of a dielectric, e.g. plastics, electrical conductivity is about 10^{-20} smaller than for metals [9]. Formula (2) suggests that the conventional depth of penetration is then higher than for metals by 10^{-10}. Therefore, the electromagnetic waves penetrate dielectrics almost completely. These cases are relatively easy to be described theoretically [10].

If the conductive qualities of the material are limited, and it proves $\mu_r \gg 1$, then partial absorption of electromagnetic waves and their partial penetration takes place. The conventional depth of penetration to such a medium is expressed by a more complicated formula [11].

$$u = \sqrt{\frac{2}{\sqrt{(2\pi f)^4 \left(\varepsilon_0 \varepsilon_r \mu_0 \mu_r\right)^2 = \left(2\pi f \sigma \mu_0 \mu_r\right)^2} - (2\pi f)^2 \varepsilon_0 \varepsilon_r \mu_0 \varepsilon_r \mu_0 \mu_r}}, \tag{3}$$

where: ε_0 – electrical permittivity of vacuum, ε_r – relative permittivity of medium.

The presented situation exists in case of the investigated ferrofluids, with magnetite particles of superparamagnetic properties or in some ferromagnetic cases, also characterized by $\mu_r \gg 1$. These particles are not good conductors of electric current. It is explained by the fact that specific conductivity of magnetite σ in the temperature of 25°C is about 10^4 S/m [12, 13]. For the sake of comparison, conductivity of metals in those conditions reaches the level of 10^5–10^6 S/m, and conductivity of insulators is included in the range 10^{-12}–10^{-17} S/m. Furthermore, the ferrofluid includes dispersive liquid and a surface-active substance, which are dielectric. Hence, the ferrofluid is inhomogenous in the microscope scale. Investigations of other authors proved that with high intensities of electric and magnetic field, both the magnetic and electric permeability depend on frequency [14, 15]. Such a situation is related to the investigated ferrofluids, and that is why they are a structure of changeable properties, hard to be described quantitatively.

The performed experiments showed that the applied microwaves transmit through the ferrofluid, and are partially absorbed. Furthermore, significant meaning for the level of absorption is borne by thickness of the ferrofluid layer, its degree of dilution and induction of the applied magnetic field. These dependencies may be explained by assuming that absorption of microwaves takes place mainly by the magnetite particles included in the ferrofluid. If amount of the particles was reduced by application of a thinner layer of the diluted ferrofluid, an increase in intensity of the transmitted beam was observed. In turn, a rise in the degree of the particles order through application of the magnetic field and creation of a column-fiber structure, suggested by Winslow, also caused an increase in the transmitted beam intensity I_B [16, 17].

The ordered structure includes areas with a reduced content of magnetite particles, where the dispersion fluid is located. The areas present a smaller ability to absorb microwaves, which is presented schematically in Fig. 7. Energy of the absorbed microwaves is dissipated as a result of changes in the direction of magnetization of the magnetite particles, polarization alterations of molecules of dispersive liquid and surface-active liquid, and induced micro-eddy-currents in magnetite particles. Energy of those micro-currents is conversed into Joule heat. Dissipation of this energy may be also supported by changes in orientation of the magnetite particles, induced by alterations of the microwaves magnetic field. These changes are suppressed by forces of viscosity of the dispersive liquid. Eventually, the energy of the absorbed microwaves cause an increase in the ferrofluid temperature. An increase in temperature would be hard to measure for insignificant power of microwaves, emitted by the applied klystron. In order to perform the measurement, it was necessary to place a ferrofluid sample in a calorimeter and carefully apply thermal stabilization.

While summing up the performed experiments it may be concluded that the ferrofluid layer, placed in the ferromagnetic field plays a role of a controlled absorbent, which enables multiple modification of the microwaves intensity. This effect is useful in innovative technological solutions, e.g. in removed filters or adaptive shields protecting against microwave radiation.

References

[1] R. Kubacki and M. Wnuk, *Broń elektromagnetyczna – broń przyszłego pola walki*, w: Z. Merczyk (red.) *Ochrona przed skutkami nadzwyczajnych zagrożeń*, Wojskowa Akademia Techniczna, Warszawa, **1** (2010), 461–470 [*Electromagnetic weapon – weapon at the future field of combat*, in: Z. Merczyk (ed.) Protection from results of the special dangers, Military Academy of Science, Warsaw (in Polish)].

[2] K. Bechta, *Broń elektromagnetyczna – istota i znaczenie broń przyszłości*, Spectrum, Biuletyn Organizacyjny i Naukowo-Techniczny Stowarzyszenia Elektryków Polskich **5-6** (2011), 16–19 [Electromagnetic weapon – principle, significance, future weapon, Spectrum, Organizational and Information Bulletin of the Polish Electrical Engineers Association (in Polish)].

[3] J. Benford, J. A. Swegle, and E. Schamiloglu, *High Power Microwaves*, Second edition, Taylor and Francis Group, New York-London 2007, 109.

[4] J. Borczyński and J. Chudroliński, *Oddziaływanie pól elektromagnetycznych małej częstotliwości na organizmy żywe i urządzenia elektroniczne*, Elektronika XLIII **5** (2002), 24–26 [*Interaction of the electromagnetic fields of low frequency with living organism and electronic devices*, Electronics (in Polish)].

[5] J. Sobiech, J. Kieliszek, R. Pluta, and W. Stankiewicz, *Modelowanie numeryczne kształtu fantomu do pomiarów pola elektromagnetycznego przez ubiór ochronny*, Przeglad Elektrotechniczny **89**, no. 12 (2013), 293–294 [*Computer modeling of the phantom shape for the electromagnetic field measurements through protective dress*, Electrical Review (in Polish)].

[6] H. Rawa, *Elektryczność i magnetyzm w technice*, Państwowe Wydawnictwo Naukowe, Warszawa 1994, 400 [*Electricity and Magnetism*, Scientific and Technology Edition, Warsaw (in Polish)].

[7] J. Hennel, *Lampy elektronowe*, Wydawnictwa Naukowo-Techniczne, Warszawa 1976, 130 [*Electronics tubes*, Scientific and Technology Edition, Warsaw (in Polish)].

[8] T. Stecewicz and A. Kotlicki, *Elektronika w laboratorium naukowym*, Państwowe Wydawnictwo Naukowe, Warszawa 1994, 63 [*Electronics in scientific laboratory*, Scientific and Technology Edition, Warsaw (in Polish)].

[9] W. Mizerski, *Tablice fizyczno i astronomiczne*, Wydawnictwo Adamantan, Warszawa 2013, 172 [*Physical and astronomical tables*, Edition Adamantan, Warsaw (in Polish)].

[10] J. D. Landau and J. M. Lifszyc, *Fizyka teoretyczna, Elektrodynamika ośrodków ciągłych*, Panstwowe Wydawnictwo Naukowe, Warszawa 2012, 511 [*Electrodynamics of continuous media*, Polish Scientific Edition, Warsaw (in Polish)].

[11] A. Wiecheć, *Rola oddziaływań magnetycznych w przemianie Verweya na podstawie badań właściwości magnetycznych magnetytu i cynkoferrytów $Fe_{3-x}Zn_xO_4$* ($x = 0.05$), Rozprawa doktorska wykonana w Katedrze Fizyki Ciala Stałego Wydziału Fizyki i Informatyki Stosowanej Akademii Górniczo-Hutniczej w Krakowie, Kraków 2008, 7.

[12] R. Aragón, R. J. Rasmussen, J. P. Shepherd, J. W. Koenitzer, and J. M. Hoang, *Effect of stechiometry changes of electrical properties of magnetite*, Journal of Magnetism and Magnetic Materials **50-54**, no. 3 (1986), 1335–1336.

[13] A. Chełkowski, *Fizyka dielektryków*, Państwowe Wydawnictwo Naukowe, Warszawa 1993, 90 [*Physics of dielectrics*, Polish Scientific Edition, Warsaw (in Polish)].

[14] S. Gąsiorek and R. Wadas, *Ferryty, zarys właściwości i technologii*, Wydawnictwa Komunikacji i Łączności, Warszawa 1987, 126 [*Ferrites outline of properties and tech-

nology, Edition of Transport and Communication, Warsaw Polish Scientific Edition, Warsaw (in Polish)].

[15] W. M. Winslow, *Induced fibration of suspension*, Journal of Applied Physics **20**, no. 12 (1949), 1137–1140.

[16] J. Černik, *Aggregation of needle-like macro-clusters in thin layers of magnetic fluid*, Journal of Magnetism and Magnetic Materials **132** (1994), 258–269.

[17] S. Bednarek and P. Tyran, *Filtr promieniowania elektromagnetycznego i jądrowego*, Opis zgłoszeniowy wynalazku, zarejestrowany w Urzędzie Patentowym Rzeczypospolitej Polskiej pod Nr 406996 (2014) [*Filter of electromagnetic and nuclear radiation*, Description of invention, registered in Patent Office of Poland Republic with No. 406996 (in Polish)].

Chair of Informatics
University of Łódź
Pomorska 149/153, PL-90-236 Łódź
Poland
e-mail: bedastan@uni.lodz.pl

Presented by Leszek Wojtczak at the Session of the Mathematical-Physical Commission of the Łódź Society of Sciences and Arts on September 10, 2015

ABSORPCJA MIKROFAL PRZEZ FERROFLUIDY STEROWANA POLEM MAGNETYCZNYM

S t r e s z c z e n i e

Opisana została budowa układu do badania oddziaływania mikrofal z ferrofluidem umieszczonym w polu magnetycznym wytwarzanym przez cewki Helmholtza. Częstotliwość mikrofal wynosiła 6.5 GHz. Indukcja pola magnetycznego skierowanego wzdłuż wiązki mikrofal była zmieniana w granicach 0–80 mT. W tym układzie badano próbki ferrofluidu o grubości 0–15 mm, zawierające nanoczastki magnetytu pokryte kwasem oleinowym i zdyspergowane w oleju mineralnym. Najważniejszym wynikiem tych badań jest wykrycie, że natężenie wiązki mikrofal przechodzącej przez ferrofluid zależy od indukcji przyłożonego pola magnetycznego. Możliwe są techniczne zastosowania tej zależności w pochłaniaczach mikrofal sterowanych polem magnetycznym.

Słowa kluczowe: ferrofluid, mikrofala, pole magnetyczne, absorpcja

PL ISSN 0459-6854

B U L L E T I N

DE LA SOCIÉTÉ DES SCIENCES ET DES LETTRES DE ŁÓDŹ

2015 Vol. LXV

Recherches sur les déformations no. 2

pp. 105–117

Tomasz Raszkowski

MODELLING OF HEAT CONDUCTION IN MODERN TRANSISTORS

Summary

In this paper the thermal analyses related to the modelling of heat transfer in modern electronic structures are presented. The comparison of two thermal models is demonstrated. The first one is a classical approach based on the Fourier-Kirchhoff equation. The second one is a model which concerns the Dual-Phase-Lag equation. Moreover, some other heat conduction models appropriate for nanosized electronic structures are listed and shortly described. Furthermore, the thermal analyses of modern 12 nm Fin-FET transistor are given.

Keywords and phrases: Fin-FET transistor, Dual-Phase-Lag equation, Fourier-Kirchhoff equation, thermal analyses, nanoscale heat transfer, modern electronics

1. Introduction

Modern electronic demands a very precise analyses of the thermal processes which occur in electronic structures during their operation. Modern electronic devices become more and more smaller. Moreover, they are increasingly faster. Accelerated operating speed together with lesser dimensions cause the cooling of the electronic elements more difficult. It is not easy to install the heat sinks or other structures dissipating the heat from each of the miniature elements which generate the heat. So, one of the most important issues, related to the proper operating of that kind of devices, is the modelling of the heat conduction in modern integrated circuits. Furthermore, an electro-thermal analyses are commonly regarded to be a basic development step in designing and constructing of a professional electronic circuits, very small power modules, nanosized transistors and other submicron structures [1].

As it turns, the mentioned kind of the analysis might be useful not only for modeling of the heat conduction but also, for example, for estimation of the conditions of devices operation. It allows, as an example, to determine the temperature dependencies of the properties of analyzed electronic devices, analysis of the operating point of integrated circuits or even to determine of the maximal operating temperature of that circuits. Apart from that, the electro-thermal analyses also allow to the power density estimation.

Generally writing, last years bring some new approaches to the problem of heat transfer in electronic systems. For almost two hundred years, up to 1990s [2], the most popular model, which was used to thermal analysis preparation, was a Fourier-Kirchhoff model. It established the classical heat transfer theory. That theory has been just introduced by heat conduction law's originator, Jean Baptiste Joseph Fourier [3]. Beginnings of this theory date back to the early 1820s. The considered theory is based on the mentioned law of the heat conduction, which is also known as a Fourier's law. The heat conduction law concludes that the heat flux density at a point ψ at a time t is proportional to the product of the gradient of a temperature at the point ψ at the time t and of the quantity called a thermal conductivity of a material which is analyzed. The mathematical form of this law presents itself in the following way:

$$q(\psi, t) = -\kappa \cdot \nabla T(\psi, t). \tag{1}$$

The symbol ψ means the location where the temperature analysis is conducted. Depending on the case, which is considered, the symbol ψ expresses the variables related to each dimensions. And, in one-dimensional case, this symbol expresses simply the only one coordinate. In two-dimensional case, the symbol ψ make the notation of two coordinates, for example x and y, easier. So, in such case, ψ can be expressed as $\psi = (x, y)$. Similarly to the previous case, when the three-dimensional structure is analyzed, the symbol ψ is an abbreviated notation of three coordinates, for example x, y and z, it can be written as $\psi = (x, y, z)$. It is worth writing that a negative sign, which is placed at the right side of the equation (1) indicates the direction of a heat propagation. The negative sign means that the heat flows from areas, where the higher temperatures are observed, towards regions characterized by cooler temperatures. The quantity κ is a thermal conductivity and it can be interpreted as a rate of the heat conduction. Of course, a variable q assumes values of the density of the heat flux. The ∇T expression, in turn, is a gradient of the temperature. The mentioned Fourier's law was a base to formulation of another very useful equation which was applied to modelling of heat conduction in almost all electronic structures up to the end of the twentieth century. The mentioned equation is called a Fourier-Kirchhoff equation. It is a parabolic partial differential equation for which the mixed boundary conditions were formulated. The mathematical form of that equation is presented below:

$$c_{vs} \cdot \frac{\partial}{\partial t} \left[r \cdot T(\psi, t) \right] = - \left[\nabla q(\psi, t) - q_{\mathrm{generate}}(\psi, t) \right]. \tag{2}$$

Similarly to the previous explanations, the variable q means the heat flux and it can be obtained using the Fourier's law. Symbol ∇q, of course, is a gradient of the mentioned heat flux. Moreover, the variable T expresses the temperature at location ψ at the time t. Of course, the explanation of the notation of the symbol ψ is the same like in the previous case, when the Fourier's law was considered. In the equation (2), a new variable appears. The variable q_{generate} expresses an international generation of the heat. Apart from that, equation (2) includes also two new quantities. First of them, c_{vs}, means the specific capacity of the heat, while the second one, r, is a notation of the density of the material, which is taken into considerations.

Both of described equations: this one, which expresses the Fourier's law as well as the Fourier-Kirchhoff equation were very important issues in the classic approach to a problem concerning the heat conduction because they allow to provide the first heat transfer theory. But now, at the age of the miniaturization, it turns that this classical model could be not appropriate for all cases, especially when the thermal processes occur very fast, for example during a few initial femtoseconds only after the electronic devices operating start. Moreover, due to the fact that some impossible behaviours are assumed using the Fourier-Kirchhoff equation, the classical heat transfer model is not sufficient in the case of microscopic structures [4]. One of the mentioned nonphysical assumptions is, for example, the instantaneous speed of propagation of the heat. Another one concerns the situation which could indicate that the heat flux and the gradient of temperature are characterized by the ability to their instantaneous changes. But, the experiments show clearly that mentioned situations are impossible [1, 5–7]. The other issue is related to continuing process of miniaturization of electronic structures and simultaneous acceleration of their speed of operation.

It causes that the Fourier-Kirchhoff equation and thereby the classical heat conduction theory can not be applied for example for electronic structures which are made in technology node smaller than about 200 nm [4]. Due to this fact, this paper includes considerations related to attempts to find new approaches to the heat transfer problems. Comparison of some most popular heat conduction models were found and listed in the next chapter of this paper.

2. Different approaches to heat transfer problem

Insufficiencies mentioned in the previous paragraph impose finding new approaches to the considered problem related to the heat transportation. It is needed to find such models which would allow to take into account most of microscale effects. Due to this need, some heat transfer models, appropriate even for the nanoscale, appears. One of them, called the Boltzmann Transport Equation, was provided in the early 1870s by an Austrian physicist Ludwig Boltzmann. The applicability of this model is available in real structure which are developed in technology down to a few nanometers. It can be also applied for larger structure, even up to few hundred nanometers.

A bit different model concerns, in turn, the molecular dynamics simulations. That model is also adequate for very small structures including such ones which technology node size is slightly bigger than 1 nm. The mentioned model was delivered in the late 1950s and it was originally applied for modelling of the biomolecules and in many branches of the science, for example in the material science or in the chemical physics.

Another one model which is adequate for nanoscale thermal modelling is based on a Schrödinger Equation. It was formulated and published in the mid 1920s by another Austrian physicist Erwin Schrödinger. This equation explains changes of a quantum state of the physical systems with the passing of the time. It is estimated that the mentioned model could be applied even in structures which technology nodes are significantly smaller than 1 nm. It denotes that the values smaller than the silicon lattice parameter could be taken into considerations.

The next model concerns the Ballistic-Diffusive equation. This model was proposed at the beginning of the XXI century by Chen [8]. It might be appropriate for nanosized electronic structures made in technology about 100 nm. An estimated scope of heat conduction models which would be apply for silicon structures is presented in the Fig. 1.

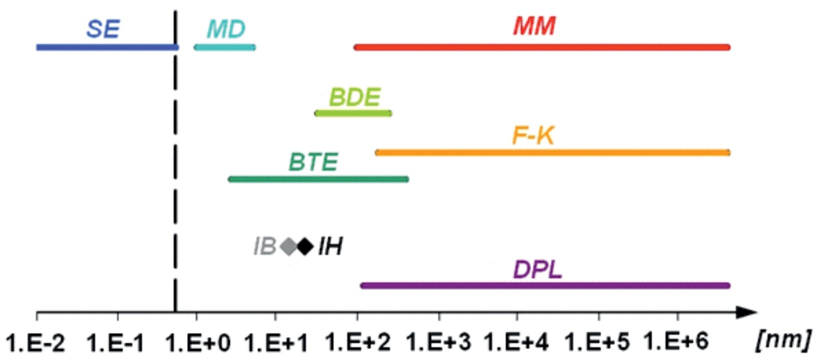

Fig. 1: An estimated scope of heat conduction model.

In the figure above different heat transfer models are compared. The notation SE is a short form of the Schrödinger Equation, while the MD means the simulations using Molecular Dynamics. The next model MM, marked by red color, is the general notation of many different macroscopic model, hence the letters used in this abbreviation. The subsequent model included in the figure Fig. 1 use the Ballistic-Diffusive Equation (BDE) to modelling the heat transfer in electronic structures. On the other hand, there is also BTE model in which the Boltzmann Transport Equation is employed. The other two model are: the Macroscopic Energy Treatment, marked by the orange color, which use the Fourier-Kirchhoff (F-K) equation and the

Dual-Phase-Lag model highlighted by the purple color. The only black dashed line indicates the value of the silicon lattice constant.

Many of the thermal models mentioned in the previous paragraph are appropriate for modelling of heat conduction in electronic nanosized structures. But most of them are characterized by a big computational complexity, so the simulation times in each of these cases are usually so long to convenient application during the research. Owing to this fact, another specific heat conduction model will be introduced and analyzed in this paper. This model is called Dual-Phase-Lag and it was formulated and proposed by Tzou at the end of twentieth century [2]. As it turns, that model is a very useful tool because it could be applied for hyperbolic heat models as well as the parabolic ones, such as the Fourier-Kirchhoff model. Apart for that, the Dual-Phase-Lag model can be commonly used to heat transfer modelling in most electronic structures, even in these which are developed in technology nodes smaller than the mentioned 200 nm and for structures which are operating at frequencies over 6 GHz [4].

As it was mentioned previously, the heat conduction modelling at nanoscale is currently very important because many new microscale structures are constructed and applied in modern electronic devices. A good example of the modern nanosized structures are for instance some families of the Intel CPUs in which the MOSFET transistors are applied. Another example concerns the nanowires and the nanotubes, a cylindrical nanostructure which are very valuable for optics, electronics, nanotechnology as well as the other fields of technology [1, 4]. There is also one structure which is worth mentioning. It is called the Fin-FET transistor [9, 11]. Due to these facts, the most of the following analyses are concerned the heat conduction in Fin-FET transistors.

3. The description of the model

The precise description of an electro-thermal model, which uses the classical Fourier-Kirchhoff equation, appropriate for the thermal analyses in the case of the Fin-FET transistor was proposed by Asenova's scientific team as it is presented in [9]. The mentioned paper includes the classic approach concerning the Fourier-Kirchhoff model, but some corrections of this model have been made. That corrections allowed applying mentioned model for nanoscale and for nanosized structures. Moreover, based on considerations presented in [2, 4, 9] and [10], the heat conduction inside the Fin-FET channel might be determined according to the following expression:

$$\frac{1}{\kappa} \cdot c_{vs} \cdot \left(\frac{\partial T}{\partial t} + \tau_q \frac{\partial^2 T}{\partial t^2} \right) \cong \Delta T + \nabla \cdot \left(\frac{\partial}{\partial t} \nabla \left(\tau_T \cdot T \right) \right) + \frac{1}{\kappa} \cdot q_{\mathrm{generate}}. \tag{3}$$

Similarly to previous equations (1) and (2), the quantity κ is a thermal conductivity, c_{vs} expressed the specific heat capacitance, T is a variables which values are related to the temperature. Moreover, t is time variable and a variable q_{generate} means the internal generated heat. There are also two new quantities, τ_q and τ_T. Their presence in the equation above is associated with the Dual-Phase-Lag equation which was a reference point to the formulation of the equation (3). Quantities τ_q and τ_T are usually called the heat flux time lag and the temperature time lag, respectively. Moreover, in many cases the value of the quantity τ_q is less than a few picoseconds. Of course, it depends on the parameters of considered materials and it may has different values for different structures.

In the following considerations, the finite slope of the changes of the mentioned heat flux is assumed. It can expressed in the following way:

$$\frac{1}{\tau_q} \cdot q_{\mathrm{gen}} > \frac{\partial}{\partial t} q_{\mathrm{gen}}. \tag{4}$$

In the inequality (4), the presented relation should be understood in a specific way that the left side of this inequality is significantly greater than the value of the expression located at the right one. Moreover, if the following expression is assumed:

$$\mathrm{r} = \begin{bmatrix} \mathbf{T} \\ \mathbf{dT} \end{bmatrix}, \tag{5}$$

the equation (3) can be also transformed to the parabolic system of the equations which is presented below in equation (6).

$$\begin{aligned} &\begin{bmatrix} 1 & 0 \\ 0 & \tau_q \cdot c_{vs} \end{bmatrix} \cdot \frac{\partial \mathbf{T}}{\partial t} - \begin{bmatrix} 0 & 0 \\ 1 & -\tau_q \cdot c_{vs} \end{bmatrix}^T \cdot \mathbf{T} - \nabla \cdot \left(\begin{bmatrix} 0 & \kappa \\ 0 & \tau_T \cdot \kappa \end{bmatrix}^T \nabla \mathrm{T} \right) \\ &= [0 \; q_{\mathrm{generate}}]^T . \end{aligned} \tag{6}$$

In equations (5) the symbol **r** means a one-column vector including the prime solution of equation (3), whereas the symbol **T** occurring in both equations (5) and (6) expresses the variable which values are related to the temperature. Moreover, the variable **dT** is the time derivative of the first order of the temperature.

4. Results of the simulations in Fin-FET transistor

As it was written earlier, the full description of the heat conduction in Fin-FET transistor, using the classic Fourier-Kirchhoff approach, was precisely documented by Asenova's team [9]. Although the very important issue, related to modern electronic circuits, are the dynamic behaviours observed in the case of very big Knudsen numbers, the quantity expressing the ratio of average free path to a characteristic length of a considered structure. Due to this fact, new considerations including approach based on the Dual-Phase-Lag equation and simulation results will be presented in this paper.

The benchmark structure used in this case is the Fin-FET transistor made in technology node 12 nm. Such kind of the transistors was described and analyzed in [9]. Projections of considered structure are presented in Fig. 2. According to the paper [9], the channel's length is 25 nm, its width is 12 nm and the height of that channel is 30 nm. The dielectric thickness placed between the gate and the thin fin is less than 1 nm, precisely writing 0.8 nm. An additional things in that structures are spacers of 6 nm thickness, situated from left and right sides of a gate. The Equivalent Oxide Thickness of the high-κ dielectric gate is also 0.8, while the Buried Oxide depth is 30 nm.

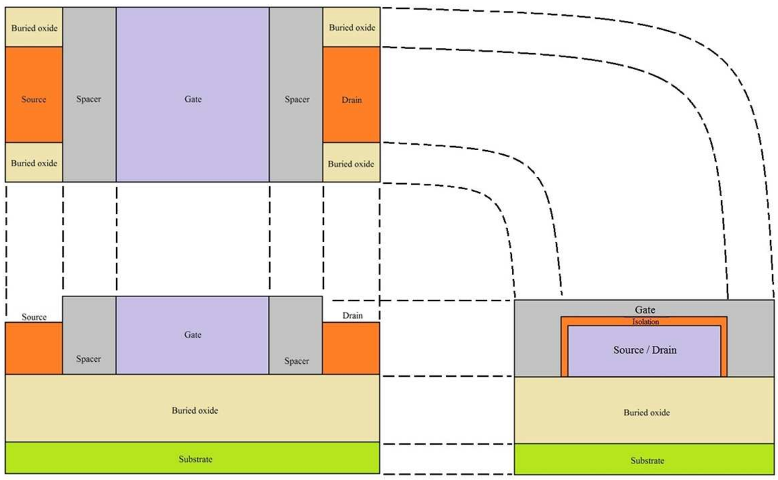

Fig. 2: The considered 12 nm Fin-FET structure.

During the simulations, the following parameters have been used:

$$c_{vs} = 1660 \left[\frac{kJ}{K \cdot m^3}\right],$$

$$\kappa = \begin{cases} 0.30E+2 \left[\dfrac{W}{K \cdot m}\right] & \text{for high-}\kappa \text{ dielectric gate,} \\ 1.38E+0 \left[\dfrac{W}{K \cdot m}\right] & \text{for the polisilicon gate,} \\ 1.48E+2 \left[\dfrac{W}{K \cdot m}\right] & \text{for others.} \end{cases}$$

Moreover, time lags in Dual-Phase-Lag equation were assumed according to the material parameters of the silicon. Therefore, the τ_q parameter is equal to 3 ps, whereas the temperature time lag τ_T is twenty times larger than the heat flux time lag and it equals 60 ps. In order to received the solution, the Finite Element Method was employed. It allows to approximate the Partial Differential Equation. Furthermore, the fifth-order algorithm, also known as the Gear's predictor-corrector method, has been used. During simulations, the two-dimensional structure, presented in Fig. 3, has been considered. In analyzed case, the following assumptions related to the initial and boundary conditions were used:

$$T(x,y,t) = 0 \quad \text{for} \quad y = -30\,\text{nm}, \tag{7}$$

$$dT(x,y,t) = 0 \quad \text{for} \quad y = -30\,\text{nm}, \tag{8}$$

$$\frac{\partial T(x,y,t)}{\partial x} = 0 \qquad \text{for} \quad x = 0\,\text{nm} \quad \vee \qquad x = 20\,\text{nm}, \tag{9}$$

$$\frac{\partial dT(x,y,t)}{\partial x} = 0 \qquad \text{for} \quad x = 0\,\text{nm} \quad \vee \qquad x = 20\,\text{nm}, \tag{10}$$

$$\frac{\partial T(x,y,t)}{\partial y} = 0 \qquad \text{for} \qquad x = 60\,\text{nm}, \tag{11}$$

$$\frac{\partial dT(x,y,t)}{\partial y} = 0 \qquad \text{for} \qquad x = 60\,\text{nm}, \tag{12}$$

$$T(x,y,t) = \begin{cases} H(t) & \text{inside the channel ,} \\ 0 & \text{outside the channel.} \end{cases} \tag{13}$$

$$dT(x,y,t) = 0 \quad \text{for} \quad t = 0. \tag{14}$$

In equation (13), a function H means the Heaviside step function. In all assumption presented in equations (7)–(14) variable T means the temperature while the variable denoted by dT is the time derivative of the temperature of the first order. The results of the mentioned simulations have been normalized. Due to this fact, obtained results express the rise of the temperature in relation to the maximal temperature of the steady state which was received using the Fourier-Kirchhoff model. The same simulations have been also conducted using the Dual-Phase-Lag model. The sample simulation result obtained for the benchmark structure is demonstrated in Fig. 3.

The figure above demonstrates the distribution of the temperature inside the 12 nm Fin-FET channel. As it was written earlier, the temperature is presented in normalized form. As it can be seen in Fig. 3, the region of the highest temperature is marked by the dark red color, while the coolest one is indicated by the dark blue color. Simulations show that the maximal temperature is observed at the point with coordinates x equals 0 and y equal to 0.291 nm. That point is located in the close proximity to the gate, made of the polysilicon material, and a dielectric gate. Increased temperature in mentioned point and in surrounding area indicates one of the most exposed to the high temperature parts of the entire structure and suggests to make precise thermal analyses.

The following figures show the simulation results received for some different time instances using the classic Fourier-Kirchhoff equation. The temperature distribution has been estimated after 20, 40, 60, 80, 100, 120, 140, 160, 180 and 200 ps after the beginning of the simulation, respectively. As it is visible in the Fig. 4. the highest

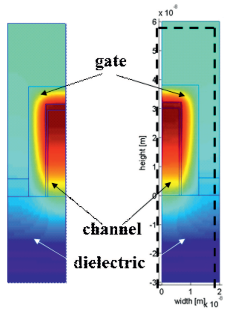

Fig. 3: The distribution of the temperature observed inside the channel of 12 nm Fin-FET transistor.

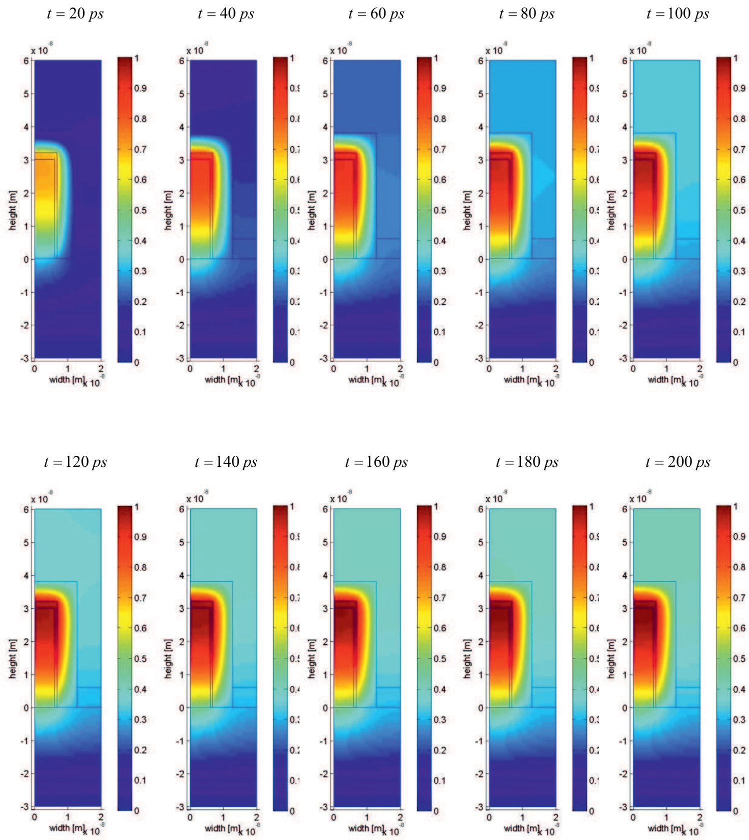

Fig. 4: The distribution of the temperature inside the Fin-FET channel estimated for chosen time instants using the Fourier-Kirchhoff approach.

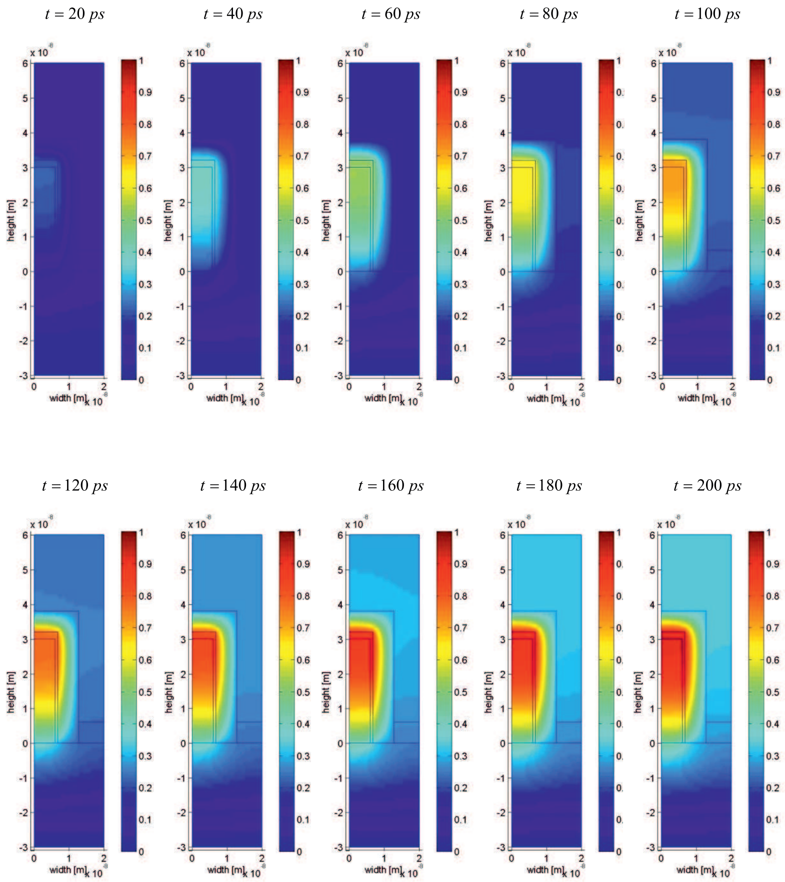

Fig. 5: The distribution of the temperature inside the Fin-FET channel estimated for chosen time instants using the Dual-Phase-Lag model.

temperature rise is observed inside the channel of analyzed Fin-FET transistor. That process occurs very fast and already after 120–200 ps the maximal recorded temperature is observed.

On the other hand, the thermal analyses in 12 nm Fin-FET channel approximated using the Dual-Phase-Lag model is presented in Fig. 5. It is clearly shown that the temperature rise inside the Fin-FET channel is significantly slower when the Dual-Phase-Lag model is used to simulate the thermal processes occurring in analyzed structure than in the case when the Fourier-Kirchhoff equation is employed. The simple comparison of both the Fourier-Kirchhoff and the Dual-Phase-Lag models is demonstrated in Fig. 6.

The figure above shows expressly that values of the temperature observed in analyzed 12 nm Fin-FET transistor are considerably lower using the Dual-Phase-

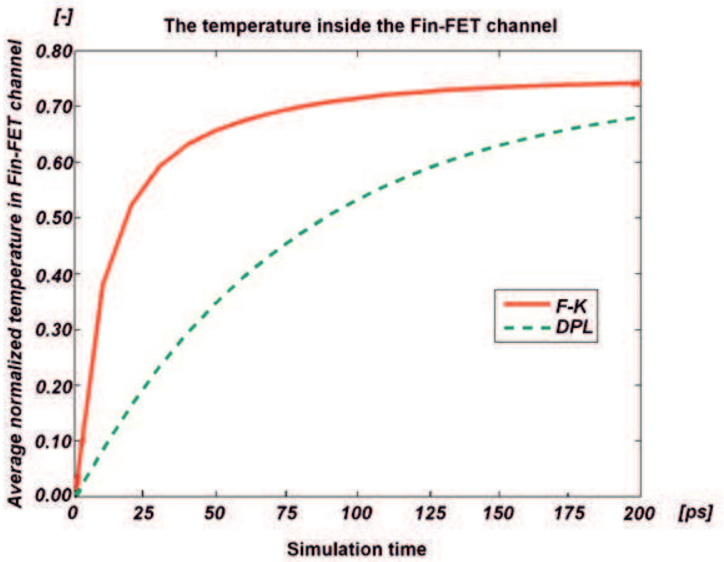

Fig. 6: Comparison of an average normalized temperature inside the Fin-FET channel using the Fourier-Kirchhoff and Dual-Phase-Lag approaches.

Lag model than in the case when the Fourier-Kirchhoff equation is applied. This situation denotes that more appropriate thermal model for modelling of the heat conduction in modern electronic nanostructures is the Dual-Phase-Lag one.

5. Conclusions

That paper demonstrates the thermal analyses which occur inside the modern transistors. The 12 nm Fin-FET transistor is considered. The comparison of dynamic behaviours of Dual-Phase-Lag model and the Fourier-Kirchhoff one is also included. Moreover, the significant number of transistors located in the close proximity was assumed. It is also worth writing that the distribution of the temperature inside the transistor channel was considered. Having regard to all mentioned assumptions, the considerably faster rise of the temperature in the Fin-FET channel is observed using the Fourier-Kirchhoff model, while the slower temperature growth is remarked in the case of the Dual-Phase-Lag one. This observation is very important in the context of the designing of modern electronic nanostructures.

Acknowledgment

This work was supported by the Polish National Science Center project No. 2013/11/B/ST7/01678, the Internal University Grant K-25/Dz. St. /1/2014 and K-25/Dz. St. /1/2015.

References

[1] M. Zubert, M. Janicki, T. Raszkowski, A. Samson, and A. Napieralski, *The heat transfer in Fin-FET transistor*, Proc. of TechConnect World Innovation Conference and Expo, June 14-17, 2015, Washington, DC, USA, vol. 4, pp. 250–253.

[2] D. Y. Tzou, *A Unified Field Approach for Heat Conduction From Macro- to Micro-Scales*, Transactions of ASME J. Heat Transfer **117**, no. 1 (1995), 8–16.

[3] J. B. J. Fourier, *Théorie analytique de la chaleur*, Firmin Didot, Paris 1822.

[4] M. Zubert, M. Janicki, T. Raszkowski, A. Samson, P. S. Nowak, and K. Pomorski, *The heat transport in nanoelectronic devices and PDEs translation into hardware description languages*, Bull. Soc. Sci. Lettres Łódź, Sér.: Rech. Déform. **64**, no. 3 (2014), 69–80.

[5] M. Zubert, M. Jankowski, P. S. Nowak, T. Raszkowski, A. Samson, and A. Napieralski, *Modeling of electromagnetic phenomena inside modern integrated semiconductor structures*, Proc. of TechConnect World Innovation Conference and Expo, June 14-17, Washington 2015, **4**, 234–237.

[6] S. E. Hebboul and J. P. Wolfe, *Lattice dynamics of insb from phonon imaging*, Zeitschrift für Physik B Condensed Matter **73**, no. 4 (1989), 437–466.

[7] R. J. Gutfeld and A. H. Nethercot, *Heat pulses in quarto and sapphire at low temperatures*, Phys. Rev. Lett. **12** (1964), 641.

[8] G. Chen, *Ballistic-diffusive equations for transient heat conduction from nano to macroscales*, J. Heat Transfer **124** (2001), 320–328.

[9] L. Wang, A. R. Brown, M. Nedjalkov, C. Alexander, B. Chenga, C. Millar, and A. Asenov, *3D coupled electro-thermal FinFET simulations including the fin shape dependence of the thermal conductivity*, 2014 International Conference on Simulation of Semiconductor Processes and Devices (SISPAD), 9-11 Sept. 2014, pp. 269–272.

[10] Mingtian Xu and Liqiu Wang, *Dual-phase-lagging heat conduction based on Boltzmann transport equation*, International Journal of Heat and Mass Transfer **48** (2005), 5616–5624.

[11] A. Kaneko, A. Yagishita, K. Yahashi, T. Kubota, M. Omura, K. Matsuo, I. Mizushima, K. Okano, H. Kawasaki, S. Inaba, T. Izumida, T. Kanemura, N. Aoki, K. Ishimaru, H. Ishiuchi, K. Suguro, K. Eguchi, and Y. Tsunashima, *Sidewall transfer process and selective gate sidewall spacer formation technology for sub-15 nm finfet with elevated source/drain extension*, Electron Devices Meeting, 2005. IEDM Technical Digest. IEEE International, pp. 844–847, Dec 2005.

Department of Microelectronics and Computer Science
Łódź University of Technology
Łódź
Poland
e-mail: traszk@dmcs.p.lodz.pl

Presented by Julian Ławrynowicz at the Session of the Mathematical-Physical Commission of the Łódź Society of Sciences and Arts on July 13, 2015

MODELOWANIE PRZEPŁYWU CIEPŁA W NOWOCZESNYCH STRUKTURACH PÓŁPRZEWODNIKOWYCH

S t r e s z c z e n i e

W niniejszym artykule zostały przeprowadzone analizy termiczne związane z modelowaniem przepływu ciepła w nowoczesnych strukturach elektronicznych. Zostało dokonane porównanie dwóch modeli termicznych. Pierwszy z nich oparty jest na klasycznym podejściu wykorzystującym równanie Fouriera-Kirchhoffa. Drugi model wykorzystuje równanie Dual-Phase-Lag. Ponadto, przedstawionych zostało kilka innych modeli termicznych, które znajdują zastosowanie w modelowaniu przepływu ciepła w nanostrukturach elektronicznych. Przeprowadzone rozważania dotyczą analiz termicznych nowoczesnych tranzystorów Fin-FET wykonanych w procesie technologicznym 12 nanometrów.

Słowa kluczowe: tranzystor Fin-FET, równanie Dual-Phase-Lag, równanie Fouriera-Kirchhoffa, analizy termiczne, przepływ ciepła w nanoskali, nowoczesna elektronika

PL ISSN 0459-6854

B U L L E T I N

DE LA SOCIÉTÉ DES SCIENCES ET DES LETTRES DE ŁÓDŹ

2015 Vol. LXV

Recherches sur les déformations no. 2

pp. 119–130

Tomasz Raszkowski and Agnieszka Samson

NUMERICAL APPROACHES TO DUAL-PHASE-LAG EQUATION PROBLEMS

Summary

In this paper the Dual-Phase-Lag model is considered for one-dimensional structure which was heated from the one side and perfectly cooled from other side. The solution for the mentioned heat transfer model was acquired using the Finite Difference Method. This result was precisely discussed and compared with classical heat conduction model which used the Fourier-Kirchhoff equation. In order to present the accuracy of considered methodology the computational complexity and the convergence of proposed algorithm were demonstrated.

Keywords and phrases: Dual-Phase-Lag model, heat transfer, nanoscale, Fourier-Kirchhoff equation, Finite Difference Method, simulations, convergence

1. Introduction

The theory of the heat transfer was established by Jean-Baptiste Joseph Fourier in 1822 [1]. It was based on a law of the heat conduction, which also is known as the Fourier's law. It states that the heat flux is proportional to the negative gradient of the temperature. A differential form of this law demonstrates that the heat flux density equals to the product of the thermal conductivity and the negative gradient of the temperature. It can be formulated as follows:

$$q(x,t) = -k\nabla T(x,t), \quad \text{for} \quad x \in R, \quad t \in R_+ \cup \{0\}, \tag{1}$$

where q is the local density of the heat flux, k is the conductivity of the considered material and ∇T is the gradient of the temperature.

The Fourier's law led to formulation of the parabolic Fourier-Kirchhoff (FK) partial differential equation with mixed boundary conditions. The mathematical form of mentioned equation presents as follows:

$$\frac{\partial T(x,t)}{\partial t} = -\frac{1}{c_{vs}} \nabla q(x,t) \quad \text{for} \quad x \in R, \quad t \in R_+ \cup \{0\}, \tag{2}$$

where c_{vs} means a volume-specific heat capacity.

Both the Fourier's law and the Fourier-Kirchhoff equation were very important issues in classical approach to the problem of modeling of heat transfer because they provided the considered heat transfer theory. This theory has been successfully applied to the end of the XX century to describe thermal processes for relatively large structures and long times of thermal analyses.

Unfortunately, the Fourier-Kirchhoff equation assumes some non-physical behaviours such as infinite speed of heat propagation. Apart from that, this equation postulates that both the heat flux and the temperature gradient could change instantaneously, but, unluckily, it doesn't agree with experiments. Moreover, due to miniaturization of electronic appliances and meaningful increase of their speed, considered model is not sufficient for structures which technology nodes are smaller than 180 nm [2]. This issue is important for example in the case of the MOSFET transistors which are used, inter alia, in family of 14 nm Intel Broadwell CPU and even in the case of prototypical 6 nm FinFET transistors or nanotubes and nanowires manufacturing technology [3].

Therefore, there exists a need for alternative solutions which would include consideration relating to the microscale effects in models of heat conduction. There exist a few mathematical models which are adequate for modeling of heat transfer in nanoscale. One of them is the Boltzmann Transport Equation (BTE). Another one concerns the molecular dynamics simulations. Both of them are described precisely in [4]. It is worth saying that mentioned approaches are characterized by big computational complexity, so simulations times are not short. It means that these models might not be appropriate in all of applications, especially in the case when the speed of simulations is one of the most important elements. Owing to this fact, the paper focus on another heat conduction model called Dual-Phase-Lag (DPL). It was proposed by Tzou in 1997 [5]. That model is relevant for the parabolic Fourier-Kirchhoff model as well as the hyperbolic models. Furthermore, considered model might be useful for heat conduction modeling in structures developed in technologies lower than 180 nm and for integrated circuits operating at frequencies even up-to 6.4 GHz [6].

In the next section the Dual-Phase-Lag model is described. Then, solution acquired for Finite Difference Method (FDM) is presented. In the consecutive section of this paper simulations and their results are discussed. In the last section the analyses related to the computational complexity and the convergence of proposed algorithm are considered.

2. Dual-Phase-Lag heat transfer model

The analysis will be begin with presenting a brief description of mentioned problem. The general heat conduction behaviour might be presented using Fourier-Kirchhoff model which is expressed in the form of the following system of equations:

$$\begin{cases} -\dfrac{1}{c_{vs}}\nabla q(x,t) = \dfrac{\partial T(x,t)}{\partial t}, \\ \\ \nabla T(x,t) = -\frac{1}{k}q(x,t), \end{cases} \tag{3}$$

for $x \in R$ and $t \in R_+ \cup \{0\}$. But in the case of nanoscale, as it was written earlier, a better description of heat transfer can be received using the mentioned Dual-Phase-Lag model [6, 7]. This model can be presented as follows:

$$\begin{cases} -\dfrac{1}{c_{vs}}\nabla q(x,t) = \dfrac{\partial T(x,t)}{\partial t}, \\ \\ k \cdot \tau_T \dfrac{\partial}{\partial t}\nabla T(x,t) + k \cdot \nabla T(x,t) + \tau_q \dfrac{\partial q(x,t)}{\partial t} = -q(x,t), \end{cases} \tag{4}$$

for $x \in R$ and $t \in R_+ \cup \{0\}$.

The system of equations above was derived using the modified Fourier's law. Quantities used in description of this model have the following explanations:

- k, which is called a thermal conductivity, can be interpreted as measure of the ratio of heat conduction,
- τ_q is called the heat time temperature flux,
- τ_T parameter means the temperature time flux.

Two last lag quantities explain existing of the word "dual" in the name of analysed model. In the case, when τ_T equals to zero this model is called the Cattaneo-Vernotte relation [8]. It leads to the hyperbolic heat transfer equation. In the other case, when τ_T and τ_q parameters are equal to zero, the second equation describing the DPL model reduces to the form notorious for the Fourier's law equation. Another case concerns the situation when the thermal conductivity is independent of the temperature and the internal heat generation does not exist. Then the considered relations can be written shortly as the following equation [8]:

$$\alpha\tau_T \frac{\partial}{\partial t}(\nabla^2 T) + \alpha\nabla^2 T = \frac{\partial T}{\partial t} + \tau_q \frac{\partial^2 T}{\partial t^2}. \tag{5}$$

In the form above it appears an additional parameter α. This is a ratio of the thermal conductivity and capacity:

$$\alpha = \frac{k}{c_{vs}},$$

which is also known as a thermal diffusivity.

In comparison to hyperbolic heat transfer model, it appears an additional term which contains the 3$^{\text{rd}}$-order mixed time and a space temperature derivative. The case, when both the temperature and heat flux time lags equal to zero, provides (5) to Fourier-Kirchhoff equations. In order to facilitation of all analyses, the DPL heat transfer equation was transformed to dimensionless form. Instead of the temperature T, the rise Θ of the temperature over ambient temperature is considered. Then the equation can (5) be demonstrated in the following form [8]:

$$B\frac{\partial}{\partial\eta}\left(\nabla^2\Theta\right)+\nabla^2\Theta=2\frac{\partial\Theta}{\partial\eta}+\frac{\partial^2\Theta}{\partial\eta^2}. \tag{6}$$

In this formula new dimensionless constants appear:

$$B=\frac{\tau_T}{2\tau_q},\qquad \eta=\frac{t}{2\tau_q}.$$

The first one presents a dimensionless time. The second one is a parameter which allows to control the transitions between different kinds of the heat conductions behaviours.

3. Finite Difference Method solution

One of the most convenient approaches, which are commonly used in solving heat transfer problems, are Green's functions. In that cases they might be understood as responses of the temperature at point x, which is a coordinate, at the time instant t due to immediate heat generation at the point x_1 at the instant t_1. The sample one-dimensional heat conduction problem was already solved using Green's functions for Fourier-Kirchhoff equation [8, 9]. This paper concerns the analogous considerations, but Finite Difference Method has been used.

The following initial and boundary conditions were used for solving Dual-Phase-Lag equation (4):

$$q(0,t)=c\cdot 1(t)\quad\text{for}\quad t\in R_+\cup\{0\},\quad c\in R, \tag{7}$$

$$T(L,t)=0\quad\text{for}\quad t\in R_+\cup\{0\}, \tag{8}$$

$$T(x,t)|_{t=0}=0\quad\text{for}\quad x\in(0,L), \tag{9}$$

where L means the thickness of the silicon slab.

The discretization mesh for considered problem has been assumed according to equations below:

$$T_i=T\left(i\cdot\Delta x+\frac{1}{2}\cdot\Delta x,t\right)\qquad\text{for}\qquad i=0,\ldots,n-1, \tag{10}$$

$$T_n=T(L,t), \tag{11}$$

$$q_i=q(i\cdot\Delta x,t)\qquad\text{for}\qquad i=0,\ldots,n. \tag{12}$$

In order to received the solution, the following system of the Finite Difference Method equations was used:

$$c_{vs} \cdot \begin{bmatrix} \dot{T}_0 \\ \dot{T}_1 \\ \vdots \\ \dot{T}_{n-1} \end{bmatrix} = \frac{-1}{\Delta x} \begin{bmatrix} -1 & & & & \\ +1 & -1 & & & \\ & +1 & -1 & & \\ & & \ddots & \ddots & \\ & & & +1 & -1 \\ & & & & +1 \; -1 \end{bmatrix} \cdot \begin{bmatrix} q_1 \\ q_2 \\ \vdots \\ q_n \end{bmatrix} + \frac{1}{\Delta x} \begin{bmatrix} q_0(t) \\ 0 \\ \vdots \\ 0 \end{bmatrix} \tag{13}$$

where the column vector $[q_1 \; q_2 \; \ldots \; q_n]^T$ is obtained according to the following system of equations:

$$-\tau_q \cdot \Delta x \cdot \begin{bmatrix} \dot{q}_1 \\ \dot{q}_2 \\ \vdots \\ \dot{q}_n \end{bmatrix} = \Delta x \cdot \begin{bmatrix} q_1 \\ q_2 \\ \vdots \\ q_n \end{bmatrix} - k \begin{bmatrix} 1 & -1 & & & \\ & 1 & -1 & & \\ & & \ddots & \ddots & \\ & & & 1 & -1 \\ & & & & 1 \end{bmatrix} \cdot \begin{bmatrix} T_0 \\ T_1 \\ \vdots \\ T_{n-1} \end{bmatrix} - \tau_T \cdot k \cdot \begin{bmatrix} 1 & -1 & & & \\ & 1 & -1 & & \\ & & \ddots & \ddots & \\ & & & 1 & -1 \\ & & & & 1 \end{bmatrix} \cdot \begin{bmatrix} \dot{T}_0 \\ \dot{T}_1 \\ \vdots \\ \dot{T}_{n-1} \end{bmatrix}. \tag{14}$$

In this case, the following boundary conditions have been established:

$$\dot{T}_n = 0, \tag{15}$$

$$q_0(t) = c \cdot 1(t) \qquad \text{for} \qquad c \in R. \tag{16}$$

4. Simulations and their results

The proposed approach using Finite Difference Method was received in Matlab environment. Moreover, the following methods for numerical solving of Ordinary Differential Equations (ODE) have been used:

a) **ode23** – the explicit Runge-Kutta expression of the 2$^{\text{nd}}$ and the 3$^{\text{rd}}$ order, known as the Bogacki-Shampine pair;

b) **ode45** – an explicit Runge-Kutta expression of the 4$^{\text{th}}$ and the 5$^{\text{th}}$ order, often called as the Dormand-Prince pair;

c) **ode15s** – a variable-order solver which is based on numerical differentiation expressions and which use Gear's method.

In all of mentioned cases, the assumptions presented below were used:

$$L = 10\,nm, \qquad n = 100, \qquad c_{vs} = 1780\frac{kJ}{K \cdot m^3},$$
$$k = 0.16\frac{kW}{K \cdot m}, \qquad \tau_q = 3\,ps, \qquad B = \frac{\tau_T}{2 \cdot \tau_q},$$

where n means the number of discretization mesh nodes.

Due to the value of the dimensionless parameter B, the following cases have been obtained [10]:

a) the Fourier-Kirchhoff solution for B equals to 0.5,

b) the hyperbolic solution when B is tending to 0,

c) and the case of the heat transfer which is observed e.g. in some metal nanostructures when B is significantly greater than 0.5.

It is worth emphasizing that the time variables and coordinates have been normalized because of the convenience of mathematical analyses and of the better comparing of observed phenomena in different approaches to the problem of the heat transfer. Mentioned normalization was determined according to the following formulas:

$$\bar{x} = \frac{x}{L}, \tag{17}$$

$$\bar{T} = \frac{T}{T_{\max}}, \tag{18}$$

where the parameter $T_{\max}$ means the maximal steady-state temperature. Moreover, in considered one-dimensional case, the heat transfer equation can be expressed in the form of the following Laplace equation:

$$\Delta T(x) = 0 \qquad \text{for} \qquad x \in (0, L), \tag{19}$$

and with boundary conditions presented below:

$$-k\frac{\partial T(x)}{\partial x}\bigg|_{x=0} = q, \tag{20}$$

$$T(L) = 0. \tag{21}$$

Therefore, the analytical solution of the mentioned maximal steady-state temperature can be determined as follows:

$$T_{\max} = \lim_{t\to\infty} T(x,t)\bigg|_{x=0} = \lim_{t\to\infty} T(0,t) = \frac{q}{k} \cdot L. \tag{22}$$

Obtained results of the simulations have been compared with results received using Green's functions [9]. The Fig. 1 presents the mentioned comparison prepared for the value of the parameter B equals to 0.5.

As it can be seen, in the figure above the normalized temperature values along the analysed structure are demonstrated. The black lines indicate the findings received using the Fourier-Kirchhoff model, while the red, green, blue and yellow lines represent that ones which were obtained for the Dual-Phase-Lag model for 25 fs, 250 fs, 1000 fs and 5000 fs, respectively. Every single line shows the temperature distribution for different values of time instants. It is clearly seen that the green solid lines coincide exactly with the red dashed ones, so in both methods the similar results are produced. This fact denotes that both methods are equivalent.

In Figs. 2 and 3 the temperature solutions obtained for Fourier-Kirchhoff model (when B equals to 0.5) and for other values of the parameter B in the Dual-Phase-Lag model are shown.

The Fig. 2. presents that the hyperbolic model, marked by dashed lines, overestimates the temperature in heat source, which is located at point 0 on the horizontal axis, but the higher average surface temperature is obtained for the Fourier-Kirchhoff model, marked by the solid lines. In the figure the results for three different time instants, respectively for 25 fs, 50 fs, 250 fs and 500 fs, are shown.

In turn, the Fig. 3 demonstrates that initially, in the case when the value of the parameter B is greater than 0.5, the heat diffusion speed is higher than in the Fourier-Kirchhoff model (B equals to 0.5). Analogously to the previous figure, different normalized temperature distributions, for time instants equals to 25 fs, 50 fs, 250 fs and 1000 fs, are presented. It is also worth noticing that the scale on the vertical axis in analysed figure is logarithmic.

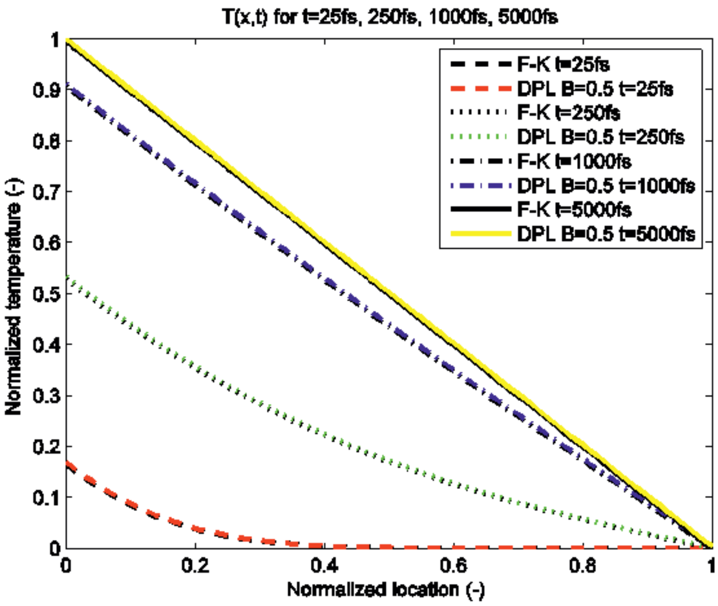

Fig. 1: The comparison of the solutions obtained for the Fourier-Kirchhoff and the dual-phase-lag ($B = 0.5$) models.

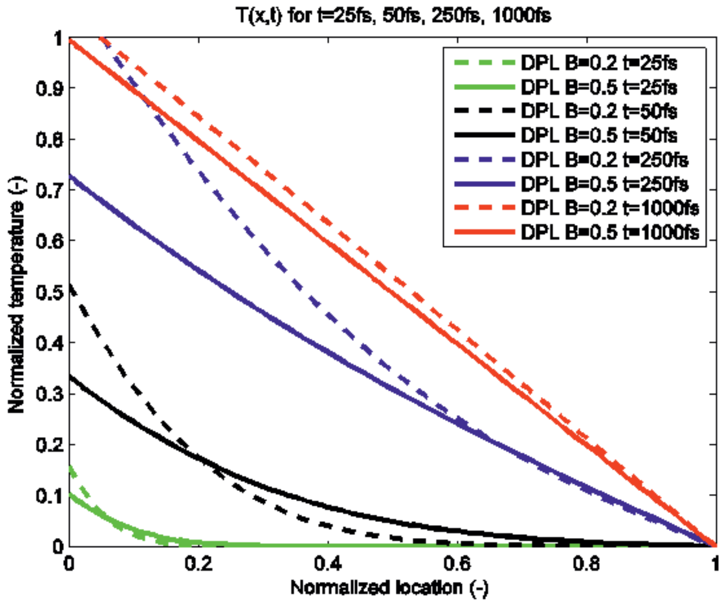

Fig. 2: The temperature solutions obtained for the selected values of the parameter B in the dual-phase-lag model.

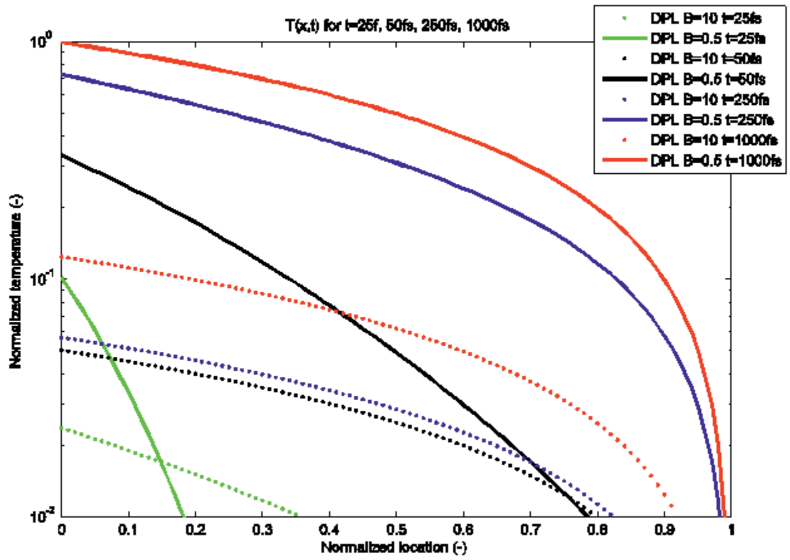

Fig. 3: The comparison of the temperature solutions received for the dual-phase-lag model for $B = 10$ and $B = 0.5$.

5. Analyses related to computational complexity and the convergence of proposed algorithm

In order to estimate the computational complexity of proposed algorithm, the temperature values, denoted by T, were computed for some values of the number of the discretization mesh nodes n. Temperature values have been yielded at point $x = 0$ and for some time instants t. All simulations have been carried out in Matlab environment. The testing machine was supported by the Intel quad-core CPU and the Microsoft Windows 7 operating system. Due to avoid the excessive CPU and RAM memory usage, the sparse matrices were implemented. Moreover, the following simulation parameter values have been fixed:

$$B = 0.5, \quad \text{RelTol} = 10^{-5}, \quad \text{MaxStep} = 10^{-16}, \quad t = 0\ fs, \ldots, 500\ ps.$$

All of the durations of the simulations have been measured by the stopwatch timer function in Matlab environment. Results of these measurements, received for the case when the value of B is equal to 0.5, for various number of discretization mesh nodes n and for all numerical methods mentioned earlier (ode23, ode45 and ode15s) are included in the Table 1. and graphically in Fig. 4. The graphical comparison of the simulation times measurement presents the figure below.

The temperature value relative error of the computation ε was established using the following expression:

$$\varepsilon = \frac{T_{k=n} - T_{1000}}{T_{1000}}, \tag{23}$$

where:

- T_{1000} means the temperature value obtained for $n = 1000$ nodes,
- $T_{k=n}$ means the temperature values yielded for $k = n$ where $n = 10$, 20, 50, 100, 200, 500 nodes.

Tab. 1: Times of simulation.

Number of nodes	Simulation time [s]		
	ode23	ode45	ode15s
5	10.014	18.214	10.126
15	11.198	20.947	10.671
25	11.326	21.183	11.059
45	11.547	21.498	12.387
75	13.745	22.921	13.549
150	47.210	61.819	21.176
250	113.012	187.984	44.876
450	449.179	617.426	142.276
750	1139.210	2084.800	333.376
1000	2242.710	4216.300	547.626

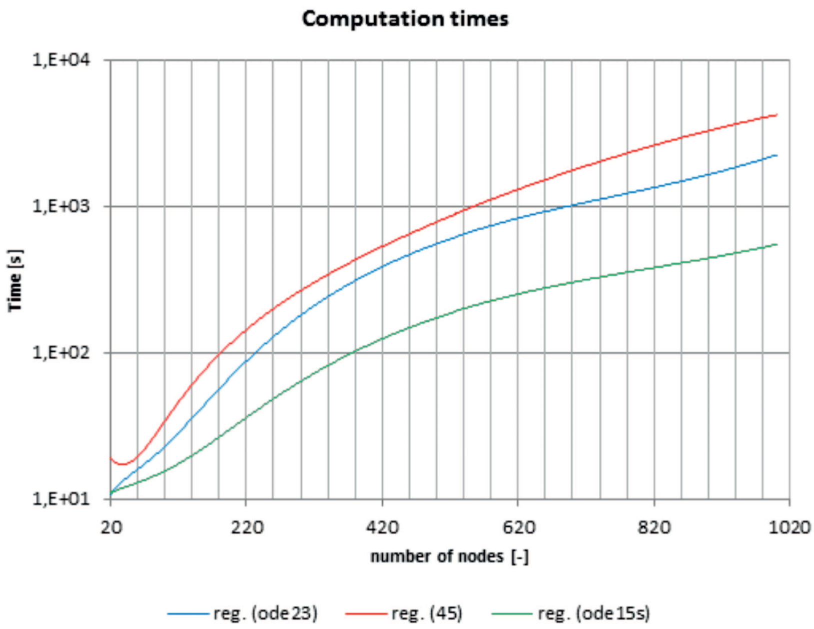

Fig. 4: Comparison of the simulation times in each numerical approach.

The Table 2 contains the relative error computed using Gear's method for $t = 500\,\mathrm{ps}$ according to the equation (23). The relative error presented in graphical form demonstrates the following figure. As it can be seen, the increase of the number of discretization nodes n causes the fast reduction of the relative error. It denotes that the proposed approach is convergent in analyzed cases.

Tab. 2: The Relative Errors for $t = 500\,\mathrm{ps}$.

Number of nodes	The relative error
5	−0.0928
15	−0.0318
25	−0.0192
45	−0.0106
75	−0.0062
150	−0.0029
250	−0.0015
450	−0.0006
750	−0.0001
1000	0.0000

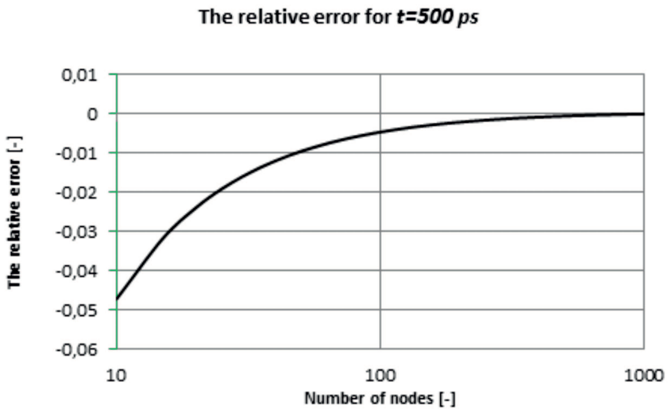

Fig. 5: The relative errors yielded for $t = 500\,\mathrm{ps}$.

6. Conclusions

This paper demonstrates the numerical approach in solving the heat transfer problem in one-dimensional structures. The Finite Difference Method solution of the Dual-Phase-Lag equation for considered problem is convergent when n tends to infinity. The best of presented numerical methods, used to solve the ordinary differential equations, is the Gear's method as it is indicated by the results of the computational complexity measurement. Apart from that, the analyzed Finite Difference Method is appropriate to describe the nanosized structures and to approximate the temperature of the real integrated circuits

Acknowledgment

This work was supported by the Polish National Science Center project No. 2013/11/ B/ST7/01678, the Internal University Grant K-25/Dz. St. /1/2014 and K-25/Dz. St. /1/2015.

References

[1] J. B. J. Fourier, *Théorie analytique de la chaleur*, Firmin Didot, Paris 1822.

[2] M. Janicki, M. Zubert, and A. Napieralski, *Convergence of Green's function heat equation solutions in electronic nanostructures*, Mixed Design of Integrated Circuits & Systems (MIXDES), Proceedings of the 21st International Conference, 19-21 June 2014, 285–288.

[3] T. Raszkowski, M. Zubert, M. Janicki, and A. Napieralski, *Numerical solution of 1-D DPL heat transfer equation*, Proc. of 22nd International Conference Mixed Design of Integrated Circuits and Systems MIXDES 2015, 25-27 June 2015, Toruń 2015, 436–439.

[4] D. G. Cahill, W. K. Ford, K. E. Goodson, G. D. Mahan, A. Majumdar, H. J. Maris, R. Merlin, and S. R. Phillpot, *Nanoscale thermal transport*, Journal of Applied Physics **93** (2003), 793–818.

[5] D. Y. Tzou, *A unified field approach for heat conduction from macro- to micro-scales*, Transactions of ASME J. Heat Transfer **117**, no. 1 (1995), 8–16.

[6] M. Zubert, M. Janicki, T. Raszkowski, A. Samson, P. S. Nowak, and K. Pomorski, *The heat transport in nanoelectronic devices and PDEs translation into hardware description languages*, Bull. Soc. Sci. Lettres Łódź, Sér. Rech. Déform. **64**, no. 3 (2014), 69–80.

[7] Mingtian Xu and Liqiu Wang, *Dual-phase-lagging heat conduction based on Boltzmann transport equation*, International Journal of Heat and Mass Transfer **48** (2005), 5616–5624.

[8] M. Janicki, M. Zubert, A. Samson, T. Raszkowski, and A. Napieralski, *Green's function solution for Dual-Phase-Lag heat conduction model in electric nanostructures*, 31th Annual Semiconductor Thermal Measurement and Management Symposium (SEMI-THERM), 15-19 March, San Jose 2015, 95–98.

[9] M. Janicki, M. Zubert, and A. Napieralski, *Green's function solution of hyperbolic heat equation suitable for thermal analysis of electronic nanostructures*, 20th International Workshop on Thermal Investigations of ICs and Systems (THERMINIC), 24-26 September 2014, 1–4.

[10] P. J. Antaki, *Solution for non-Fourier dual phase lag heat conduction in a semiinfinite slab with surface heat flux*, International Journal of Heat and Mass Transfer **41**, no. 14 (1998), 2253–2258.

Department of Microelectronics and Computer Science
Łódź University of Technology
Łódź, Poland
e-mail: traszk@dmcs.p.lodz.pl

Presented by Julian Ławrynowicz at the Session of the Mathematical-Physical Commission of the Łódź Society of Sciences and Arts on July 13, 2015

NUMERYCZNA IMPLEMENTACJA ALGORYTMÓW ROZWIĄZYWANIA RÓWNANIA DUAL-PHASE-LAG

S t r e s z c z e n i e

W niniejszym artykule rozważane jest równanie Dual-Phase-Lag dla struktury jednowymiarowej. Struktura ta jest ogrzewana z jednej strony i chłodzona z drugiej strony. Rozwiązanie dla tak skonstruowanego modelu przepływu ciepła zostało uzyskane przy użyciu Metody różnic skończonych. Wyniki zostały szczegółowo omówione i porównane z rezultatami otrzymanymi za pomocą klasycznego modelu Fouriera-Kirchhoffa. W celu ukazania dokładności rozważanej metodologii przeprowadzone zostały badania dotyczące złożoności obliczeniowej i zbieżności zaproponowanego algorytmu.

Słowa kluczowe: model Dual-Phase-Lag, przepływ ciepła, nanoskala, równanie Fouriera-Kirchhoffa, metoda różnic skończonych, symulacje, zbieżność, algorytmy

Rapporteurs – Referees

CONTENU DU VOLUME LXV, no. 3